Effect of Capillary Dimensions on Extrudate Swell of Molten Polymers

By

© (STEVE) FEI-KUI HO , B. Eng.

A Thesis

Submitted to the School of Graduate Studies

in Partial Fulfilment of the Requirements

for the Degree

Master of Engineering

McMaster University

November , 1980

MASTER OF ENGINEERING (1980) McMASTER UNIVERSITY

(Chemical Engineering) Hamilton, Ontario,

Canada.

TITLE : Effect of Capillary Dimensions on Extrudate Swell of Molten Polymers

AUTHOR : (STEVE) FEI-KUI HO , B. Eng. Sc.

(University of Western Ontario, Canada)

SUPERVISOR : Dr. John Vlachopoulos

NUMBER OF PAGES : xiv, 207

ABSTRACTS

The effect of capillary dimensions on the extrudate swell of molten polymers is studied with three branched low-density polyethylenes (LDPE) and a broad distribution polystyrene (PS) samples. The polystyrene and one of the low-density polyethylene samples (DHDY-6873) are tested in detail at three extrusion temperatures ranging from 160°C - 220°C, while the other two low-density polyethylene samples are run at one temperature only.

For all polymers, extrudate swell decreases exponentially with increasing length-to-diameter (L/D) ratio of capillaries. For a die-orifice (L/D → 0), extrudate swell increases with entry angle up to 150° and decreases thereafter. At constant reservoir diameter D_R, extrudate swell also increases with D_R/D ratio up to 10 and then drops.

An empirical decay equation is found to correlate well with the extrudate swell data for low-density polyethylenes. However, there is no direct correlation for polystyrene.

Huang and White's new expression predicting extrudate swell with long capillaries does not correlate reasonably well with the experimental data for polystyrene. However, the model as

previously suggested by Graessley gives better approximation. Tanner's new inelastic theory on extrudate swell plays no significant part in the present study. The effect of "frozen-in-stresses" on extrudate swell is found to be small.

Huang and White's new model predicting extrudate swell for an orifice-die correlates well with the polystyrene data at low shear rate region (< 30 1/sec), but indicates considerable discrepancy at high shear rate region. At present, there is no reliable predictive theory for extrudate swell at higher shear rates both with short and long capillary dies.

ACKNOWLEDGEMENTS

The author wishes to express his gratitude to his research supervisor, Dr. John Vlachopoulos for his constant guidance and advice during the course of his study and the preparation of his thesis.

Financial support from the Department of Chemical Engineering, McMaster University is gratefully acknowledged.

Thanks are extended to Mr. G. Innocente of the mechanical work shop for making the extrusion dies, and Mr. W. Hutton - the computer assisstant, for his guidance in typing up the thesis.

At last but not at least, the author would also like to thank all the folks in the Department, no one in particular, whose presence has made his stay enjoyable.

TABLE OF CONTENT

LIST OF FIGURES

LIST OF TABLES

CHAPTER 1

INTRODUCTION

When a polymer melt emerges from a die, orifice or any other kind of flow channel, it exhibits an appreciable increase in cross-sectiona area. This phenomenon is known as extrudate swell (Fig. 1.1). Alternative terms describing this behavior are die swell, memory, puff-up and Barus effect. It is a flow defect and occurs at both low and relatively high shear rates. However, beyond a critical shear rate, extrudate distortion takes place (Figs.4.2 a & b).

Extrudate swell can be described quantitatively in terms of the swell ratio, d/D, which is the ratio of the diameter of the extrudate to that of the die. The reasons for increased interest in this phenomenon are numerous, ranging from a desire to define the viscoelastic response of polymeric materials to the need to obtain direct relations between extrudate swell and such polymer processing characteristics as swell in blow molding, thickness in extruded wire and cable covering, as well as the "draw-down" and "neck-in" in sheet extrusion. However, there has not been much progress in relating extrudate swell to polymeric structure.

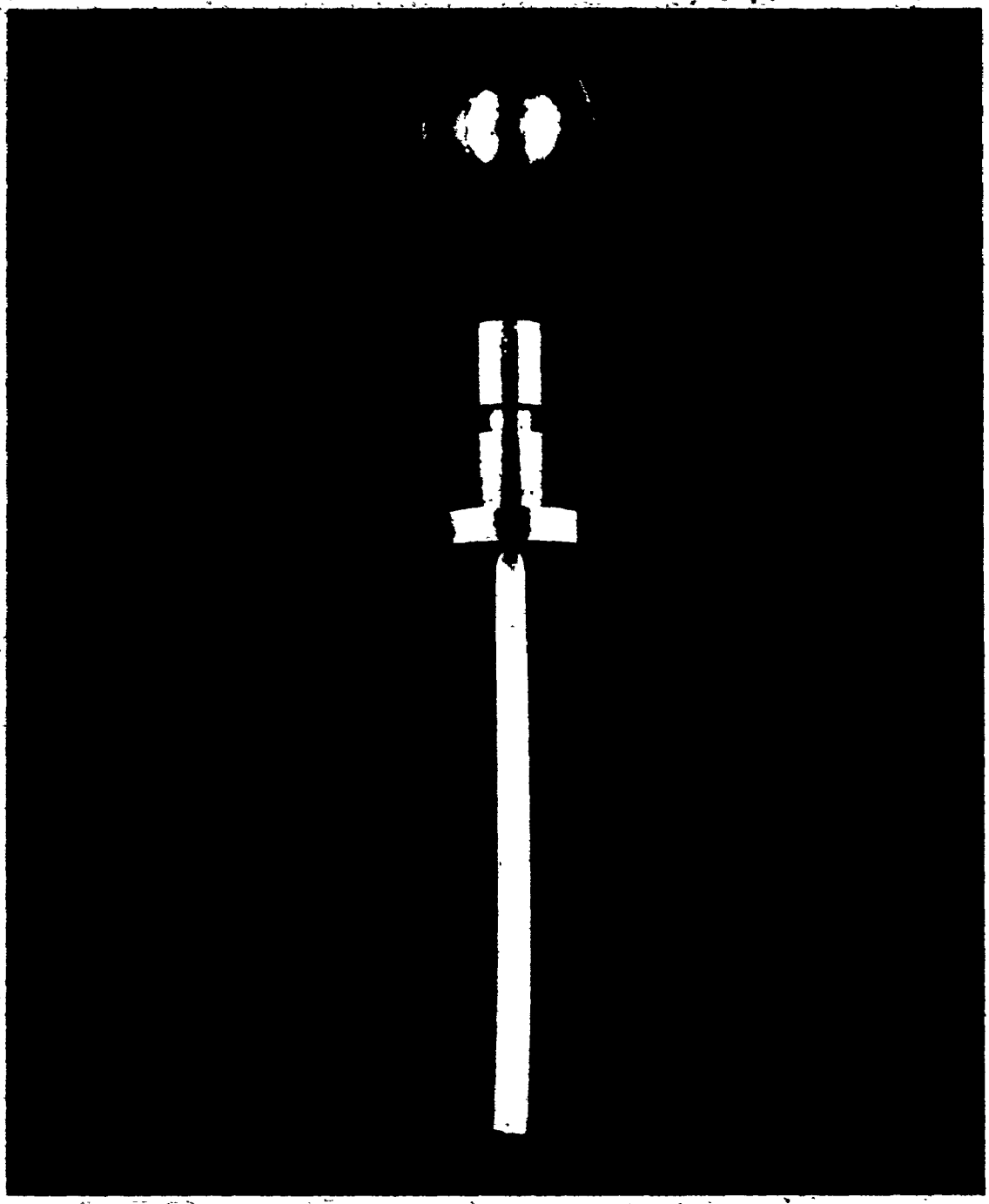

Figure 1.1 : Extrudate Swell of Polymer Melt.

Top and Side Views

This phenomenon is not unique to polymer melts, non-elastic liquids exhibit die swell of about 1.10 at low Reynolds number. For high Reybolds number flow, the liquid jet contracts by about 13%. However, there is a smooth transition between the two extreme limits and this effect is small compared to the large die swell observed with viscous polymer melts.

Studies on extrudate swell using long capillary dies have been extensive, but not much work has been done with short capillaries and zero-length dies. It has been observed that die swell depends greatly on capillary dimensions which can be described in terms of the L/D ratio (Fig.1.2). Despite the effort that has been devoted to investigate this behavior, the explaination still remains unclear.

The objective of this thesis is:

1. to investigate the effect of capillary length, diameter, and its included entrance angle on die swell for low-density polyethylene and polystyrene samples,
2. to study the effect of extrusion variables of shear rate, shear stress and temperature on die swell phenomenon,
3. to investigate the effect of "frozen-in-stresses" on extrudate,
4. to investigate new models which will predict extrudate swell with short and long capillary dies.

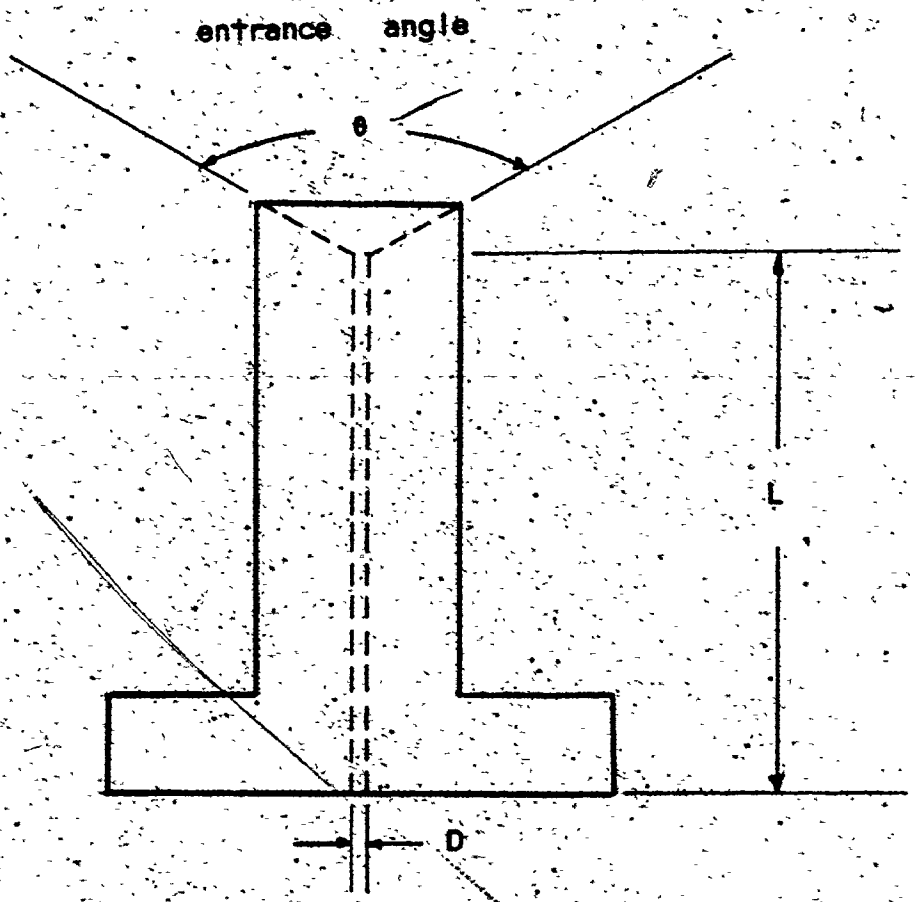

Fig.1.2 Schematic Illustration of Capillary Die Geometry

CHAPTER 2

LITERATURE SURVEY

2.1 On General Use of Study of Extrudate Swell

The problem of die swell in rubber industry was recognized as early as 1933 by Dillon and Johnston (1,2). They related extrudate swell to rubber processing behavior and concluded that at constant output rate, the amount of swelling decreased with increasing temperature.

Since 1945, the speeding growth of the thermoplastic industry led to the study of extrudate swell as a significant processing and characterization parameter. Recent advances in theoretical development have made the work on this phenomenon more comprehensive. Investigations of this "elastico-viscous" effect are particularly useful in the processing of thermoplastic materials in blow molding, sheet extrusion, wire and cable insulation and related areas (3,4).

In the bottle-blowing process, Wechsler and Baylis (5) studied the effect of temperature, shear rate, density and melt index on extrudate swell. Wilson (6) also discussed die swell as an important variable in the extrusion blowing of polyethylene bottle and showed its dependence on polymer composition and die design.

In extending his work, Beynon and Glyde (7) observed die swell an increasing function of shear rate up to a critical value beyond which certain flow defects occurred. They agreed with Dillon and Johnston (1,2) that die swell decreased with increasing temperature, but larger swells were also attainable at higher temperatures.

Following Wilson's work, Burgess and Lewis (8) discussed the importance of study of extrudate swell in die design. They concluded that in addition to temperature and extrusion rate, die swell is also a complicated function of the molecular weight, molecular weight distribution and branching of polymer as well as length of the die-land. The general conclusion was that the higher the molecular weight and the shorter the die-land, the larger was the swell.

Effect of draw-down and neck-in (3) are very important in the processes of extrusion coating and sheet extrusion of polymers. The former refers to the ability of the polymer to coat evenly down to very low coating weights over a wide range of coating speeds. The latter is a phenomenon associated with cast film extrusion and is the term given to the reduction in film web as it leaves the die. Polymer with a larger swelling ratio exhibits low "neck-in".

Kaltenbacher et al (9) compared draw-down characteristics with apparent viscosity, melt elasticity as assessed by die swell measurement; high degree of correlations between draw-down behavior in a coating process with the melt viscosity and die swell were obtained. They also compared neck-in with melt viscosity, melt elasticity, molecular weight and molecular weight distribution, and confirmed that the greater the elastic properties, the better is the polymer. The coated width was correlated with swelling ratio and melt flow index. It was found that these factors would reduce neck-in but would also reduce maximum coating speeds.

Emphasis on the importance of die swell as a characterizing variable in sheet extrusion and extrusion coating was also discussed (10-12). It was noted that draw-down and neck-in are related to die swell in such a way that any change made to improve one property will adversely affect the other; a common but depressing observation. Other applications on the study of extrudate swell have also been discussed by Brydson (3).

2.2 On Extrudate Swell

2.2.1 Mechanism

The earliest quantitative study is perhaps that of Dillon and Johnston (1,2) on rubbers. Since then a number of investigators (13-17) suggested that stress relaxation is responsible for swelling. It should be noted, however, that even Newtonian jets swell by about 13% at very low Reynolds number (Re<16) (18). This value of swell has been found both experimentally (19) and theoretically (20). The swelling of Newtonian jets is probably due to the streamline adjustments as the liquid comes out of an opening into air and acquires a free surface. Thus, both stress relaxation and Newtonian swell give contribution to extrudate swell.

Nakajima and Shida (21) considered the extrudate swell problem as a consequence of elastic energy recovery. Following Lodge's idea (22) of elastic recovery of a KBKZ fluid (23) when released from a state of stress, Tanner (24) proposed an elastic recovery theory to determine the swelling due to a sudden and unconstrained recovery from a long duration Poiseuille flow in a die (see also section 3.3). White (25) performed a general analysis of the unconstrained elastic recovery in viscoelastic fluids. Formulation of Tanner's the-

ory has been modified by a number of authors (26-28).

Recently, Phuoc and Tanner (29) discovered that a Newtonian fluid with a temperature-dependent viscosity exhibits a swelling (see also section 6.3). For typical low-density polyethylene viscosity value and usual extrusion conditions a swelling of about 70% was reported (29,30). To explain this phenomenon, Tanner (30) developed an inelastic theory by considering the extrudate as consisting of two layers - the outer layer is in tension and the inner layer is in compression. He assumed that the swelling is caused by an increased resistance to deformation of elongated filaments near the extrudate surface. By means of an appropriate formulation of force and mass balances for the two layers, Tanner (30) showed that swelling is predicted for variable-viscosity Newtonian, second-order, power-law and Maxwell fluids. Some direct observations that support Tanner's two layer model were made earlier by Kiselev and Kanavets (31).

Therefore, it can be argued that four mechanisms are responsible for extrudate swell: A Newtonian swell, an elastic recovery, an inelastic (thermal) swell and stress relaxation. The contribution due to Newtonian is about 13%.

The contribution due to stress relaxation is perhaps few % for low-density polyethylene and polystyrene, but becomes quite significant for high-density polyethylene (see also section 2.2.3). No experimental observations on polymer melts is available to justify Tanner's new inelastic theory on extrudate swell. The idea that elastic recovery is the major contribution to extrudate swell is generally accepted (21,24-28,32-35).

2.2.2 Effect of Die Geometry

Past experience has indicated that die swell is a complex problem. Most of its previous investigations were based on long flow channels of simple constant cross-section so that the problem can be understood better in terms of well-defined flow histories.

Early studies on extrudate swell using capillary dies were made by Spencer and Dillon (13,14); but their analysis on die swell has been criticized by Mooney (36) and Bagley et al (37). The latter investigators used low-density polyethylene and observed that extrudate swell decreases exponentially with capillary length. They explained this behavior in terms of a memory effect and introduced the concept of the average time transit, t, through the die to obtain the following equat-

ion:

$$(B-B_\infty)=(B_o-B_\infty)\exp(-kt) \qquad (2.1)$$

where B is the swelling index defined as the ratio of extrudate diameter to die diameter, i.e. d/D. B_o and B_∞ are values of B at zero and infinite transit times, and k is a decay constant.

In an attempt to relate the swelling index to the capillary die length to radius ratio, L/R, Bagley et al (37) suggested a volume average transit or residence time, t_a, estimated by means of the following equation:

$$t_a=\pi R^2 L/Q \qquad (2.2)$$

where Q is the constant volumetric flow rate. Eq.(2.2) can be written as

$$\dot{\gamma}_a=4(\pi R^3/4Q)(L/R)=4(L/R)/\dot{\gamma}_a \qquad (2.3)$$

where $\dot{\gamma}_a$ is the pseudo shear rate of the wall (to be discussed in section 3.1).

Bagley et al (37) used the effective capillary length-to-radius ratio (L/R +e) (see section 3.2.6) sothat eq.(2.1) becomes

$$(B-B_\infty)=(B_o-B_\infty)\exp[-(4k/\dot{\gamma}_a)(L/R+e)] \qquad (2.4)$$

They found that for the low-density polyethylene studied, k varies linearly with $\dot{\gamma}_a$ and therefore

$$k=(C/4)\,\dot{\gamma}_a \qquad (2.5)$$

where C is a constant and eq.(2.4) may be written as

$$(B-B_\infty)=(B_o-B_\infty)\exp[-C(L/R+e)] \qquad (2.6)$$

Rogers (38) studied the dependence of die swell on capillary length using 18 samples of commercial and experimental polyethylenes and found good agreement with Bagley et al results (37), but the experiment was not designed to elucidate a mechanism nor develop an expression relating the swelling ratio to capillary geometry.

Kawasaki, Tatsusaka and Ono (39) considered the extruding process as a series of deformation mechanisms and after leaving the flow-channel, recovery of the remaining strain takes place and causes die swell. An Oldroyd model which consists of a series of dash-pots (dynamic viscosity μ_1) and Voigt element (dynamic viscosity μ_2 and relaxation modolus G_2) is employed as the representative rheological model for molten polymers. This led them to an equation relating the swelling index B of the extrudate to the L/R of the capillary.

$$\ln\left\{1-\frac{1}{(B-A)^2}\right\}=-\ln\left\{\frac{\gamma(t_1)}{\gamma_2(t_1)}\right\}-\frac{1.74}{\dot{\gamma}_a\beta}(L/D) \qquad (2.7)$$

where $\beta=\dfrac{\mu_1+\mu_2}{G_2}$, $\dot{\gamma}_a$ is defined previously in eqs.(2.1) and (2.3).

By varying the capillary length only hence changing values of L/R while fixing $\dot{\gamma}_a$, a linear relation exists between $\ln\{1 - \frac{1}{(B-\Delta)^2}\}$ and L/R. However, the parameter Δ is not clearly defined (40).

On the contrary, Vlachopoulos et al (41) used capillaries (10< L/D <24) to study die swell of polystyrene and found, in good agreement with Graessley's result (35), that the swelling ratios are almost independent of L/D. The latter investigator also used relatively long capillary dies with L/D ratios ranging from 13-100; the swelling index of polystyrene samples may perhaps be insensitive to capillary length change in this ratio range. On the other hand, Mori and Funatsu (42) indicated that the swelling ratios decrease rapidly with increasing L/D up to a L/D of about 20 for polypropylene and polyethylene samples - the same conclusion as drawn by Han et al (43).

The dependence of die swell for polyethylene on die entry geometry was investigated by Arai and Aoyama (44) using capillary dies. The dies have the same L/D of 1.0 and same diameter of 1.0 mm with entrance angles ranging from 30^0 - 180^0. No appreciable change in swelling ratio was observed.

White and Roman (27) used capillaries with L/D ratios rang-

ing from 5.0 to 47.5 to examine the die swell of low- and high-density polyethylene, polypropylene and polystyrene. Results indicated that swell of low-density polyethylene is most pronounced to capillary length change while polystyrene the least.

Recently, Huang and White (45,46) made experimental and theoretical investigations of extrudate swell of polystyrene and polypropylene from large and small length/cross-section ratio slit and capillary dies. They found that the effect of die entry geometry, i.e. entrance angle of dies, is pronounced for zero-length (L/D=0) and very short dies (L/D<3). For the two polymer samples studied, they concluded that extrudate swell decreases with decreasing entrance angle of the die (see also section 3.3).

2.2.3 Effect of Various Methods of Measurement

Different methods have been employed and improved to measure die swell of polymer melts. Bagley et al (37) studied die swell of polyethylene using a gas-driven capillary viscometer and measured the diameter of the frozen extrudate with a micrometer. The diameter of extrudate is corrected for the density difference between room temperature and extrusion temperature, i.e.

$$d/d_o = (\rho_o/\rho)^{1/3} \qquad (2.8)$$

where d=diameter of extrudate corrected to extrusion temper-

ature

d_o=diameter of frozen polymer at room temperature

ρ_o and ρ are densities of polymer at operating and room temperatures respectively.

Once extruded, the polymer melt is allowed to cool and solidify at room temperature. They realized that die swell measurement determined in this way is not accurate because solid densities depend on crystallization kinetics. Also, the draw down effect due to the increasing weight of the extrudate will stretch the diameter, but they suggested that all measurement be taken at 1/4 inch from the emergent end.

When molten polymer comes out of the die to room temperature, solidification will take place prior to complete relaxation of the extrudate thereby "freeze" part of the stress. The effect of frozen-in-stresses becomes more pronounced with those molten polymers which have long relaxation times.

Han and Charles (47) proposed a new photographic technique to accurately measure die swell. In their method polymer melt is extruded to a chamber which is maintained at the same temperature as the operating temperature, and pictures are taken of the suspended stream at various time intervals until the melt has fully relaxed. High-density polyethylene sam-

ples were examined. It was found (47) that for shear rate ranging from 200-800 1/sec, measurement obtained from the frozen extrudate were lower by 9.3% than those obtained by the photographic technique.

In an attempt of developing an even better technique of measuring die swell, Utracki et al (48) designed a new device for this purpose. They suggested that accurate measurement can only be made provided that the extruded strand undergoes complete isothermal relaxation in the absence of gravitational sagging and interfacial tension effects. Methods in which the extrudate was either allowed to quench into cold water (49) or relax in hot gas chamber (50,51) have been employed. Extrusion into a hot gas chamber increases the effect of gravitational sagging and interfacial tension while quenching introduces an additional thermal history, which in the case of crystallizable polymers, introduces an additional stress (32).

In Utracki et al (48) investigation, samples of polystyrene, polyethylene and polyvinyl chloride (PVC) were examined. Extrusion sample was allowed to emerge into a thermostated fluid of proper density and interfacial tension in a thermostating chamber, collected and photographed. The melt diameter

was then determined by comparison of the extrudate diameter in the developed film to that of a standard. Measurements made in this way were found to be reproducible, reliable and accurate.

Annealing is a process in which the molten polymer has been frozen and returned to a silicon bath at a temperature above its melting temperature for some time. White and Roman (27) studied die swell of low- and high-density polyethylene, polypropylene and polystyrene using various methods. High-density polyethylenes were found to exhibit much greater stress recovery in the annealing process than polystyrene and polypropylene. Variation of magnitude of die swell does depend on the type of measurement, and the values are largest for the isothermal extrusion into hot silicone oil and lowest for the frozen extrudates. The differences in extrudate diameter from different methods of measurement range from 10-30% for high-density polyethylene (27). However, measurements on die swell with polystyrene (35) and low-density polyethylene (52) showed the difference is relatively small.

2.2.4 Effect of Molecular Weight and its Distribution

Polymers are composed of macromolecules and therefore their elastic properties are characterized by their molecular weight,

molecular weight distribution and degree of long-chain branching.

Rogers (38) studied the dependence of die swell on molecular weight and molecular weight distribution using different polyethylene samples. By and large, extrudate swell was greater for broad distribution than narrow distribution polymers of similar weight-average molecular weight. He observed that swelling increases linearly with increasing weight-average molecular weight, but some ethylene-butene copolymers showed greatest deviation from the linear plot and could possibly form another family of curves. A similar trend was also observed with molecular weight distribution. However, it has been shown (53) that when the molecular weight of polymer reaches an approximate value of 400,000 swell does not increase appreciably.

On the contrary, Sieglaff (54) examined the rheological properties on commercial PVC and concluded that the degree of swell at low shear rates is less for higher molecular weight samples while at high shear rates, prior to a critical value at which extrudate distortion occurs, the extent of swell is not sensitive to molecular weight changes.

Graessley et al (35) used three narrow distribution polystyrenes to study die swell. A constant swelling ratio of 1.10 was observed in the Newtonian region, but in the non-Newtonian region

the ratio increases rapidly. They also found that swell increases both with molecular weight and molecular weight distribution. Similar conclusion was drawn by Vlachopoulos et al (41), and Racin and Bogue (55) that the broader is the distribution, the larger the extrudate swells.

Mendelson and Finger (52) examined the effect of long-chain branching on the melt elasticity in shear of polyethylenes. Results have shown that both low and high molecular weight branched high-density polyethylenes undergo less elastic deformation and hence swell less than the linear ones. They also found that the long-chain branched low-density polyethylene samples have higher melt elasticity and therefore swell more than the high-density polyethylene samples.

2.2.5 Effect of Temperature and High Shear Rate

The dependence of die swell on temperature has been examined by a number of investigators (1-3,7,35,52,56). For polystyrene and polymethylmethacrylate (PMMA), it is generally agreed (1-3,35, 46) that the swelling index decreases with temperature at constant shear rates. On the other hand, Horie (56) observed the anomalous behavior with low-density polyethylene whose swelling ratio increase with temperature - a disagreement with earlier results

from Beynon and Glyde (7), and Dillon and Johnston (1,2). He noted that the polyethylene sample studied is branched polymer while the polystyrene and PMMA commercial samples are linear samples - die swell of branched polymer is usually more complicated than that of a linear one.

Swell increases with extrusion rate up to a critical shear rate, equivalent to a die wall shear stress of 10^5 Pa, beyond which the emergent extrudates become distorted for all polymers (7,45,46,56-59). Extrudate distortion is observed in the form of surface roughness, sharkskin and melt fracture (3,60). This flow defect is believed (61-63) to be a consequence of flow instability in the die entry region. It has been indicated (58,60) that the onset of melt fracture occurs at higher shear stress in slit dies than in capillaries.

Experimental studies on melt fracture of commercial samples of low- and high-density polyethylene, narrow and broad molecular weight distribution polystyrene, polypropylene, linear and branched polyethylene were made extensively by Vlachopoulos and his co-workers (57-59). They concluded that critical shear stress increases slightly with temperature thereby the maximum attainable swelling ratio also increases with temperature. In addition, the critical shear stress was found to be independent of molecular

weight distribution and that increasing the weight-average molecular weight of the polymer will decrease the critical shear stress.

CHAPTER 3

THEORETICAL BACKGROUND

3.1 Capillary Flow

The flow of a fluid in a capillary can be described by the equations of continuity, momentum and energy. Generally, the momentum equation takes the form of:

$$\rho \frac{D\bar{V}}{Dt} = - \nabla P - \nabla.\bar{\bar{\tau}} + \Sigma \rho \bar{F} \qquad (3.1)$$

By assuming that

(1) the flow is steady,

(2) the flow is in the axial direction only,

(3) the axial velocity is a function of the distance from the axis alone,

(4) there is no slippage at the wall,

(5) the fluid is incompressible,

(6) the flow is isothermal,

(7) the capillary is sufficiently long so that end effects are negligible,

(8) external forces are negligible,

(9) the fluids is time-independent, i.e. $\tau = f(\dot{\gamma})$ only,

(10) viscosity does not change appreciably with change in pressure

down the capillary,

and expressing in cylindrical co-ordinates as shown in Fig.3.1, eq.(3.1) reduces to

$$0 = -\frac{\partial P}{\partial z} - \frac{1}{r}\frac{\partial}{\partial r}(r \ \tau_{rz}) \qquad (3.2)$$

Rearranging eq.(3.2) and integrating yields

$$\tau_{rz} = \tfrac{1}{2} r \frac{\partial P}{\partial z} = \tfrac{1}{2} r \frac{\Delta P}{L} \qquad (3.3)$$

At the wall

$$\tau_w = \tfrac{1}{2} R \frac{\Delta P}{L} = \tfrac{1}{4} D \frac{\Delta P}{L} \qquad (3.4)$$

From equations (3.3) and (3.4),

$$\tau_{rz} = (r/R)\, \tau_w \qquad (3.5)$$

In a capillary of radius R, the volumetric flow rate is

$$Q = \int_0^R 2 \pi r v_z(r)\, dr \qquad (3.6)$$

Integration by parts gives

$$\tfrac{1}{2} \frac{Q}{\pi} = \tfrac{1}{2} r^2 v_z \Big|_0^R - \int_0^R (\tfrac{1}{2} r^2)\, dv_z \qquad (3.7)$$

At r=R, $v_z = 0$, the first term on the right-hand side of eq.(3.7) vanishes. Therefore,

$$Q = -\pi \int_0^R r^2\, dv_z = -\pi \int_0^R r^2 (dv_z/dr)\, dr \qquad (3.8)$$

Differentiation of r in eq.(3.5) w.r.t. τ gives

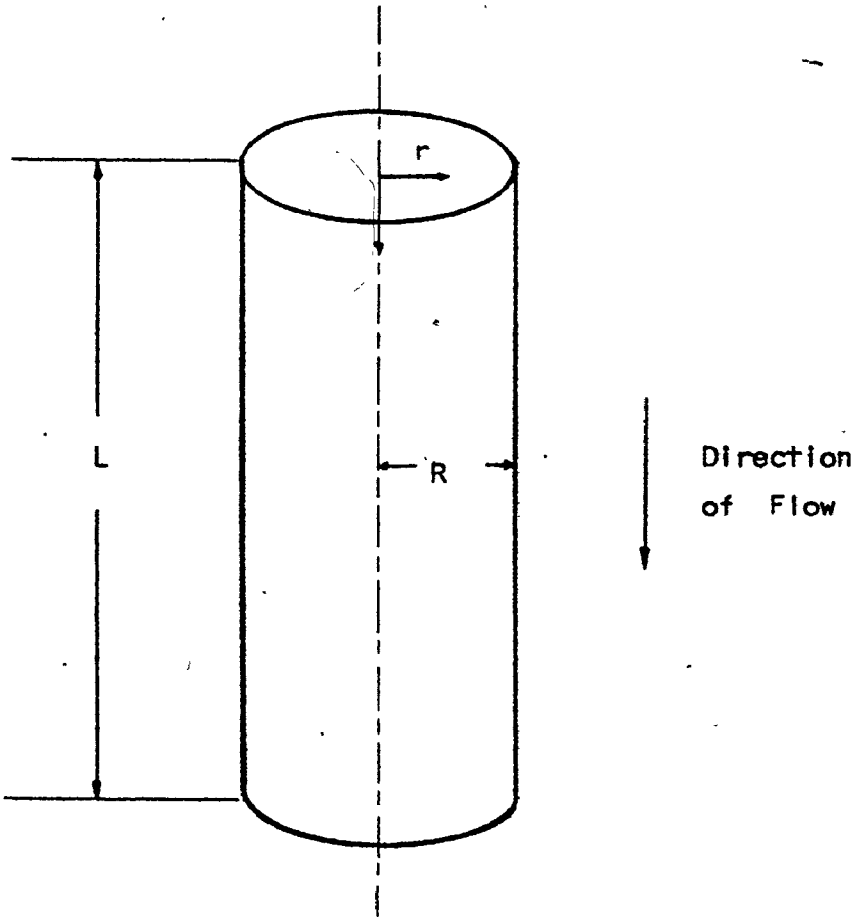

Fig.3.1 Schematic Illustration of Capillary Flow

$$dr = (R/\tau_w)\, d\tau \qquad (3.9)$$

By writing $\dot{\gamma} = (-\frac{dv_z}{dr})$, using eq.(3.5) and combining eqs.(3.8) and (3.9) so that

$$Q = \frac{\pi R^3}{\tau_w^3} \int_0^{\tau_w} \dot{\gamma}\ \tau^2\, d\tau \qquad (3.10)$$

Rearranging eq.(3.10) yields

$$\frac{Q\,\pi^3}{\pi R^3} = \int_0^{\tau_w} \dot{\gamma}\,\tau^2\ d\tau \qquad (3.11)$$

Differentiating eq.(3.11) w.r.t. τ_w and employing Leibnitz's rule gives

$$\left(\tau_w^3 \frac{dQ}{d\tau_w} + 3\tau_w^2\, Q \right) / \pi R^3 = \dot{\gamma}_w \tau_w^2 \qquad (3.12)$$

Dividing eq.(3.12) by τ_w^2 and rearranging in terms of $4Q/\pi R^2$

$$\dot{\gamma}_w = \frac{3}{4}\left(\frac{4Q}{\pi R^3}\right) + \frac{\tau_w}{4} \frac{d(4Q/\pi R^3)}{d\tau_w} \qquad (3.13)$$

The second term on the right-hand side of eq.(3.13) represents Rabinowitch's correction (64) for non-Newtonian fluid flow in a capillary. $4Q/\pi R^3$ is called pseudo-shear rate $\dot{\gamma}_a$ and is the true shear rate at the wall for Newtonian fluids.

3.2 Errors in Capillary Flow

Derivation of equations in the preceding section is based on assumptions which may result in experimental errors. Standard textbooks (3,65-67) are available to discuss in detail the validity of these assumptions, the resulting errors as well as the methods of correcting them. For the major possible errors, only the entrance effect is considered in detail; other effects are described in brief.

3.2.1 Isothermal Flow

Polymer melts are characterized by their high viscosities. Heat generation through the action of viscous heating can cause significant temperature changes across the shear fields. In deriving viscometric equations, isothermal conditions have been assumed and since viscosity is temperature-dependent, this assumption needs to be justified. However, under usual operating conditions in capillary viscometers, the temperature rise due to viscous dissipation is less than 1°C (67). Therefore, the change in viscosity can be neglected.

3.2.2 Laminar Flow

For Newtonian fluids the criterion of transition from laminar to turbulent flow in tubes is given by the critical Reynolds number of 2100 (65). For non-Newtonian fluids fitted to the

power-law model, such as pseudoplastic fluids, the onset of turbulence takes place at slightly higher numbers (68). Because of the highly viscous nature of polymer melts, Reynolds numbers of this order of magnitude can never be attained in polymer melt flows.

3.2.3 Slippage at the Wall

No slip at the capillary wall requires zero velocity there. If a fluid has a finite velocity at the wall, a change in boundary condition should be taken into account in deriving viscometry equations. It has been shown (69) that if slippage occurs, a plot of pseudo-shear rate against reciprocal of radius at fixed shear stress and temperature will give a straight line with a slope equal to four times the slip velocity. A horizontal line indicates no slippage. Polystyrene and polyethylene under usual processing conditions do not exhibit slip at the wall.

3.2.4 Fluid Expansion

Under usual operating conditions in viscometry, the compressibility of polymer melts appears to be negligible (3). Expansion of fluid would lead to a change in its volumetric flow rate whose correction has been discussed by Spencer and Gilmore (70). Pezzin (71) used their method and showed that even under extreme conditions, the correction for fluid expansion is only 3.9%.

3.2.5 Time-Independence

A material is time-dependent if its apparent viscostiy changes when passing through a tube.

If entrance effects (see section 3.2.6) are corrected for and the flow curves for dies of different dimensions still do not superimpose then this could be due to either time-dependence or slip at the wall (section 3.2.3). To distinguish this difference, a series of dies of same radius but of lengths, such that each die is longer than the preceding one by the same amount, could be used and the flow rate for each die determined. No difference in flow rates between successive dies indicates time-independence of the material. If the viscosity decreased with time, progressive increase in capillary length would have less and less effect so that the difference in flow rates between successive dies would decrease. The consequence of the time drift effects leads to difficulty in obtaining a unique and reliable flow curve which would be useful in quantitative applications. However, no known reports of time-dependent effects have been observed with polymer melts (3).

3.2.6 Entrance Effect.

Assumption has been made in deriving eq.(3.4) to calculate shear stress at the wall that flow is fully developed even at the

capillary entrance. As fluid enters the die, a change in velocity profile occurs resulting in a considerable amount of pressure drop there (Fig.3.2). These entrance effects are independent of the length of the capillary and may be considered as increasing the effective length of the die (72). Therefore, the use of long dies can diminish and even make this effect negligible (71). Merz and Colwell (73) indicated that capillary geometry will not affect shear stress data when using dies with an L/D of about 60 for polystyrene, and about 30 for polyethylene at the pseudo-shear rate of 100 1/sec. Because of the highly viscous nature of polymer melts, working with long dies becomes difficult and relatively short dies are generally used. Bagley's end correction (72) is commonly employed to account for the entrance effects.

In his empirical method, an effective capillary length, (L+Nc.D), greater than the actual length of the capillary is assumed. From eq.(3.4), the true shear stress can be calculated from the equation

$$\tau_w = \frac{D}{4} \frac{\Delta P}{L + Nc.D} = \frac{\Delta P}{4(L/D + Nc)} \qquad (3.14)$$

If the fluid is time-independent, then

$$\tau_w = f(\dot{\gamma}_w) \qquad (3.15)$$

Substitution of eq.(3.13) into eq.(3.15) yields

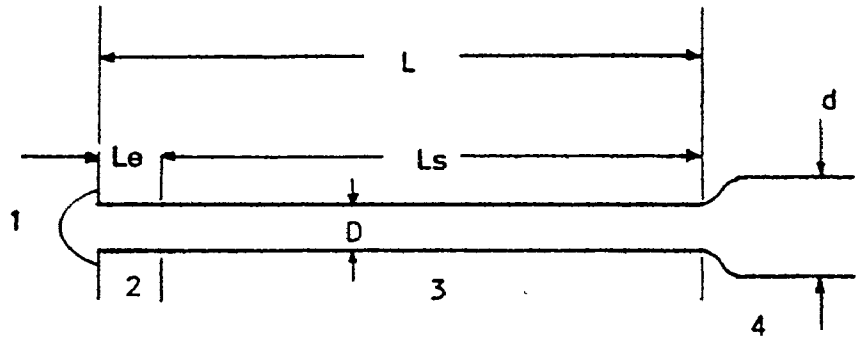

1. Tapered Entrance
2. Entrance Region
3. Region of Steady Flow
4. Exit Region

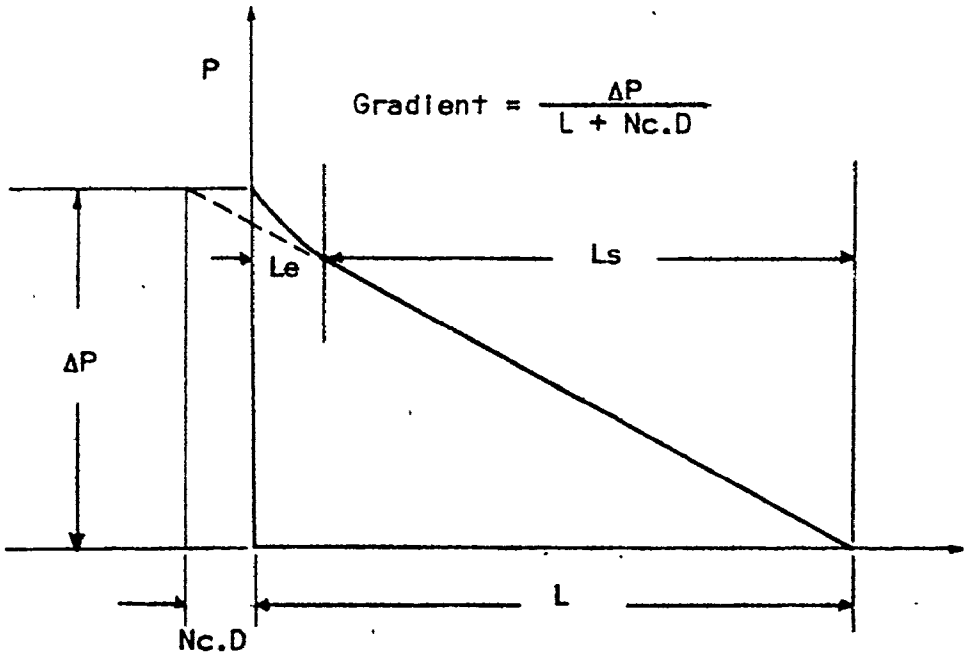

Fig.3.2 Correction of Tube Length by the Addition of Length Nc.D to Account for Entrance Effect

$$f\left\{\frac{3}{4}\left(\frac{4Q}{\pi R^3}\right) + \frac{\tau_w}{4}\frac{d(4Q/\pi R^3)}{d\tau_w}\right\} = \tau_w \qquad (3.16)$$

Alternatively,

$$\tau_w = f(4Q/\pi R^3) = f(\dot{\gamma}_a) \qquad (3.17)$$

where $\dot{\gamma}_a = 4Q/\pi R^3$ is the pseudo-shear rate.

Also from eqs.(3.14) and (3.17), after rearranging,

$$\Delta P = 4(L/D + Nc)\, f(\dot{\gamma}_a) \qquad (3.18)$$

A number of capillaries with constant radius R but different L/D are used and flow curves are obtained by plotting ΔP against $\dot{\gamma}_a$; the former can be read off at arbitrarily chosen values of $\dot{\gamma}_a$ and plotted against L/D. From eq.(3.18) at $\Delta P=0$, $Nc=-L/D$. Therefore the value of Nc can be obtained from the negative intercept of the L/D axis. Also from eq.(3.14), true shear stress at the wall can be estimated.

Shroff et al (74) suggested another method of obtaining τ_w using a die-orifice (L/D=0) and a relatively long capillary (e.g. L/D=19.4), having the same diameter of 0.087 cm. By means of the zero-length die the pressure drop due to entrance effect can be measured directly, and the true shear stress can be evaluated from the following equation:

$$\tau_w = (\Delta P_{L/D} - \Delta Po)/4(L/D) \qquad (3.19)$$

where $L/D' \geq 20.0$.

Notably, the Instron Rheometer whose diameter is 0.953 cm is not suitable for making measurements with orifice dies. The barrel effect (75) becomes quite important when studying resins of high molecular weight or of low melt index. Operating at low shear rates makes accurate measurement almost impossible.

Commercial samples of high- and low-density polyethylene, polystyrene and polypropylene were examined in their experiment (74). The values of ΔP_o were compared with those extrapolated values obtained via the conventional Bagley plot (72). These values were found in good agreement. However, this method is not 100% reliable as discussed by Colbert and Ziegel (76).

3.3 Expressions Predicting Extrudate Swell

In an attempt to relate swelling index (d/D) to recoverable shear strain (σ), several expressions centered on the concept of elastic recovery of the swelling process have been proposed.

The recoverable shear strain is usually defined from Hooke's law which seems to hold for most polymers:

$$\sigma = \tau_{12} J_o \tag{3.20}$$

where τ_{12} is the shear stress and J_o the shear compliance ($J_o = 1/G$, where G is the shear modulus). Coleman and Markovitz (77) relate J_o and τ_{12} to the first and second normal stress τ_{11} and τ_{22} by

$$\tau_{11} - \tau_{22} = 2 J_o \tau_{12}^2 \tag{3.21}$$

Combining eqs.(3.20) and (3.21) yields the "stress ratio"

$$\sigma = (\tau_{11} - \tau_{22})/2\tau_{12} \tag{3.22}$$

Several questions have been raised in the past as to the numerical factor 2, but it is generally included for polymer melts.

Nakajima and Shida (21) used the concept of rubber elasticity and assumed that the polymer in a capillary is in an elongated state in the direction of the capillary axis thereby stored elastic energy in the same sense as the potential

energy of a stretched spring. Upon leaving the capillary, this energy will recover and cause die swell. They estimated the tensile stress for the elastic deformation of the extrudate until its diameter equals to that of the capillary, and arrived at the following equation

$$\frac{\tau_t}{NacT} = \lambda - 1/\lambda^2 \qquad (3.23)$$

where $\lambda=(d/D)^2 = B^2$, τ_t is the tensile stress, Na and c are the number of chains per unit volume and Boltzmann's constant, and T is the absolute temperature. Shear modulus G is defined (78) by

$$G = NacT \qquad (3.24)$$

Analogous to recoverable shear strain, $\tau_t/NacT$ has a meaning of tensile strain. Next, a bold assumption was made that the tensile strain is taken as the quantitative expression for the recoverable strain in the flow:

$$\bar{\sigma} = \tau_t / NacT = B^2 - B^{-4} \qquad (3.25)$$

where $\bar{\sigma}$ is the average recoverable strain and is different from the recoverable strain at the wall σ_w. These quantities will be discussed shortly.

This assumption, in a strict sense, is not true since stored energy is carried out at the capillary exit but not

strain. The free recovery is interpreted in some what analogous manner to creep recovery where a sudden removal of the stress is treated as if a reverse stress were applied to null the previous stress and the new stress were held constant over the period of recovery.

Assuming a parabolic velocity profile, it has been shown (41,56) that

$$\sigma_w = \sqrt{3}\,\bar{\sigma} \qquad (3.26)$$

and in case of a flat velocity profile

$$\sigma_w = \sqrt{2}\,\bar{\sigma} \qquad (3.27)$$

From eqs.(3.25) and (3.26), one obtains

$$\sigma_w = \sqrt{3}\,(B^2 - B^{-4}) \qquad (3.28)$$

for a parabolic velocity profile.

Following Nakajima and Shida's analysis, Bagley and Duffey (79) used a one-constant energy function for a Mooney material (78) and arrived at another equation:

$$\bar{W} = C_1 (I_1 - 3) \qquad (3.29)$$

where C_1 is a constant and I_1 is the first strain invariant defined by

$$I_1 = \lambda_1^2 + \lambda_2^2 + \lambda_3^2 \qquad (3.30)$$

Assuming fluid incompressibility and simple elongation process,

the principal extension ratios are given by

$$\lambda_1 = \lambda$$
$$\lambda_2 = \lambda_3 = \lambda^{-\frac{1}{2}} \tag{3.31}$$

Therefore,

$$\bar{W} = C_1(\lambda^2 + 2/\lambda - 3) \tag{3.32}$$

and the force acting along the axis of capillary is, in case of simple elongation,

$$f_b = dW/d\lambda = 2C_1(\lambda - \lambda^{-2}) \tag{3.33}$$

Thus the tensile stress t_{zz} acting on the cylinder in the final elongated state is

$$t_{zz} = f_b = 2C_1 (\lambda^2 - 1/\lambda) \tag{3.34}$$

Treloar (78) has shown that

$$G = 2C_1 \tag{3.35}$$

Bagley and Duffey (79) assumed that

$$\bar{\sigma}^2 = t_{zz}/G \tag{3.36}$$

and arrived at a new expression relating recoverable shear strain to die swell:

$$\bar{\sigma}^2 = \lambda^2 - 1/\lambda = B^4 - B^{-2} \tag{3.37}$$

They also carried out an energy balance analysis along Graessley's (35) line. Treloar (78) indicated that the strain energy function in shear inside the capillary is

$$\bar{W}_{shear} = G\bar{\sigma}^2/2 \tag{3.38}$$

In the course of elongation, the stored strain energy per unit volume of the material in passing from unstrained to strained case is, from eq.(3.32),

$$\bar{W}_{elongation} = (G/2)(\lambda^2 + 2/\lambda - 3) \qquad (3.39)$$

At the die exit, $\bar{W}_{elongation}$ must equal $\bar{W}_{shear}$ so that

$$\bar{\sigma}^2 = B^4 + 2B^{-2} - 3 \qquad (3.40)$$

In the above equations, the value of $\bar{\sigma}$ is that existing in the tube immediately on exiting and is not the value at the tube or capillary entrance except for zero-length die.

Based on the elastic recovery of a Poiseuille flow of KBKZ fluid (23), another expression has been proposed by Tanner (24). He made the following assumptions:

(1) the flow is incompressible and isothermal,

(2) the die is long,

(3) inertial effects in the flow are negligible,

(4) gravity, other body and surface tension forces are ignored,

(5) the flow at exit may be approximated by a sudden strain which takes the fluid from the viscometric stress inside the tube instantaneously to the zero stress state outside the tube,

(6) as a constitute equation for their material, the KBKZ (23) form is assumed.

On the basis of these assumptions, Tanner obtained the following equation:

$$\sigma_w^2 = 2(B^6 - 1) \qquad (3.41)$$

Since it is well-known (19,20,25) that the swelling index approaches a value of about 1.10 for slow Newtonian flow, he suggested a modification of the above equation so that

$$\sigma_w^2 = 2[(B - 0.1)^6 - 1] \qquad (3.42)$$

Vlachopoulos et al (41) made an evaluation of the above expressions predicting die swell. Following the energy balance analysis of Graessley (35) and assuming a parabolic velocity profile inside the capillary and that polymer melts behaves as power law fluids, they obtained an expression relating the average recoverable strain $\bar{\sigma}$ to the recoverable strain at the wall σ_w :

$$\sigma_w = \sqrt{3}\,\bar{\sigma} \qquad (3.43)$$

Since the evaluation of these expressions requires the independent determination of the recoverable strain which is half the ratio of the first normal stress difference over the shear stress. While the latter stress can be obtained from viscometry, the first normal stress difference is difficult to measure accurately (80) . Graessley et al (35) used Weissenberg rheogoniometer to measure the normal stresses of polystyrene samples

and their blends. They concluded that those expressions based on the concept of rubber elasticity introduce an elastic shear modulus which is not easily defined; in this sense, therefore, Tanner's elastic recovery theory on die swell has advantages over other expressions.

Rokudai (34) made an evaluation of die swell theories in terms of a non-linear constitutive equation. Polystyrene samples were examined and he found that the theory of Graessley et al (35) failed to agree with the experimental results. However, Tanner's elastic recovery theory (24) well predicted the experimental results at low and medium shear rates.

Mori and Funatsu (42) employed the elastic theory of large deformations by Rivlin (81) and suggested that

$$\sigma = (\tau_{11} - \tau_{22})/\tau_{12} \qquad (3.44)$$

without the numerical factor of 2 (c.f. eq.3.22). In addition, they assume that the mechanism of die swell can be characterized as follows:

(1) the polymer element flowing in a capillary tube induces a recoverable shear strain in the material,

(2) the recoverable shear strain is a function of the initial condition of the strain at the starting point of the

fully developed flow region and the residence time between the starting point and the die exit,

(3) the recoverable elongation is produced by the recoverable shear strain,

(4) upon leaving the die, the polymer element responds in a manner similar to a viscoelastic solid which has been stretched and released,

(5) the extrudate swells gradually to reach a final state, at a rate controlled by its relaxation time.

On the basis of these characterizations, they arrived at a new expression relating the recoverable shear strain at the wall σ_w to die swell B, i.e.

$$\sigma_w = \{ B^2 \left[1 + \frac{\partial(\ln B)}{\partial(\ln \tau_w)} \right]^2 - 1 \}^{\frac{1}{2}} \qquad (3.45)$$

Based on the unconstrained recovery theory from Poiseuille flow as suggested by Tanner (24) and assumed that the shear modulus is constant, Huang and White (45) derived another equation for long capillary dies:

$$B = 0.1 + \{ 1 + \frac{1}{4a} (\frac{N_{1w}}{\tau_w})^2 \}^{1/6} \qquad (3.46)$$

where $N_1 = \tau_{11} - \tau_{22}$ = first normal stress difference, subscript "w" refers to the wall and "a" is defined by the empirical power law relation (82)

$$N_1 = A(\tau_w)^a \qquad (3.47)$$

The values of A and a are available (82) for commercial polystyrene with narrow or moderate molecular weight distribution. The numerical factor 0.1 is to account for swell in Newtonian fluids.

Recently, Huang and White (46) derived new equations which predict die swell for short slit and capillary dies. They suggested that the extrudate swell from short dies should be determined from the character of the entrance flow because this is the only known flow history of the polymer melt. They employed a dimensionless analysis and related the swelling ratio as a function of the entrance angle θ, non-dimensional ratios of viscoelastic constitutive parameters, and the Weissenberg number We defined by

$$We = t_{ch}\ Vch/Lch \qquad (3.48)$$

where t_{ch}, Vch and Lch are the characteristic time, velocity and length respectively. Also from their previous studies on long capillaries (45), We takes the form of

$$We = t_{ch}\frac{Vch}{Lch} = \bar{\tau}\,\dot{\gamma}_w = \frac{N_{1w}}{2\tau_w\dot{\gamma}_w}\dot{\gamma}_w = \frac{N_{1w}}{2\tau_w} \qquad (3.49)$$

where N_{1w}, τ_w and $\dot{\gamma}_w$ are previously described.

For die swell from short capillaries the ratio Vch /Lch is

given by the elongation rate $\partial v_z/\partial z$ defined by

$$\frac{Vch}{Lch} = \dot{\gamma}_{Ez} = \frac{\partial v_z}{\partial z} = \frac{d\,(Q/Ao)}{dz} = -\frac{Q}{Ao}\,\frac{dAo}{dz} \qquad (3.50)$$

with $A_o = (r_o \tan\frac{\theta}{2})$ where $r_o = \frac{D}{2\tan(\frac{1}{2}\theta)}$ (Fig.3.3) is a radius vector pointed backward into the die entry region so that the elongation rate is given by

$$\dot{\gamma}_{Ez} = \frac{Vch}{Lch} = \frac{16Q}{\pi D^3}\tan(\tfrac{1}{2}\theta) \qquad (3.51)$$

and Q is the volumetric flow rate.

By considering the dependence of $\bar{\tau}$ (eq.3.49) on the second invariant of the rate of deformation tensor, they obtained the following:

$$\dot{\gamma}_w = \sqrt{3}\,\dot{\gamma}_{Ez} \qquad \text{for capillary} \qquad (3.52)$$

From the previous knowledge of entrance flow for low-density polyethylene and polystyrene (61,63), Huang and White (46) assumed that the shear flow contribution is small compared to elongational flow and that polymer melt behaves as a Maxwellian fluid (3). Their expression, after a minor correction, should read

$$B = \left\{\frac{1 + 0.5\,\bar{\tau}\,\dot{\gamma}_{Ez}}{1 - \bar{\tau}\,\dot{\gamma}_{Ez}}\right\}^{1/6} \qquad (3.53)$$

The existence of vortex-like flows (Fig.3.4) in the die

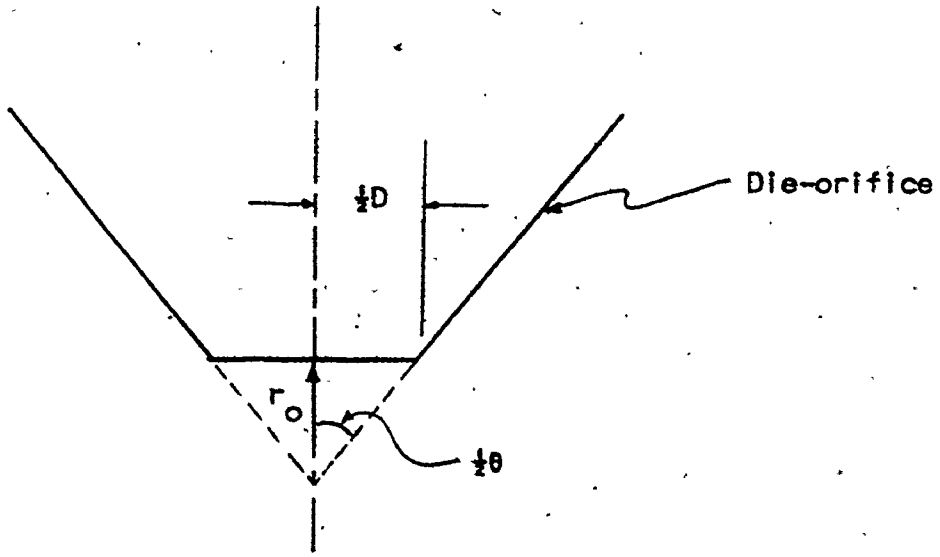

Fig.3.3 Position of the Radius Vector r_o

corners have been observed for low-density polyethylene and polystyrene (63) and their melts exhibit significant vortices (46). The latter authors suggested the θ in eq.(3.52) should be replaced by the natural flow angle α (Fig.3.4), which has been correlated with the experimental data obtained from the Weissenberg rheogoniometer and the Instron capillary rheometer for low-density polyethylene and polystyrene (63).

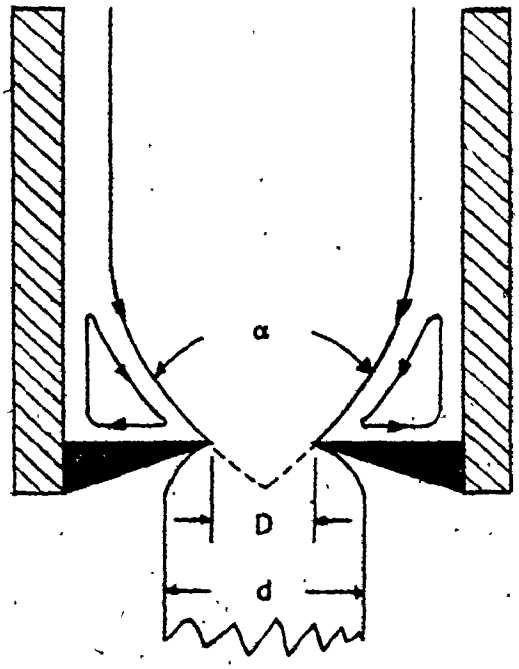

Fig.3.4 Elongational Flow Characteristic of Die Entrance Region

CHAPTER 4

EXPERIMENTAL PROCEDURE

4.1 Equipment

4.1.1 Rheometer

Fig.4.1 shows the essential features of the Instron Model 3211 capillary rheometer in which rheological measurements were carried out. Basically the rheometer consists of an extrusion barrel assembly, a temperature control and distribution system, a push-button operated drive system, and an electronic force measuring and readout system.

The extrusion barrel assembly consists of a cylindrical reservoir made of hardened steel, 0.953 cm in diameter, enclosed in an aluminium jacket to which four cylindrical heating elements are clamped. A die is inserted into the bottom of the reservoir and is held by a simple clamping nut.

Heating of the extrusion barrel assembly is provided by the temperature control and distribution system to any temperature ranging from 40°C to 399°C. The thermal controller can maintain the desired temperature within ±1°C and the distribution system is accurate enough to keep the temperature difference between the top and bottom of the reservoir (includ-

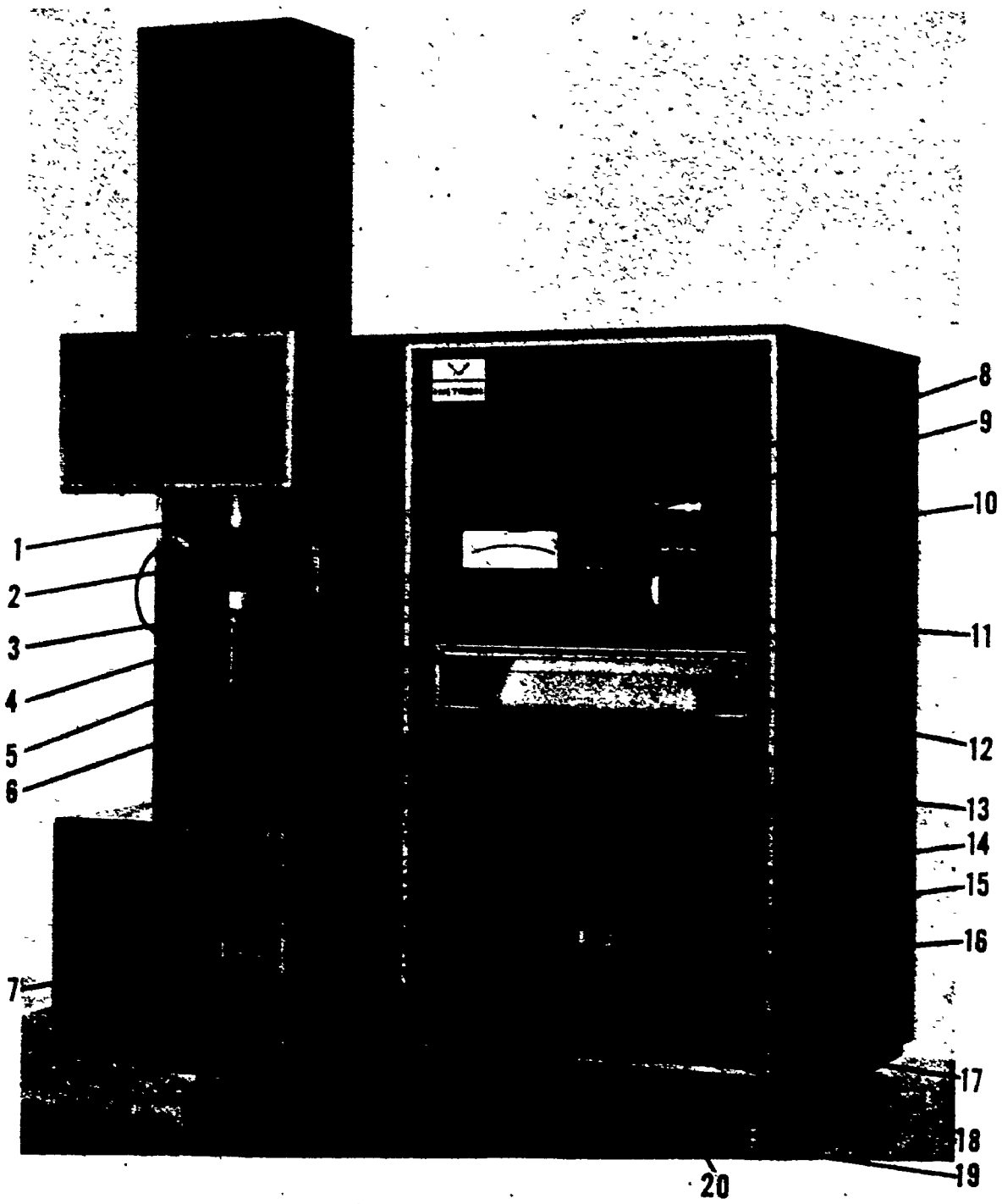

Fig.4.1 Instron Model 3211 Capillary Rheometer

Table 4.1

Essential Components of The Instron
Model 3211 Rheometer

1. Drive Leadscrew
2. Load Cell
3. Plunger Retractor Slide
4. Reference Scale
5. Lower Limit Switch Positioning Thumbwheel
6. Plunger
7. Barrel Access Door
8. Load Meter
9. Preheat Power Switch
10. Temperature Controller
11. Controller Power Switch
12. Optional Strip Chart Recorder
13. Load Cell Amplifier
14. Plunger Direction Pushbuttons
15. Plunger Speed Selector Pushbuttons
16. Limit Function Switch
17. Drive Motor Power Switch
18. Main Power Switch
19. Leveling Foot
20. Gearbox Access Door

ing the extrusion diel to within ±2°C.

The drive system consists of a synchronous motor and a gearbox so that the plunger can be driven at various constant speeds by changing gears. A set of electromagnetic clutches permits instantaneous push-button selection of six plunger speeds over a 333:1 range with a given set of gears. The force on the plunger is transmitted by a compression load cell to a recording system - a readout meter or a strip chart recorder. More accurate measurements can be made by means of the chart recorder which gives reading of 50-lb to 5000-lb at full scale.

Both the force and speed readings can be converted into pressure drops and pseudo-shear rate by means of conversion constants provided in the rheometer operating manual.

4.1.2 Optional Heating Bath Used to Measure True Extrudate Swell

The simple device was used in conjunction with the Instron Model 3211 rheometer. It consists of a beaker with a thermometer and a magnetic stirrer. Heating is provided by a hot-plate type electric heater with a magnetic stirring mechanism. Polymer melts are extruded isothermally into the thermostated liquid, carefully selected for each polymer, or annealed. The liquid must be thermally stable, of proper density and thermo-

dynamic and interfacial properties. Table 4.2 shows the specifications of the liquids selected for polystyrene and low-density polyethylene samples.

Actually this experimental set-up is not accurate enough to measure true die swell; a more sophisticated reliable device has been suggested (48). The attempt was made simply to get an idea of how much the die swell measurements differ using various methods.

4.1.3 Extrusion Dies

Only capillary dies were used in this study and most of them were made of brass. Each of the short and relatively long dies has an entrance angle, θ, of 90.0 degrees with the L/D ratios ranging from 3 to 25. Die-orifice of different entrance angles were also used; specifications of the dies are shown in Table 4.3.

A capillary was formed by drilling a circular hole of a certain diameter through a cylinder of brass/stainless steel, 0.950 cm in diameter. The entrance angle of the die was made by means of a special type of driller in such a way that the length of the capillary meets specification (see also Fig. 1.2).

Table 4.2

Thermostating Liquids Used in Extrudate Swell Experiment

Polymer	Liquid	No.*	TB, ^{o}C	Viscosity at 25^{o}C (Pa.s)	Density at 25^{o}C (kgm^{-3})	Flash Point ^{o}C
LDPE	silcone fluid	200	155	0.0046	920	135
PS	silcone fluid, 78 wt% + 22% di-(n-octyl) phthalate	200	150	0.1942	971	315

* Dow Corning Silicone Fluids

Table 4.3

Dimensions of Capillaries Used

(Set A)

D = 0.133 cm θ = 90°

Length L (cm)	L / D
3.302	24.76
2.667	20.00
2.131	15.98
1.318	9.89
1.062	7.96
0.714	5.35
0.384	2.99
0.0	0.0

(Set B)

D = 0.099 cm θ = 90°

Length L (cm)	L / D
1.240	12.51
0.792	8.0
0.546	5.51
0.297	3.0
0.0	0.0

(Set C)

D = 0.066 cm θ = 90°

Length L (cm)	L / D
0.826	12.50
0.528	8.0
0.361	5.50
0.198	3.00
0.0	0.0

(Set D)

D = 0.118 cm L / D = 0.0

θ (degrees) : 180.0 , 150.0 , 120.0 , 60.0

4.2 Materials

Commercial samples of polystyrene and low-density polyethylene were used in the experiment in the temperature range of 160°C-220°C. Polyethylene samples were supplied by Union Carbide in the form of white pellets and the Dow Chemicals polystyrene is transparent crystals. Polymer characteristics of these samples are summarized in Table 4.4.

Table 4.4

Characteristics of Polymers Investigated

Type	Trade Name	Supplier	(a) $\bar{M}w \times 10^{-5}$	(a) $\bar{M}w/\bar{M}n$	(b) $\frac{\bar{M}z\bar{M}z+1}{\bar{M}w}$	M.I. g/10min	Density kgm^{-3}
PS	667	Dow Chemical	2.03	2.14	4.87	8.0	1040
LDPE	DHDY-6873	Union Carbide	-	-	-	2.5	930
LDPE	DFDY-6600	Union Carbide	-	-	-	0.3	920
LDPE	DFDQ-4400	Union Carbide	-	-	-	2.0	919

(a) from GPC measurement

(b) the "most probable" distribution is assumed

4.3 Operation of Equipment

The barrel of the rheometer is first preheated to test temperature, a die is then placed in position. The polymer to be studied is loaded into the reservoir in small amounts to minimize air entrapment (Figs.4.2 a and b). When working with relatively long dies (L/D>10), loading of polymer up to 3/4 of the reservoir volume is recommended by the manufacturer. However, for smaller L/D ratio capillaries or die-orifice, the loading should perhaps not exceed 1/5 of the volume of the reservoir so that the relatively small barrel effect can be neglected.

With the plunger in position the electronic circuits are calibrated and balanced. The plunger is then allowed to run carefully through the reservoir until it is 3-4 inches inside the reservoir. Both the sample and the plunger are allowed to heat up for about 30 minutes.

At selected speeds the plunger is run through the reservoir. When the force on the plunger becomes steady, the air-bubble free extrudate sample can be cut and collected. Before each reloading, the reservoir must be cleaned thoroughly using cotton.

Figure 4.2a : Extrudate Samples for LDPE at Pseudo-Shear Rate of:From top- 390, 260, 185 & 130 1/sec
Bottom: Air Entrapment.

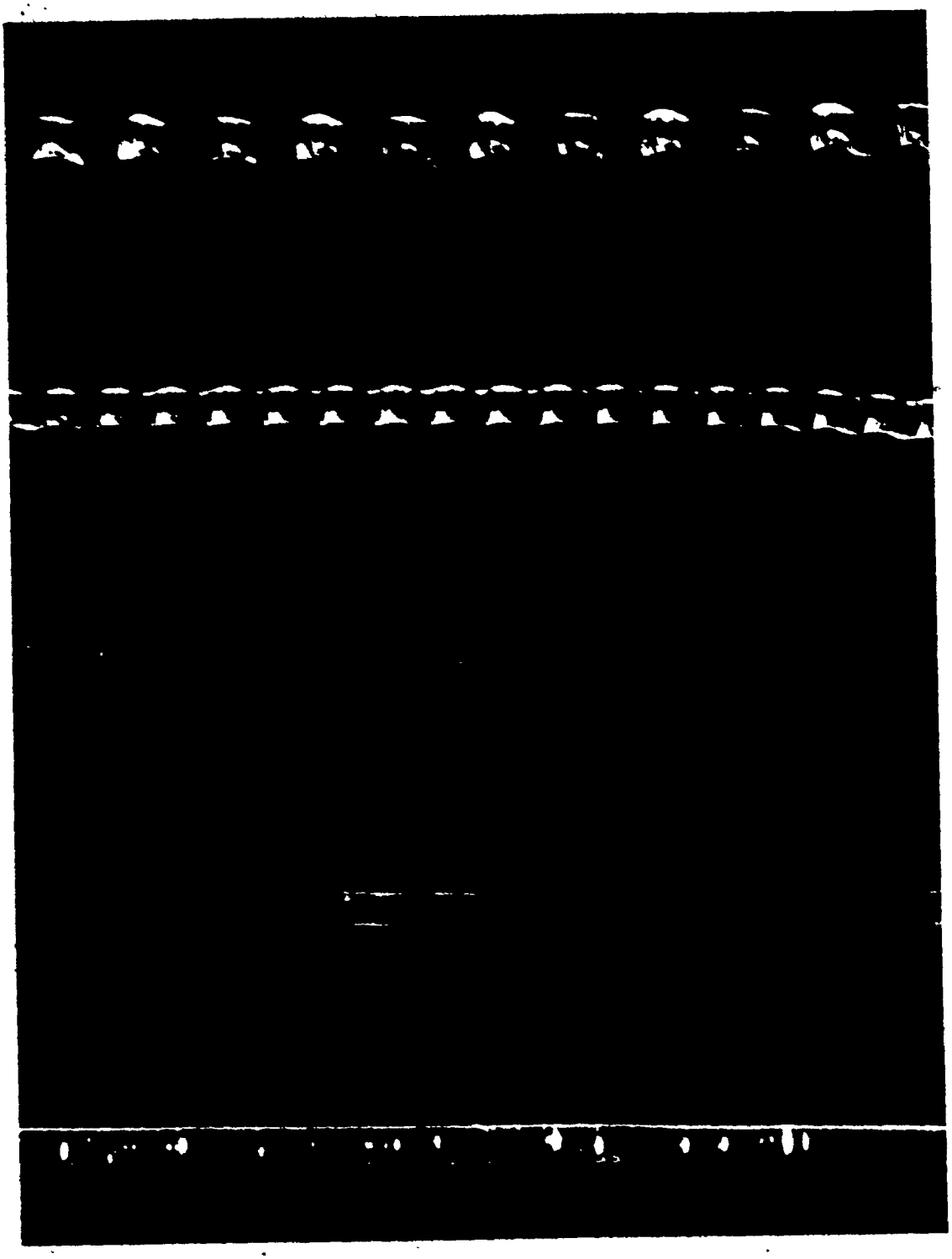

Figure 4.2b : Extrudate Samples for PS at Pseudo-Shear Rate of-From top: 390, 260, 185 & 130 1/sec
Bottom: Air Entrapment

4.4 Measurement of Extrudate Swell

As fresh extrudate emerges to air, it remains soft for some time and therefore its increasing weight causes elongation and decreases the diameter. To obtain a specimen for measurement, the extruding molten filament is cut short at the capillary. When the extrudate is about 5 cm in length, it was clamped, cut, collected and allowed to cool in ambient termpeature. Using a micrometer, all diameter measurements are made four times for each sample at about 1/4 inch from the lower end where elongation is negligible. The extrudate diameter is corrected to the extrusion temperature using eq.(2.8).

On the other hand, the polymer melt can be extruded isothermally into a bath of hot liquid described previously, left suspended for about 15 minutes, removed from the bath and allowed to cool in room temperature. The specimen is wiped to dryness before any diameter measurement is taken (see also section 2.2.3).

4.5 Construction of Flow Curves

In the experiment the plunger speed Vp and the force Fp on the plunger were measured directly. The pseudo-shear rate at the wall $\dot{\gamma}_a$ is calculated from the volumetric flow rate Q which is in turn estimated from the plunger speed ($Q=\pi Dp^2 Vp/4$, where Dp=diameter of the plunger). The apparent pressure drop ΔP through the capillary is obtained from $\Delta P=Fp/\pi(Dp/2)^2$. By means of these two variables shear stress and shear rate at the wall are obtained as follows:

1. Pseudo-shear rate $\dot{\gamma}_a$ is calculated from $\dot{\gamma}_a=4Q/\pi R^3$.
2. Values of $\dot{\gamma}_a$ and the corresponding values of ΔP are plotted for each capillary (Fig.4.3).
3. At arbitrarily chosen values of $\dot{\gamma}_a$, corresponding pressures are obtained and cross-plotted against the L/D ratios (Fig.4.4).
4. The intercepts on the abscissa give Bagley's end corrections which are used to estimate the true shear stress τ_w via eq.(3.14).
5. From the plot of τ_w versus $\dot{\gamma}_a$ (Fig.4.5), it is possible to obtain the slope of the curve at a given value of τ_w, and the true shear rate $\dot{\gamma}_w$ can be calculated from eq. (3.13).

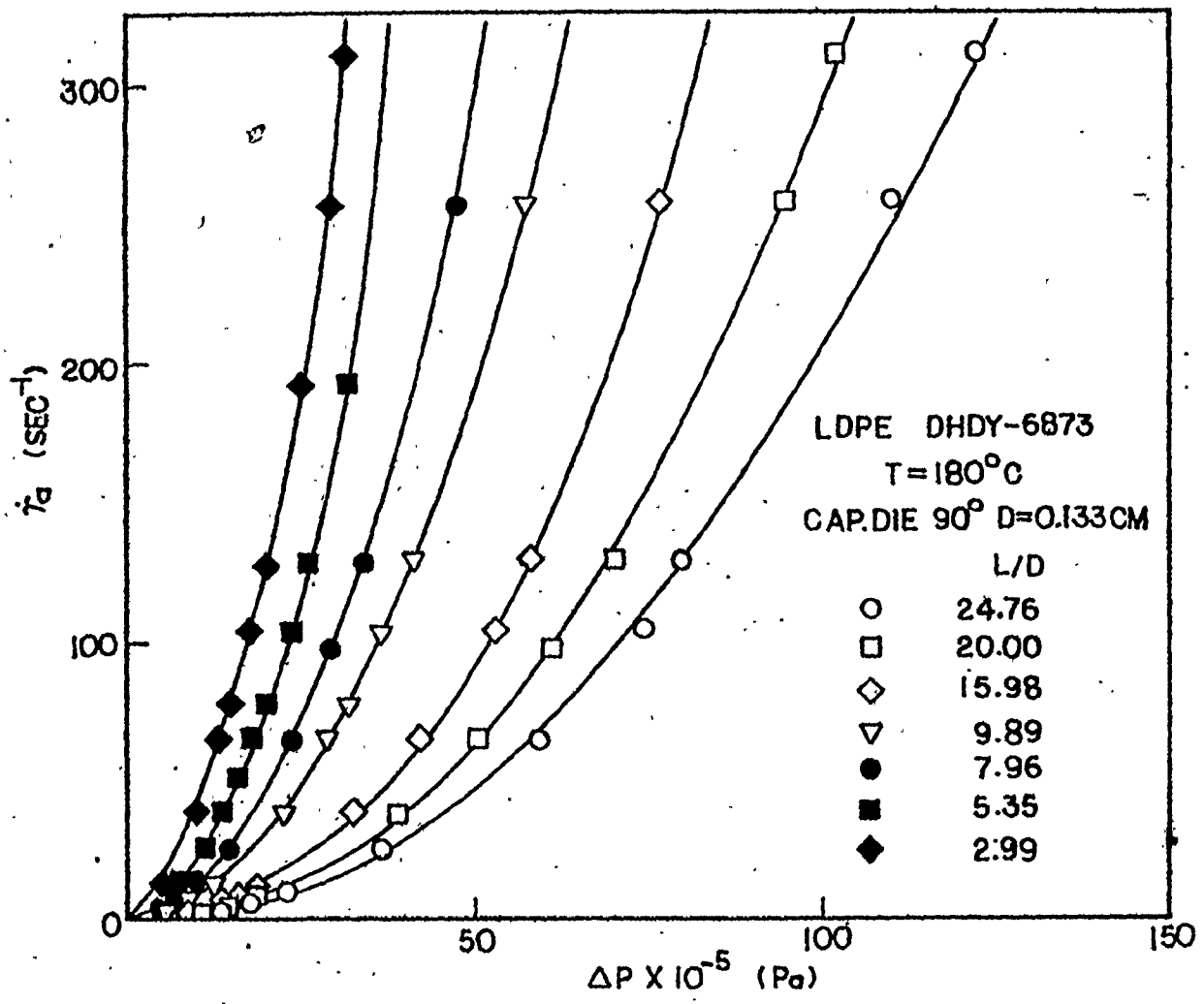

Fig.4.3 Plot of Pseudo-Shear Rate vs. Pressure Drop

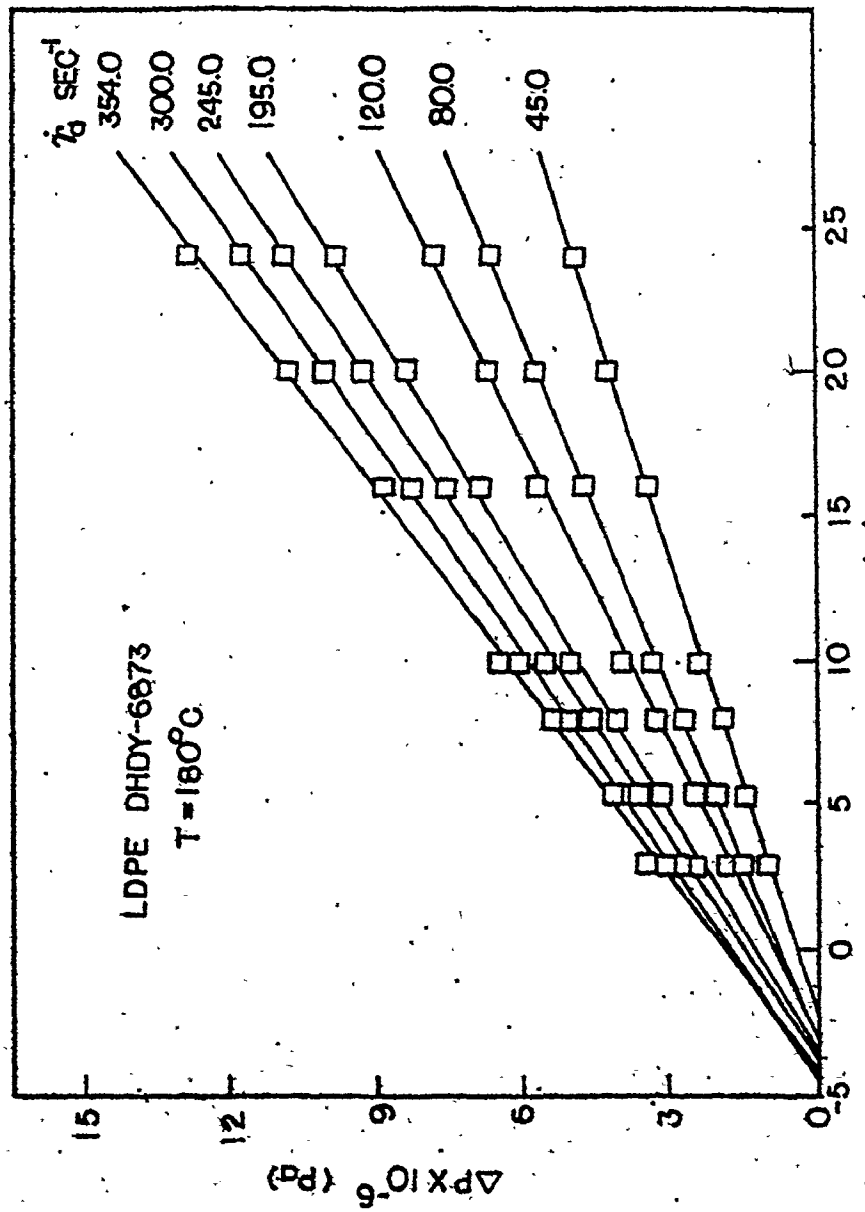

Fig.4.4 Plot of Pressure Drop vs. L/D of Capillaries

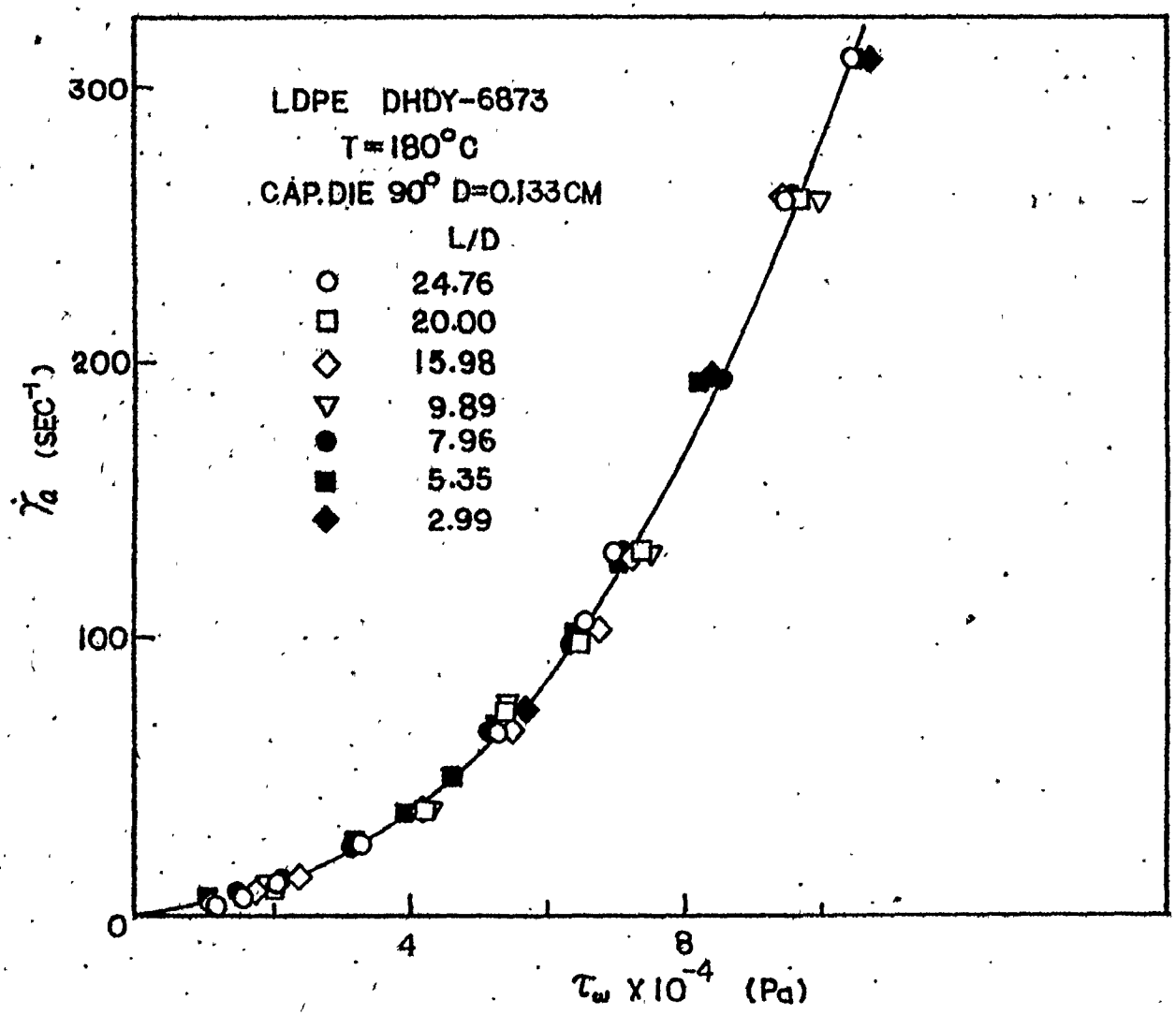

Fig.4.5 Plot of Pseudo-Shear vs. True Shear Stress

The plot of $\dot{\gamma}_w$ versus τ_w is called the flow curve and is shown in Fig.4.6. Values of ΔP, $\dot{\gamma}_a$, τ_w , $\dot{\gamma}_w$ and swelling ratio for all polymers studied are given in Appendix.

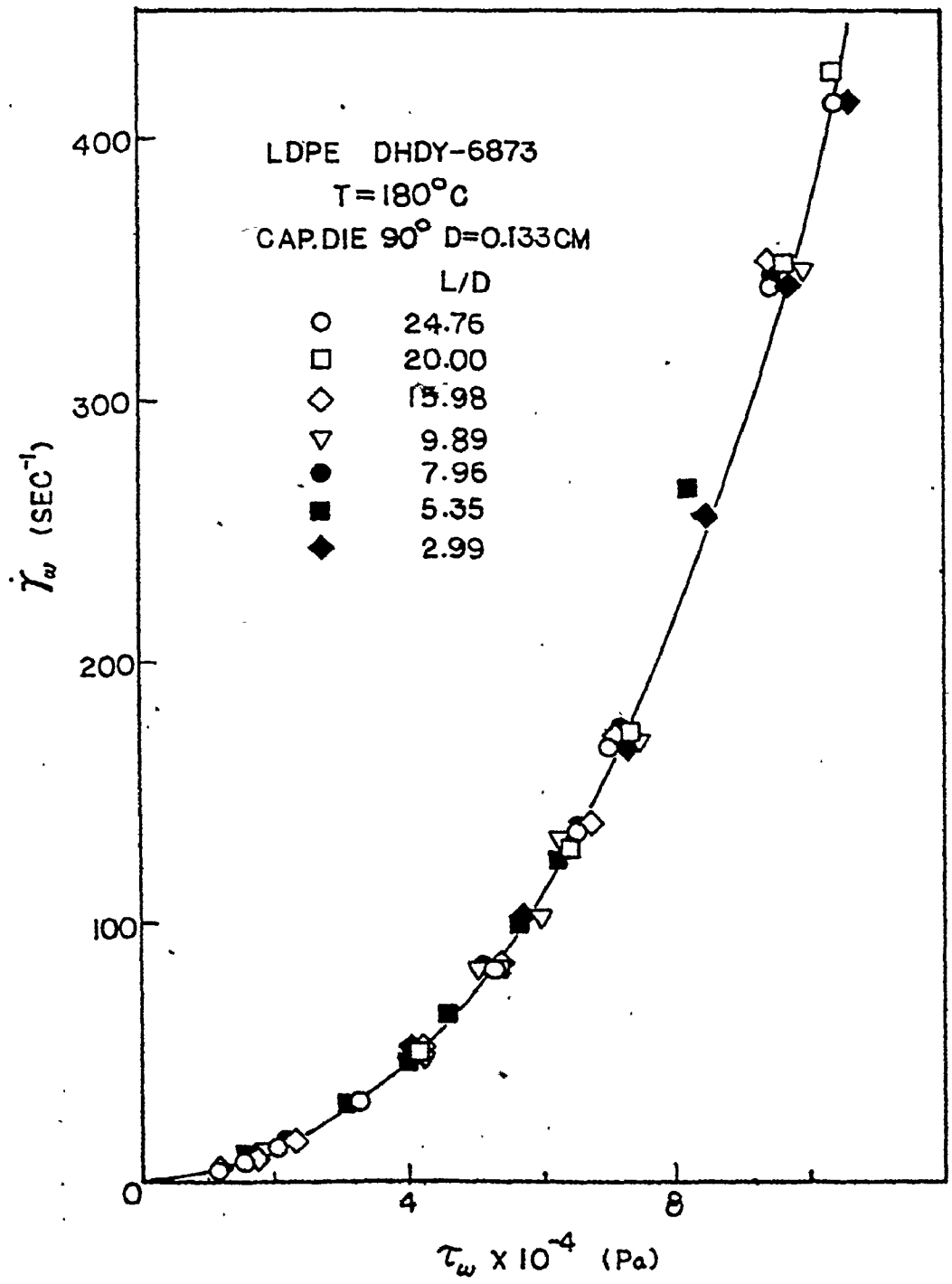

Fig.4.6 Plot of True Shear Rate vs. True Shear Stress

CHAPTER 5

RESULTS AND DISCUSSIONS

5.1 Reproducibility

The measurement of extrudate diameter was repeated four times to check the reproducibility of these values. Readings on forces were obtained within 2% for all dies while the diameter of the extrudate was found reproducible within 1%. All measurements were taken in a standard way as described in the preceding section. It was observed that the draw down effect by weight did not affect the measurement of the extrudate diameter. While the absolute diameters of the extrudate might be doubtful because of "frozen-in" mechanism, the standard way of measurement made the comparison between these values of different capillaries sensible.

5.2 Power Law Approximation

The power law implies that the logarithmic plot of true shear stress τ_w versus true shear rate $\dot{\gamma}_w$ (or $\dot{\gamma}_w$ vs. τ_w) should be a straight line. Previous study on low-density polyethylenes and polystyrenes (60) showed that these polymer melts behave as power law fluids over about one decade in shear rate, but when extended over several decades, the plot is not usually straight (67,83) as indicated in Figs.5.1 and 5.2 for low-density polyethylene and polystyrene. Accordingly, the power law takes the form of

$$\tau_w = K (\dot{\gamma}_w)^n \qquad (5.1a)$$

where K is the consistency index and n is the flow index.

Alternative representation of the power law is

$$\dot{\gamma}_w = E (\tau_w)^m \qquad (5.1b)$$

where $E=(\frac{1}{K})$ and $m=1/n$.

Both indices are temperature-dependent. The value of K depends on the arbitrarily chosen standard state of $\dot{\gamma}_w$ or τ_w ; but $\dot{\gamma}_w$ is usually taken as 1 1/sec or τ_w as 1 Nm^{-2} . The values of K and n for low-density polyethylene and polystyrene at different temperatures and shear rate range are shown in Table 5.1.

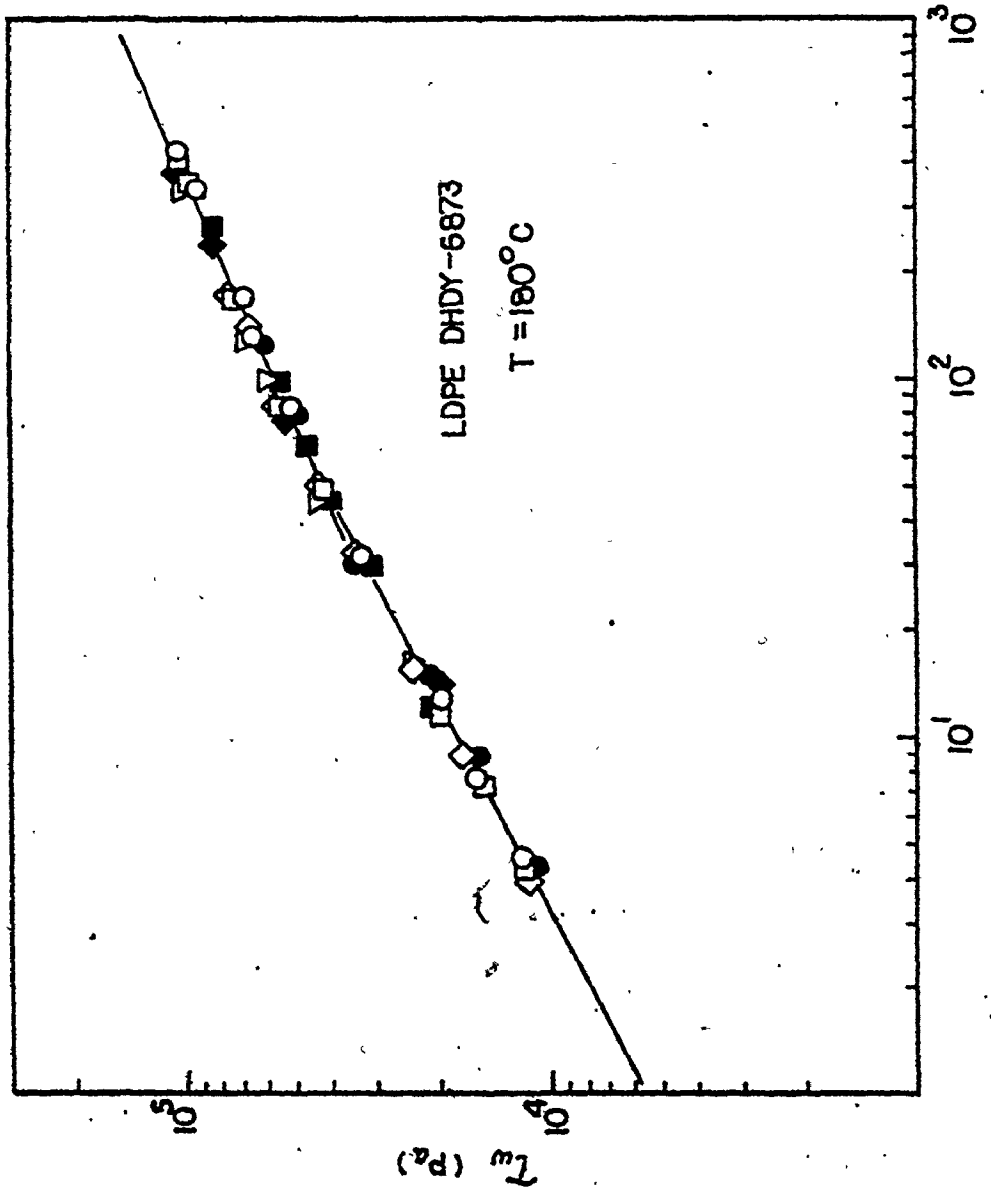

Fig.5.1 Log-log Plot of True Shear Stress vs. True Shear Rate for Low-density Polyethylene

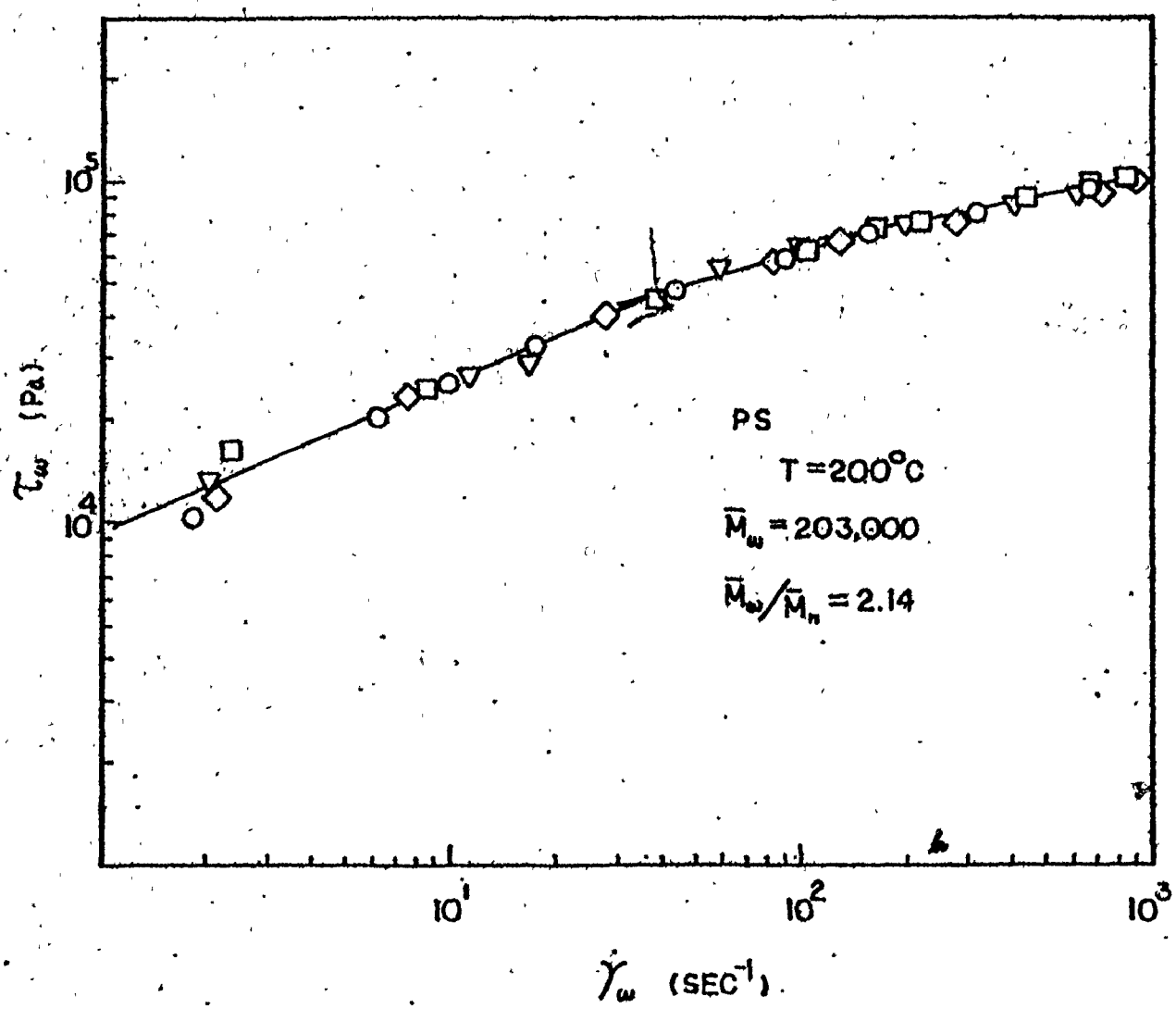

Fig.5.2 Log-log Plot of True Shear Stress vs. True Shear Rate for Polystyrene

Table 5.1

Temperature Dependence of K and n

(a) LDPE DHDY-6873

Temp. °C	$\dot{\gamma}_w$ (1/s) 1	$\dot{\gamma}_w$ (1/s) 4 - 50	$\dot{\gamma}_w$ (1/s) 1	$\dot{\gamma}_w$ (1/s) 50 - 500
	K	n	K	n
160	7.0×10^3	0.51	9.8×10^3	0.42
180	5.5×10^3	0.52	7.8×10^3	0.43
200	4.4×10^3	0.53	6.0×10^3	0.44

(b) PS

Temp °C	$\dot{\gamma}_w$ (1/s) 1	$\dot{\gamma}_w$ (1/s) 2 - 40	$\dot{\gamma}_w$ (1/s) 1	$\dot{\gamma}_w$ (1/s) 40 -200	$\dot{\gamma}_w$ (1/s) 1	$\dot{\gamma}_w$ (1/s) 200 - 2500
	K	n	K	n	K	n
180	1.8×10^4	0.36	2.6×10^4	0.26	-	-
200	9.5×10^3	0.43	1.55×10^4	0.29	2.5×10^4	0.2
220	4.3×10^3	0.48	9.2×10^3	0.31	1.25×10^4	0.27

By definition (3), the apparent viscosity η_a for polymer melt is

$$\eta_a = \frac{\tau_w}{\dot{\gamma}_w} \qquad (5.2)$$

Also, it has been suggested (83) that the temperature dependence of η_a can be expressed through an equation of the form of the Arrhenius equation:

$$\eta_a = b_1 \exp(b_2/T) \qquad (5.3)$$

where b_1 and b_2 are constants, T is the absolute temperature. Substitution of eq.(5.2) into eq.(5.3) gives

$$\tau_w/\dot{\gamma}_w = b_1 \exp(b_2/T) \qquad (5.4)$$

At $\dot{\gamma}_w = 1$ 1/sec,

$$\tau_w = K = b_1 \exp(b_2/T) \qquad (5.5)$$

Thus,

$$\ln K = b_1 + b_2/T \qquad (5.6)$$

As shown in Figs.5.3 and 5.4, the plots of lnK against 1/T appear to be straight lines at different range of shear rates.

Again from eqs.(5.1a) and (5.2), one has

$$\eta_a(\dot{\gamma}_w) = K(\dot{\gamma}_w)^{n-1} \qquad (5.7)$$

which is another representation of the power law model. It is obvious from Figs.5.1 and 5.2 that the flow index is not constant over a wide range of shear rates; it decreases with increasing shear rate and is less than unity - a characteristic of pseudoplastic fluids.

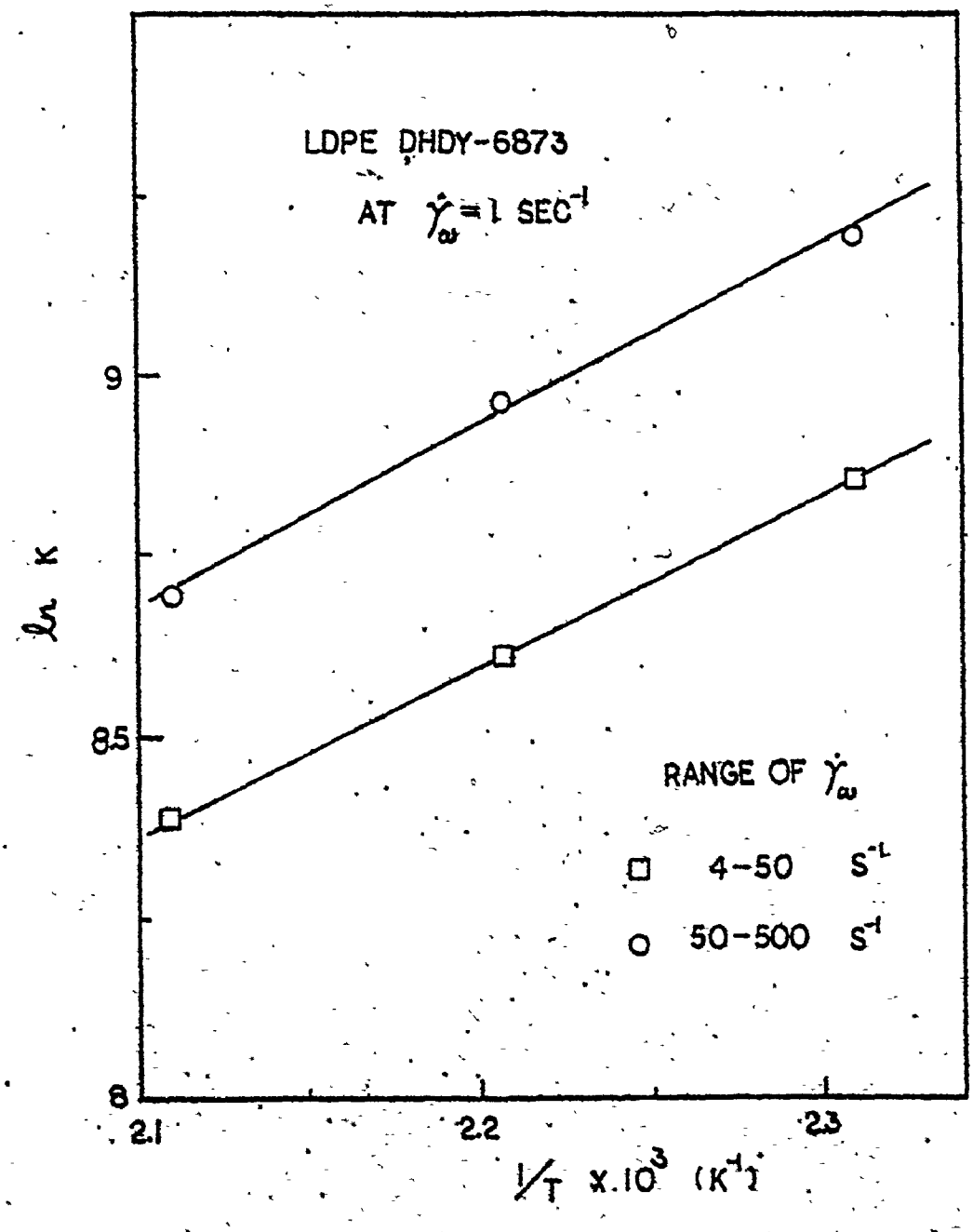

Fig. 3.3 Plot of Log of Consistency Index vs. Reciprocal of Absolute Temperature for Low-density Polyethylene

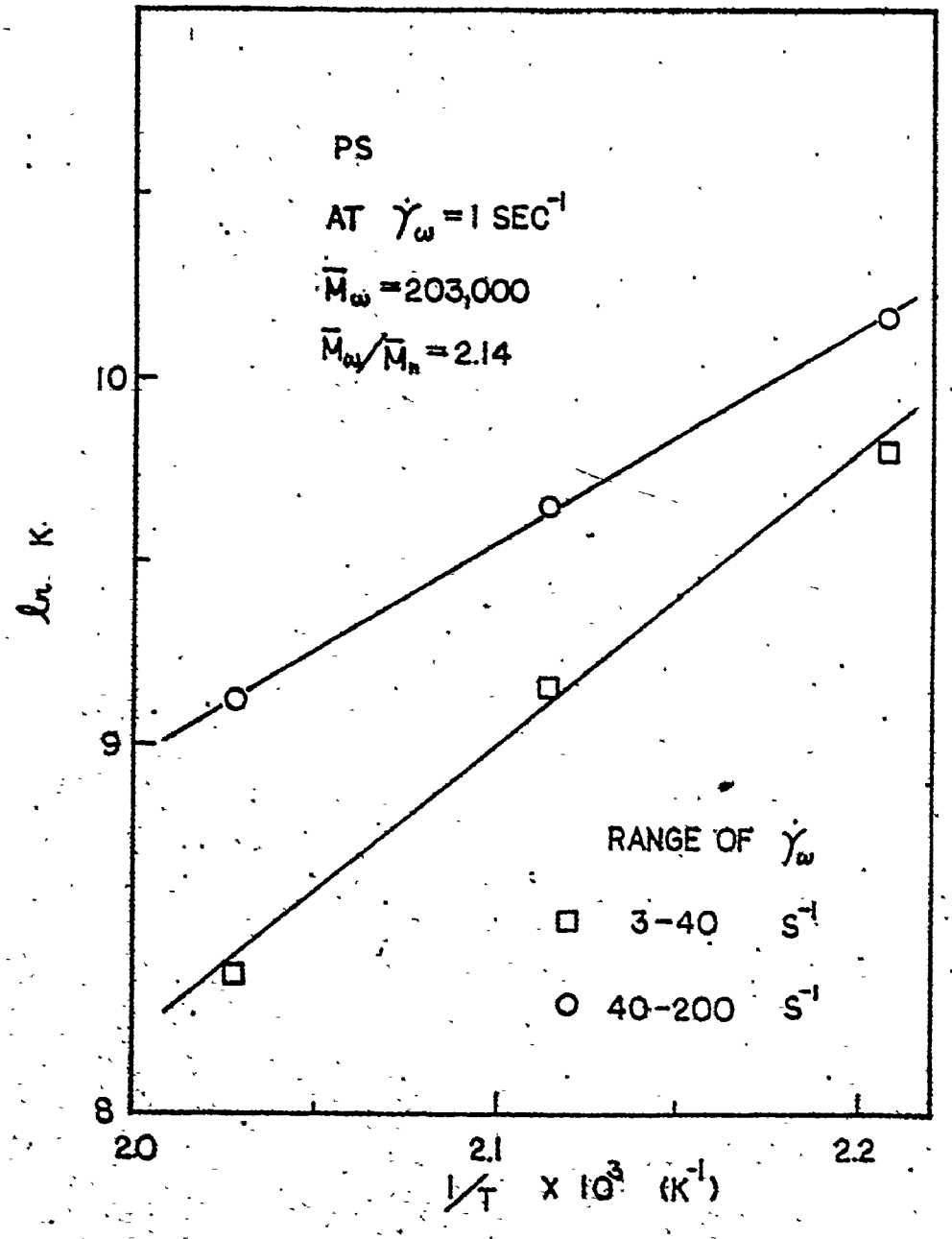

Fig.5.4 Plot of Log of Consistency Index vs. Reciprocal of Absolute Temperature for Polystyrene

As the shear rate decreases further to an order of about 0.1 1/sec which cannnot be achieved by the Instron capillary rheometer, the fluid is said to reach Newtonian region (84) and the flow index approaches unity; the viscosity is no longer dependent on shear rates - a characteristic of Newtonian fluids. (c.f. Figs.5.5 and 5.6). The consistency index becomes identical to the dynamic viscosity of the Newtonian fluid.

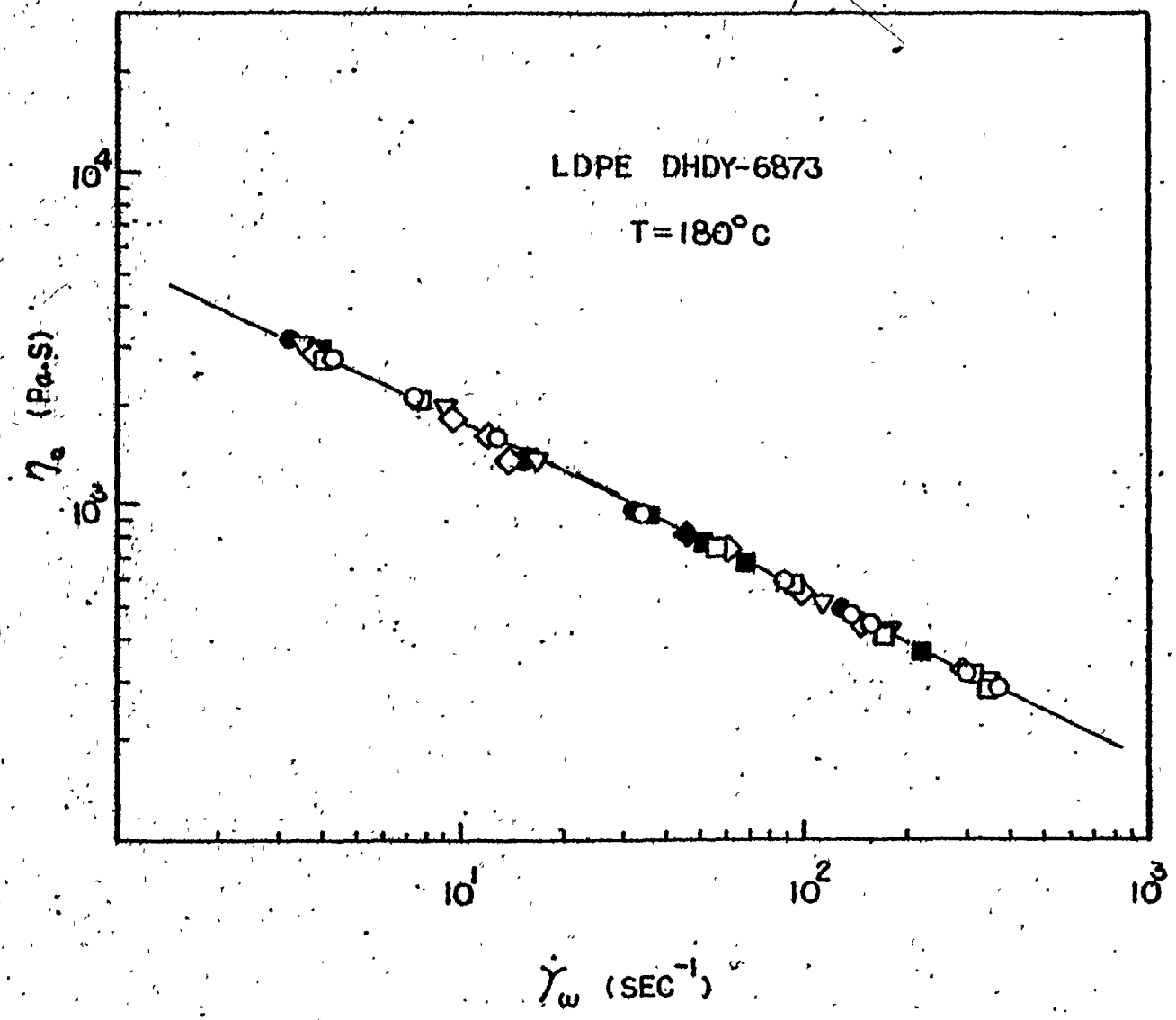

Fig.5.5 Plot of Apparent Viscosity vs. True Shear Rate for Low-density Polyethylene

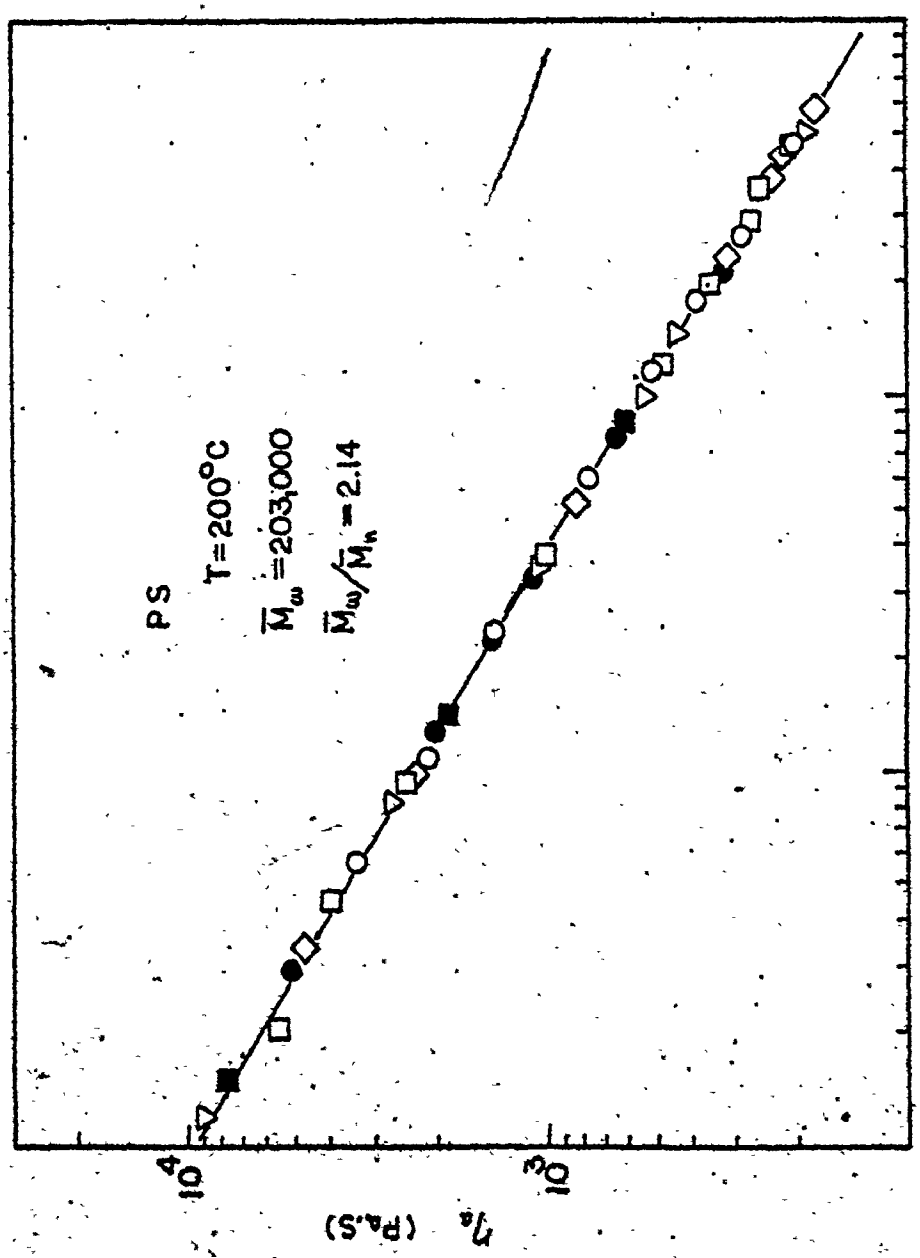

Fig.5.6 Plot of Apparent Viscosity vs. True Shear Rate for Polystyrene

5.3 Effect of Temperature on Extrudate Swell

The temperature dependence of die swell for low-density polyethylene and polystyrene is shown in Figs.5.7 to 5.12. The following conclusions can be drawn:

1. at constant shear rate the swelling ratio decreases with increasing temperature for both polymers,
2. both the critical shear rate and the maximum attainable die swell increase with temperature for the two polymers,
3. die swell is found to be almost independent of temperature at a fixed shear stress for both polymers,
4. the critical shear stress is found to be about 10^5 Pa for the polymers tested and nearly independent of extrusion temperature.

Conclusions (1) and (2) are in definite agreement with bulk of literature (1-3,7,35,56), but disagree with Horie's result for low-density polyethylene (56). The latter author failed to give an explanation for the anomalous behavior for this polymer - a branched polymer is more complicated than that of a linear one. However, the low-density polyethylene used in the present study is also a branched polymer and together with previous experimental results, it can be argued that Horie's results (56) for low-density polyethylene is

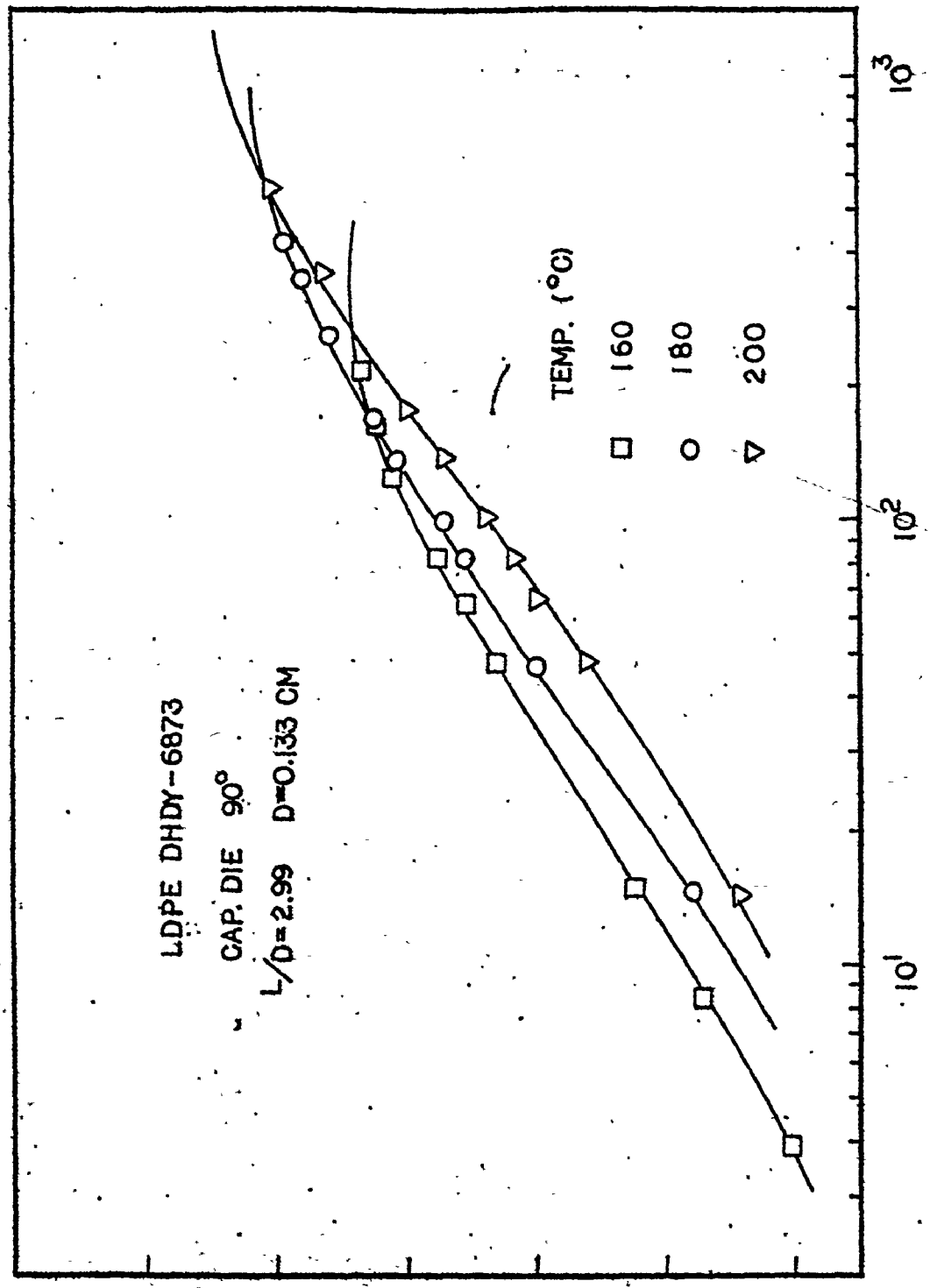

Fig.5.7 Effect of Temperature on Swelling Ratio for Low-density Polyethylene

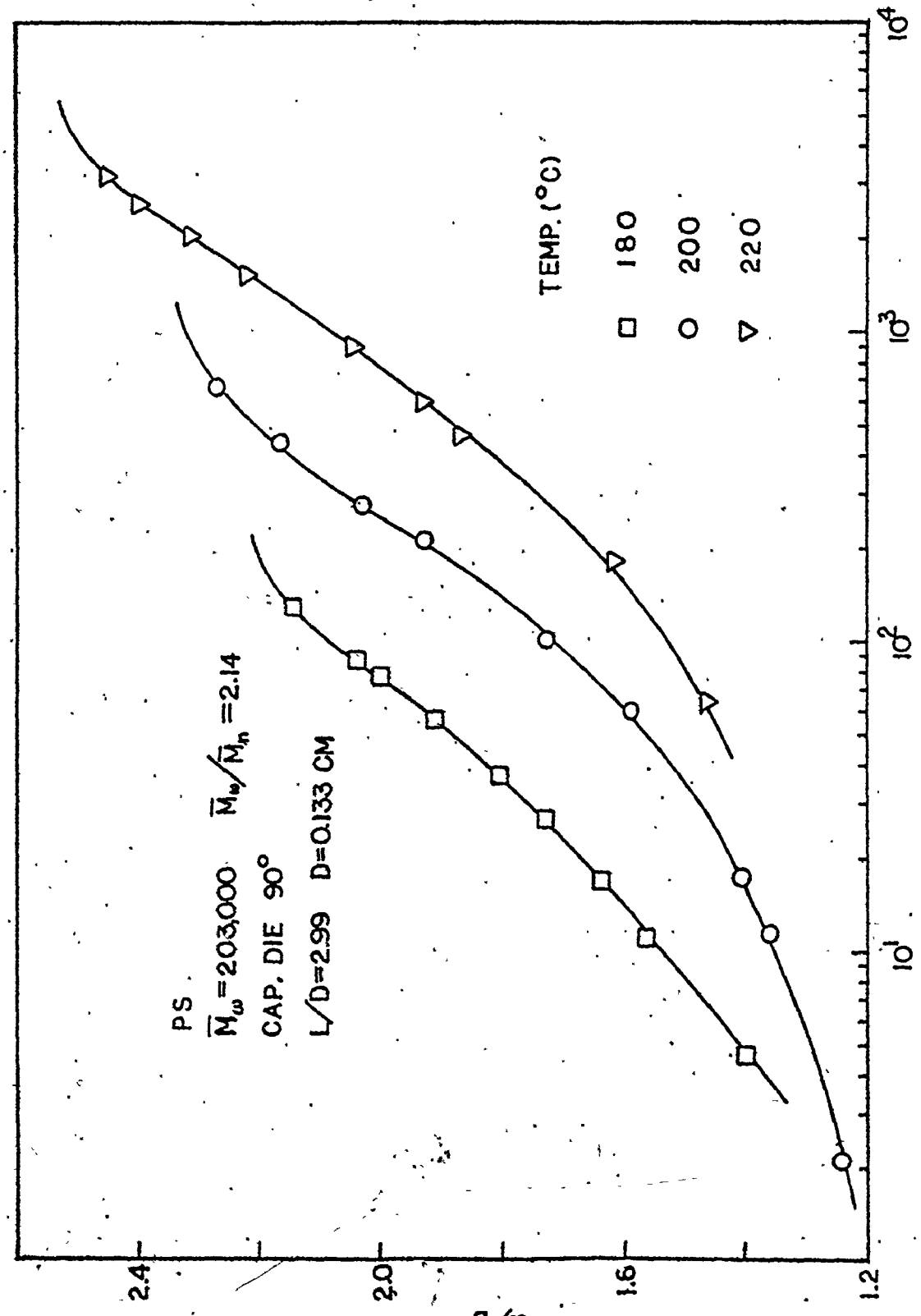

Fig.5.8 Effect of Temperature on Swelling Ratio for Polystyrene

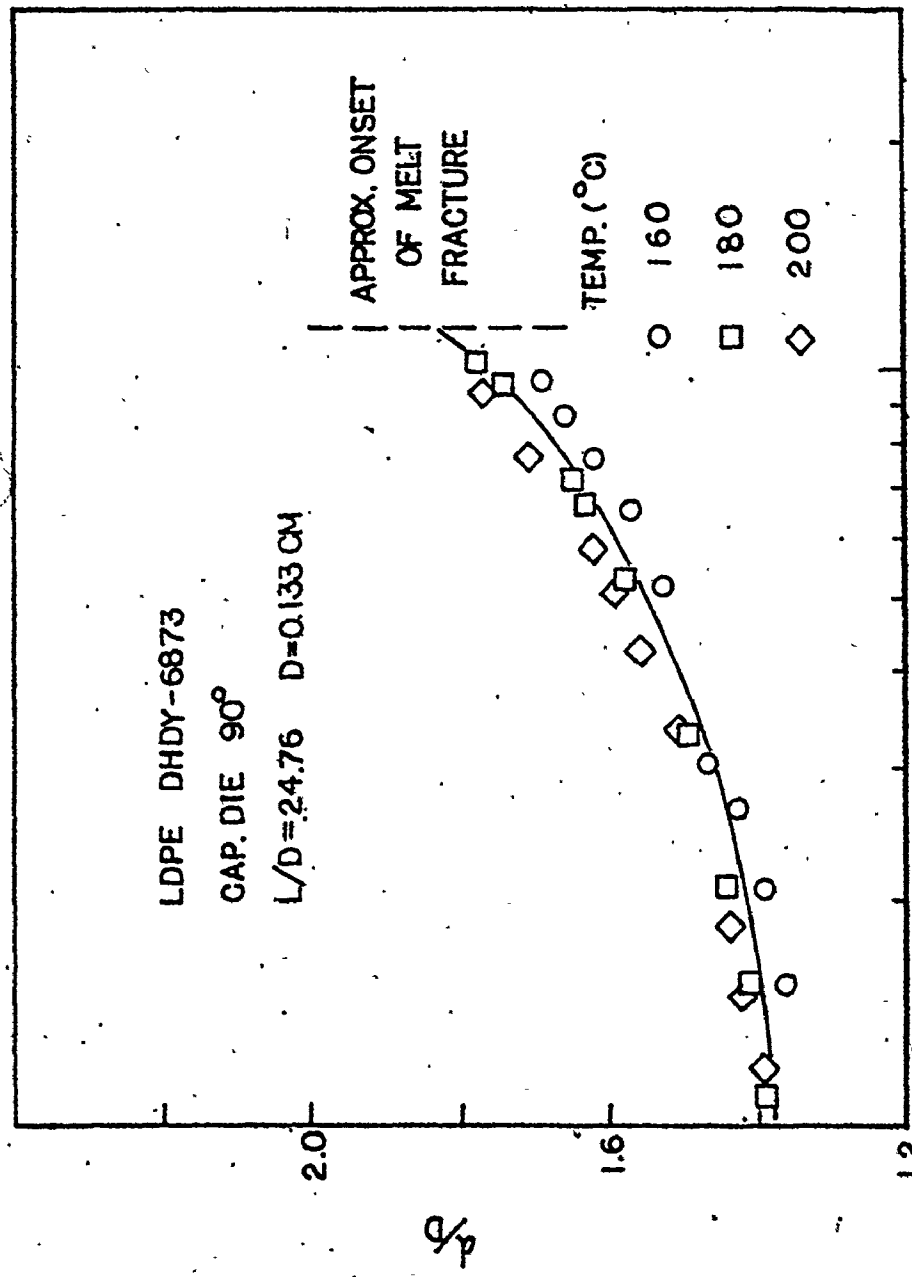

Fig.5.9 Dependence of d/D on Shear Stress for Low-density Polyethylene With Long Capillary Die

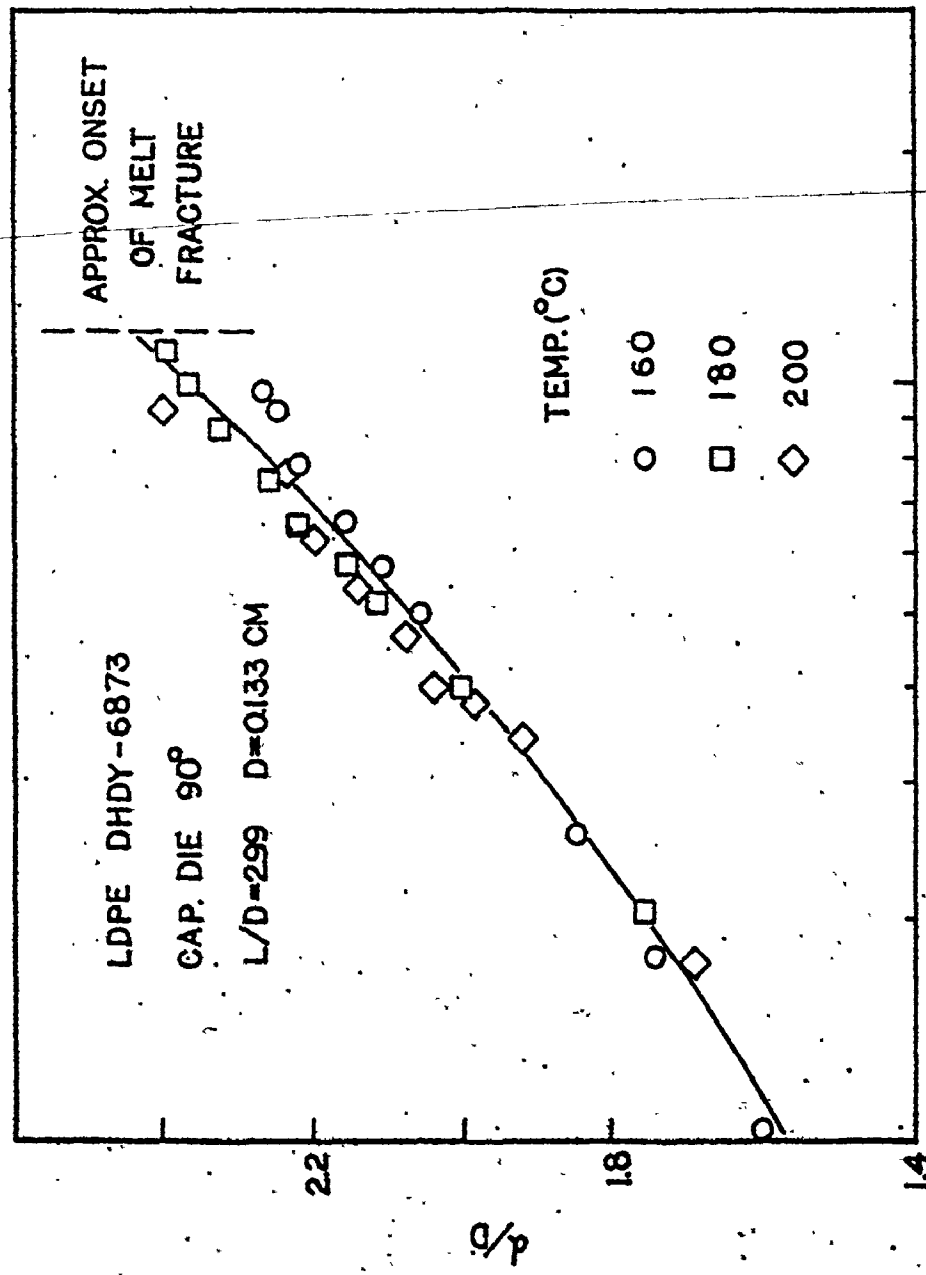

Fig.5.10 Dependence of d/D on Shear Stress for Low-density Polyethylene With Short Capillary Die

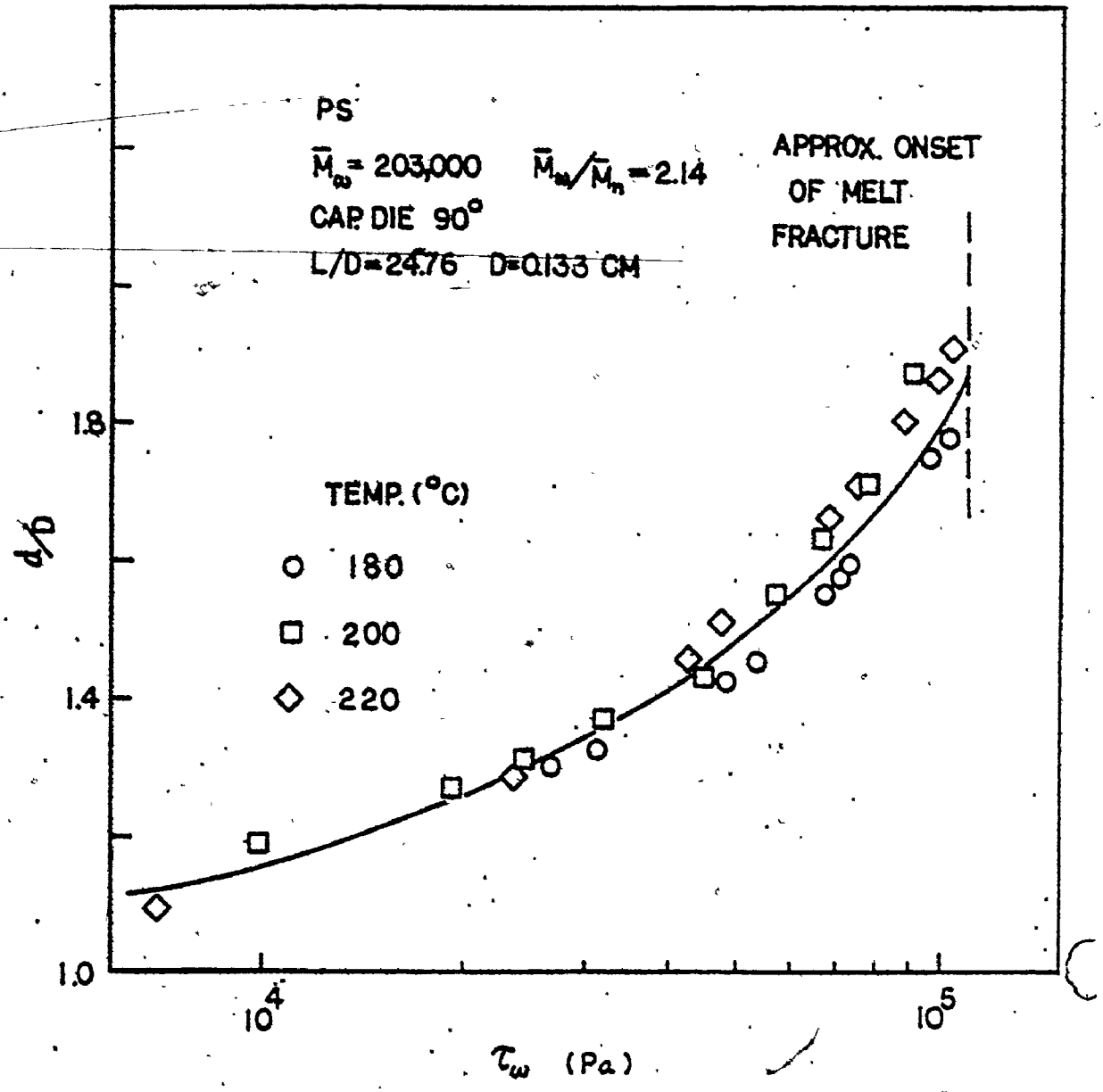

Fig.5.11 Dependence of d/D on Shear Stress for Polystyrene With Long Capillary Die

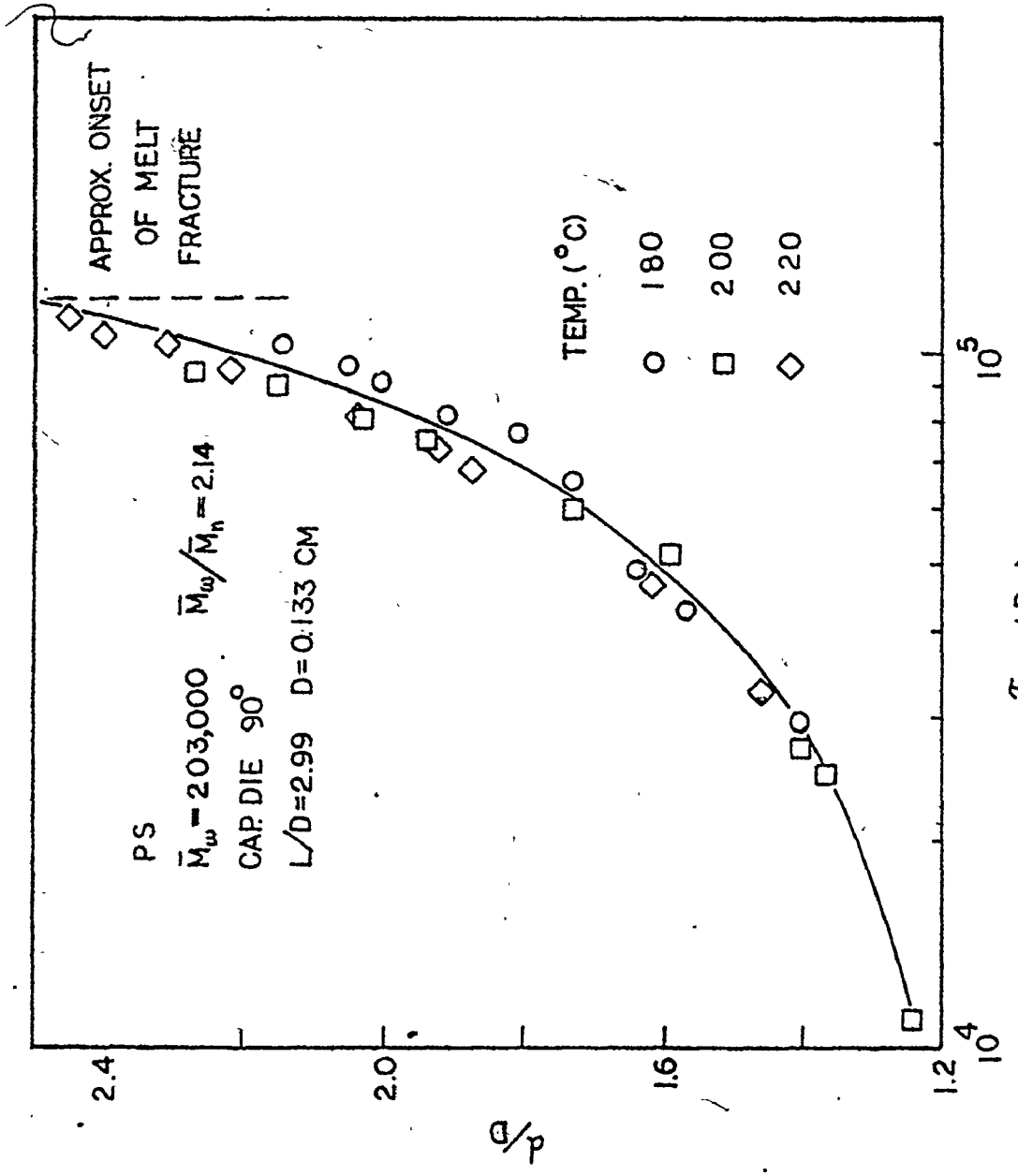

Fig.5.12 Dependence of d/D on Shear Stress for Polystyrene With Short Capillary Die

open to question.

Conclusion (3) agrees with Graessley et al (35) and Smelkov (84) but disagrees with Beynon and Glyde (7).

Conclusion (4) indicates absolute agreement with Beynon and Glyde (7), Vlachopoulos and his co-workers (57-59), Horie (56) and Huang and White (46).

5.4 Effects of Shear Rate and Shear Stress on Extrudate Swell

From Figs.5.7 to 5.18 it is apparent that

1. die swell increases with shear rate
2. die swell also increases with shear stress

The present experimental investigation with low-density polyethylene and polystyrene was carried out in the temperature range of 160°C to 200°C for the former, 180°C to 220°C for the latter sample. Except for the polystyrene tested at 220°C, all die swell measurements were made up to the critical shear rate. It is believed that distortion of the polystyrene extrudate will not be observed at this temperature unless the extrusion rate be increased still further.

Within critical shear rates, the conclusions agree with the bulk of literature (1,2,7,8,44,54,56) and can apply for the polymers studied here.

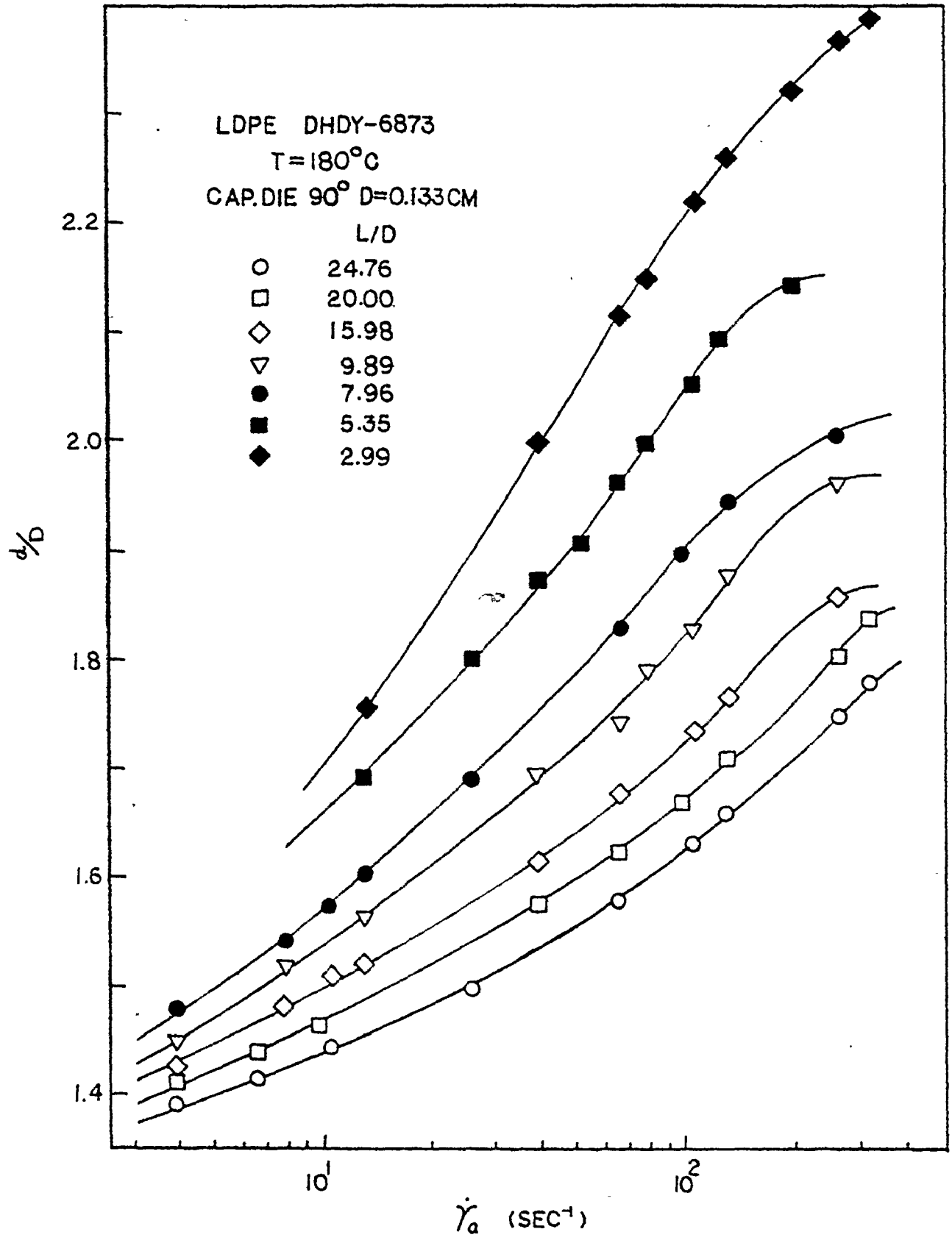

Fig.5.13 Dependence of d/D on Pseudo-Shear Rate for Low-

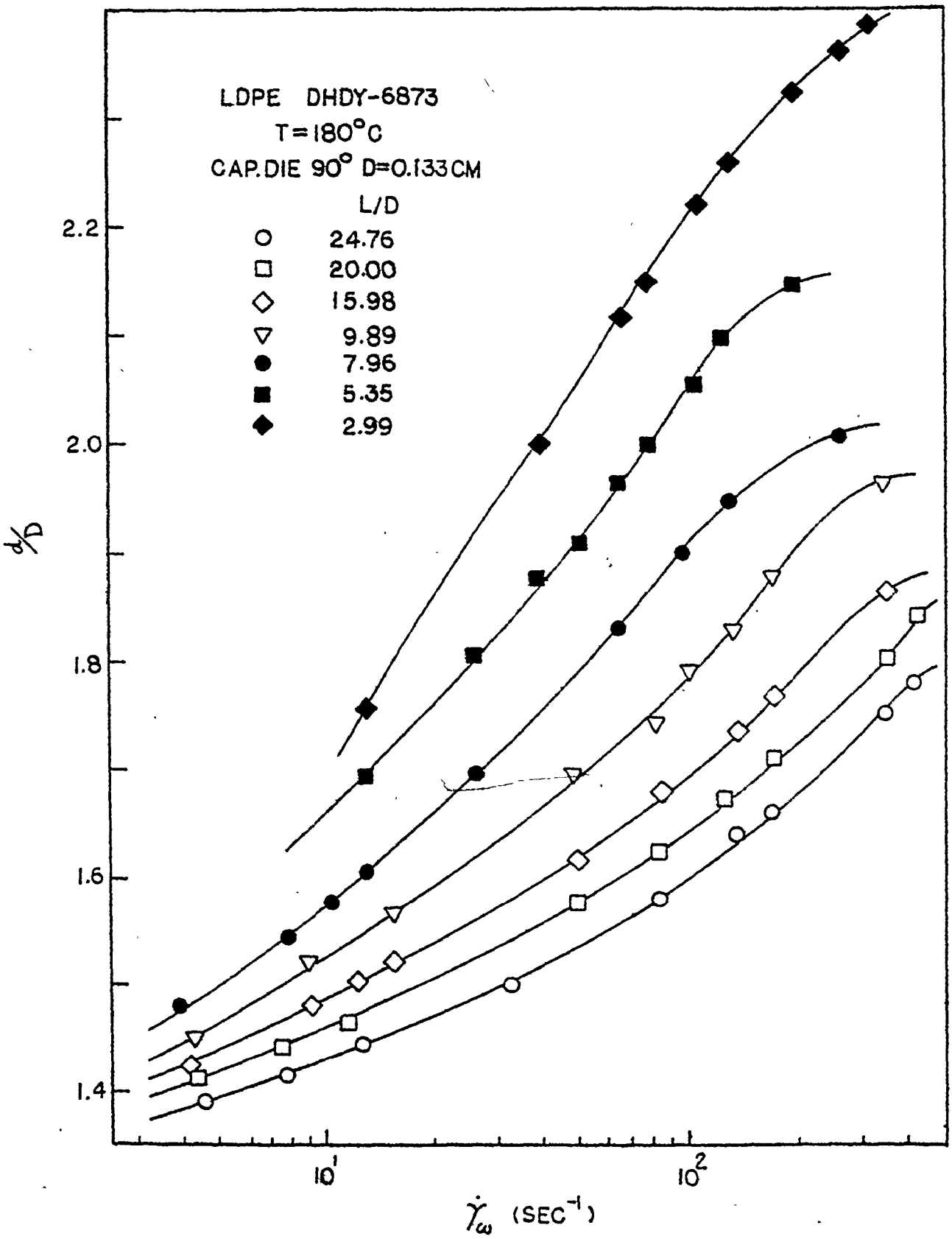

Fig.5.14 Dependence of d/D on True Shear Rate for Low-density Polyethylene

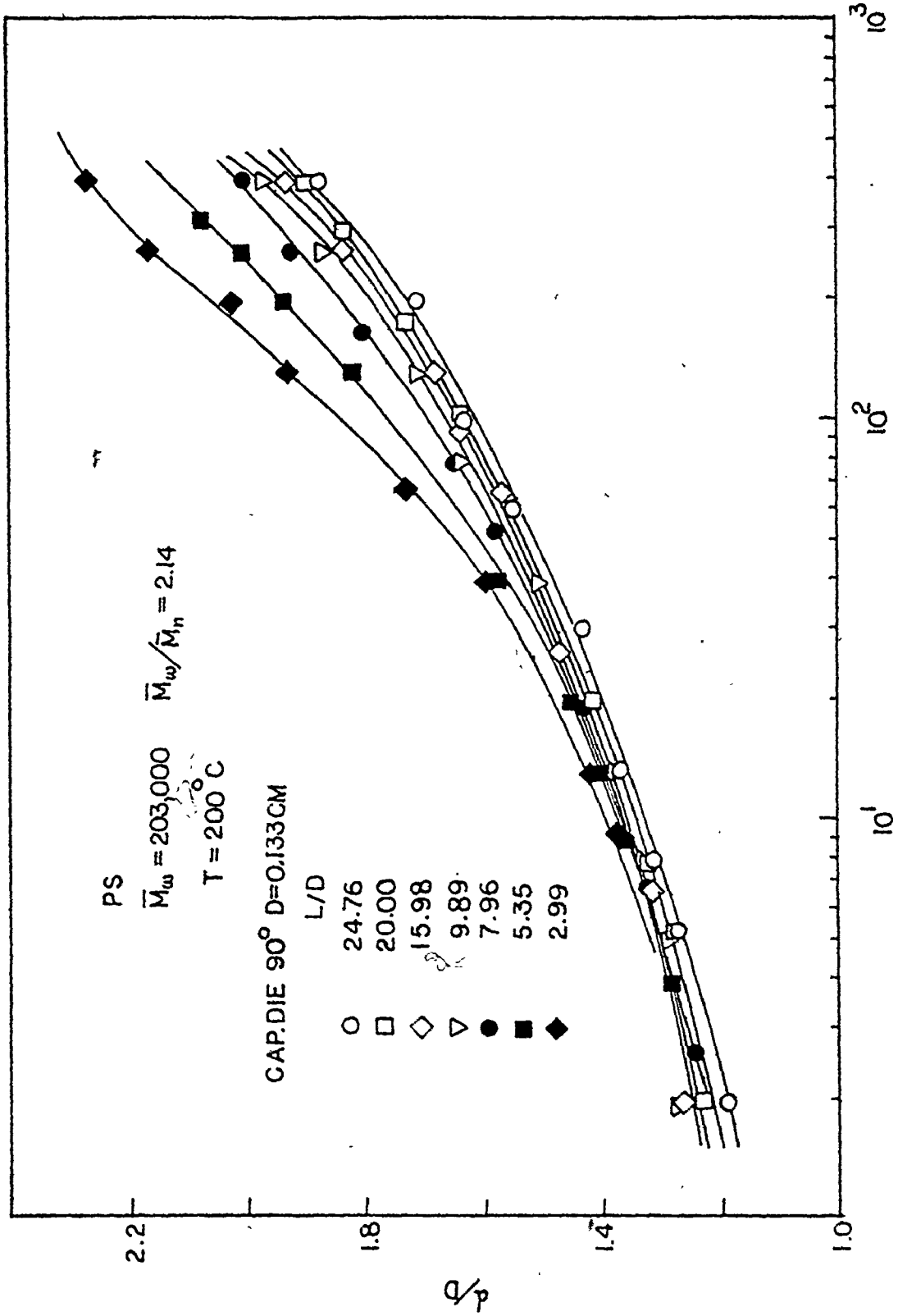

Fig.5.15 Dependence of d/D on Pseudo-Shear Rate for Polystyrene

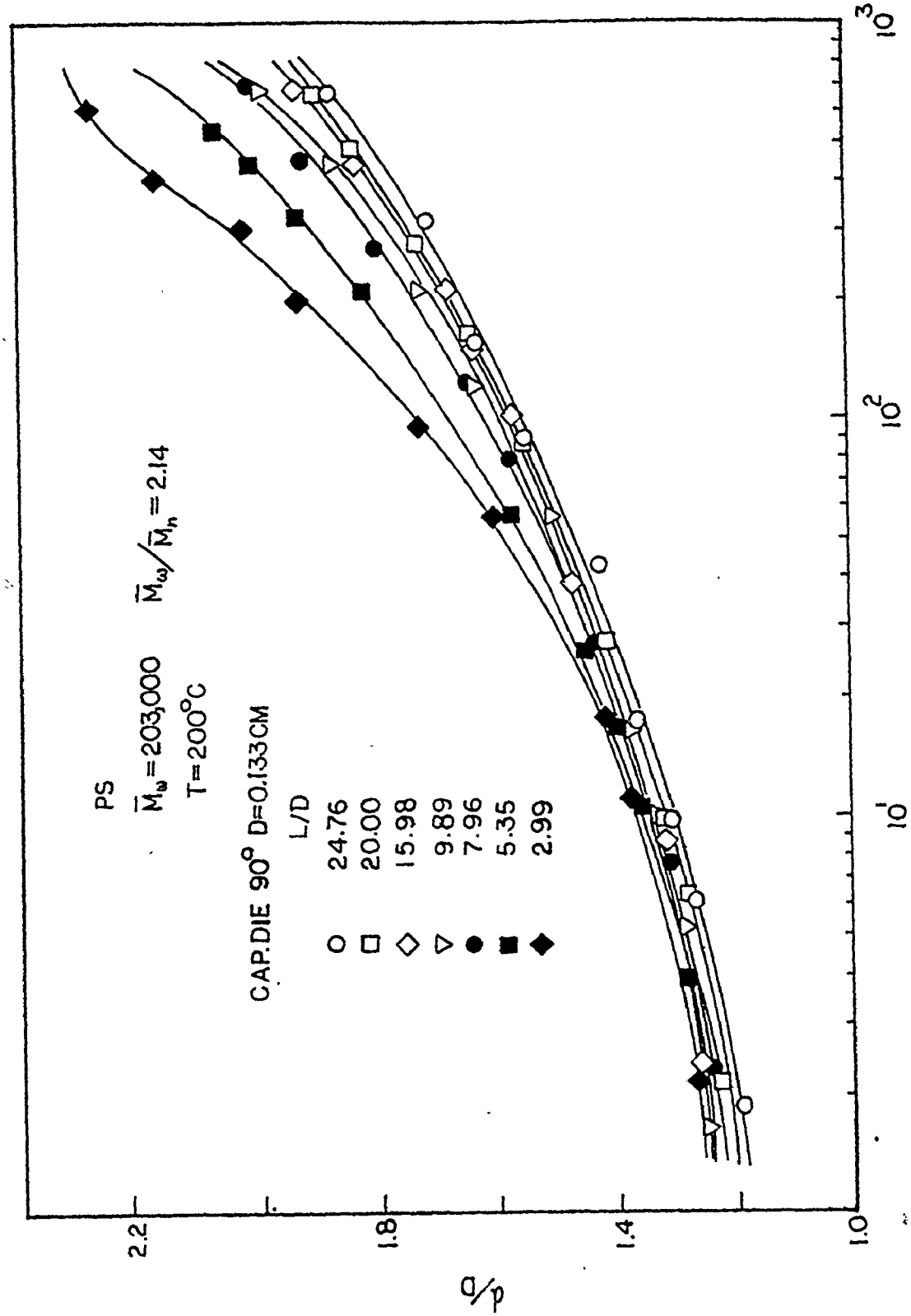

Fig.5.16 Dependence of d/D on True Shear Rate for Polystyrene

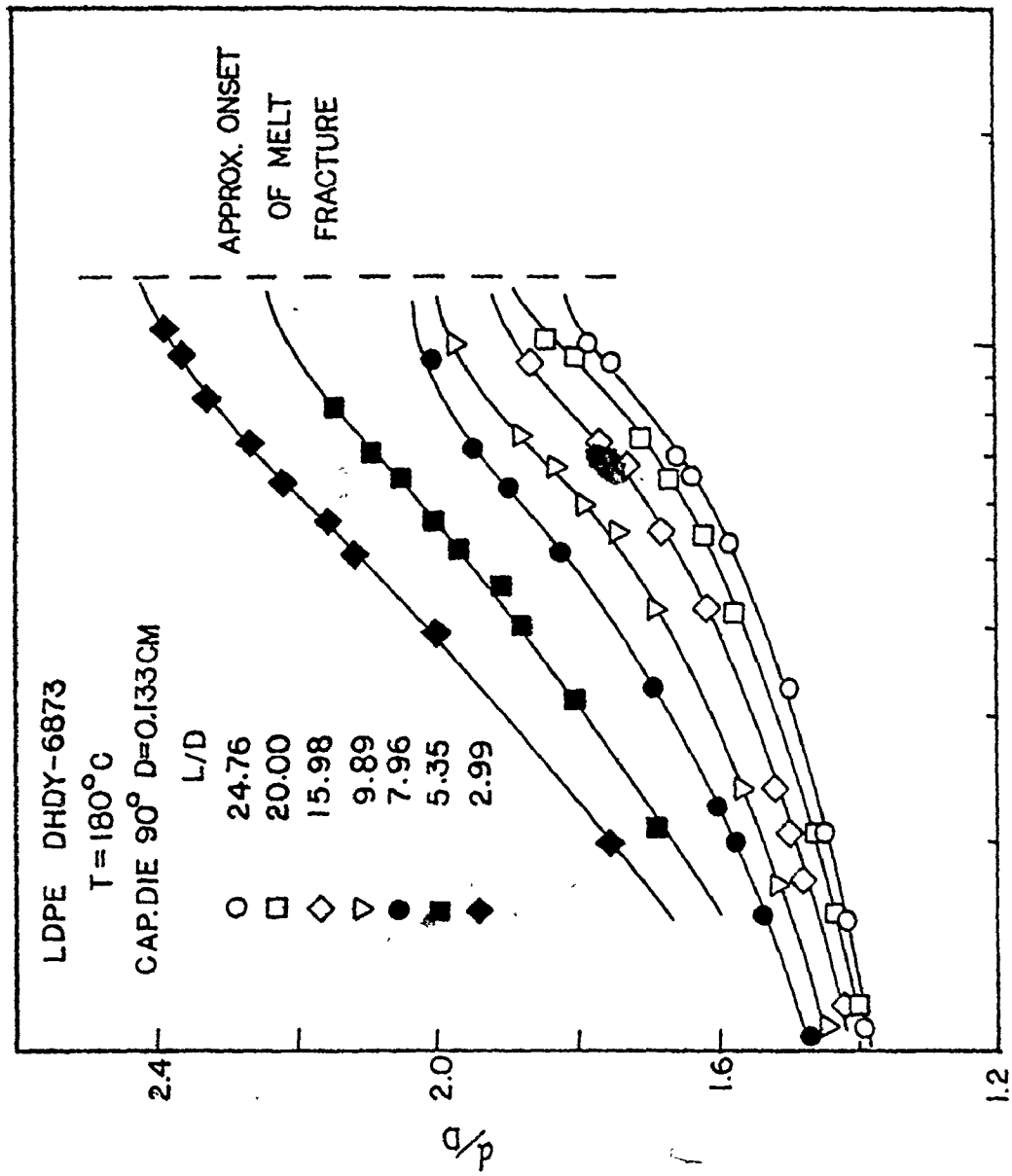

Fig.5.17 Dependence of d/D on True Shear Stress for Low-density Polythylene

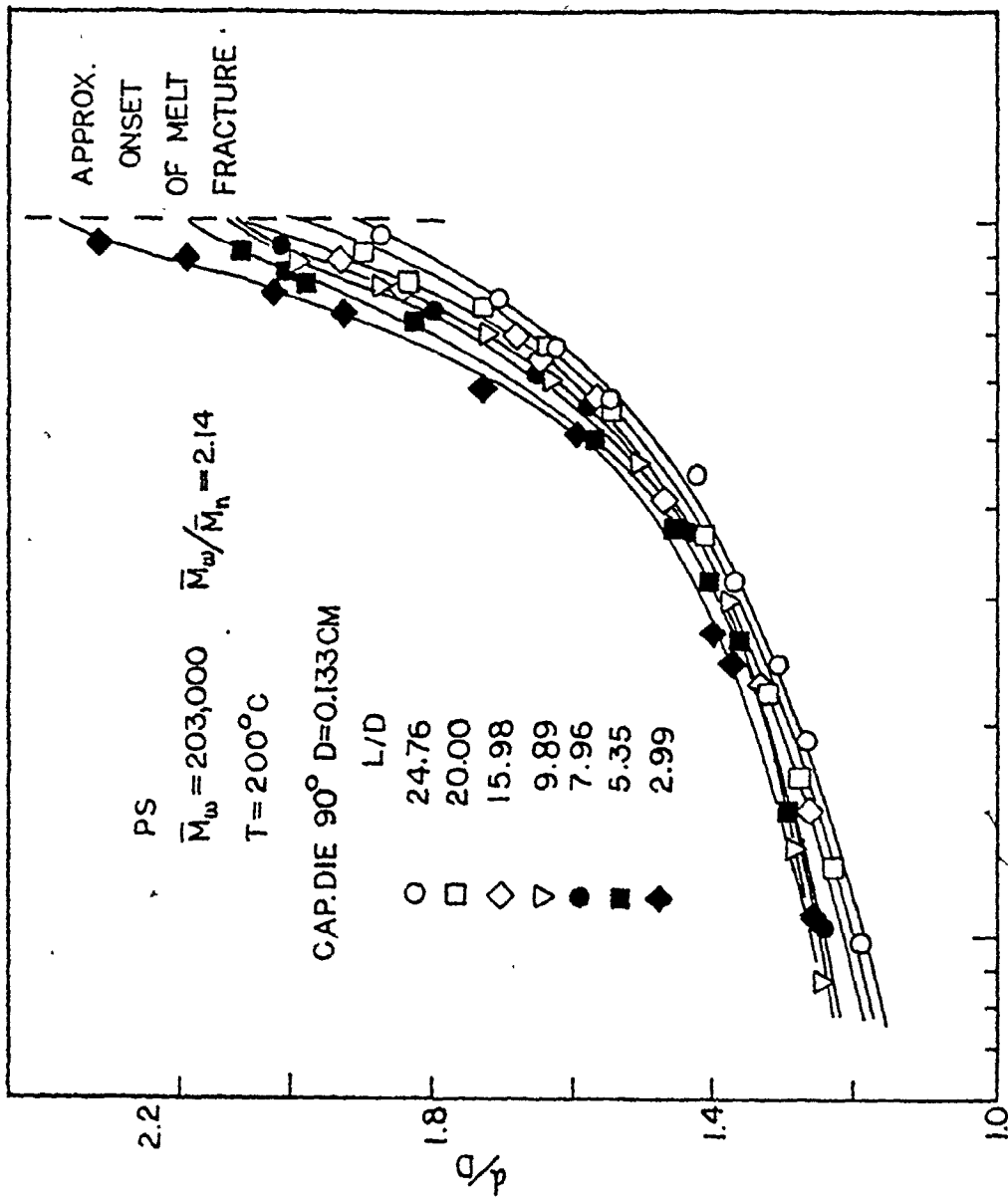

Fig.5.18 Dependence of d/D on True Shear Stress for Polystyrene

5.5 Effect of Methods Measuring Extrudate Swell

In the present study, three different techniques were used to measure extrudate swell. In the first method, the polymer melt was allowed to cool in air and the diameter of the frozen extrudate was measured using a micrometer. In the second method, the polymer melt was extruded isothermally into a bath of silicone oil maintained at the extrusion temperature. The strand was suspended in the bath for about 15 minutes, removed and cooled in air and its diameter was measured using a micrometer. In the last method, the samples were "annealed" in the hot oil bath to achieve a constant diameter. The extrudates were removed, cooled and again measured with a micrometer. For all the techniques employed, the swelling ratios were corrected to the extrusion temperature using eq.(2.8) and compared.

Fig.5.19 and 5.20 show the dependence of extrudate swell on various methods of measurement at constant shear rate. Table 5.2 indicates a comparison of extrudate swell measurements using different techniques. The following conclusions can be drawn:

1. For the low-density polyethylene (DHDY-6873) and polysty-

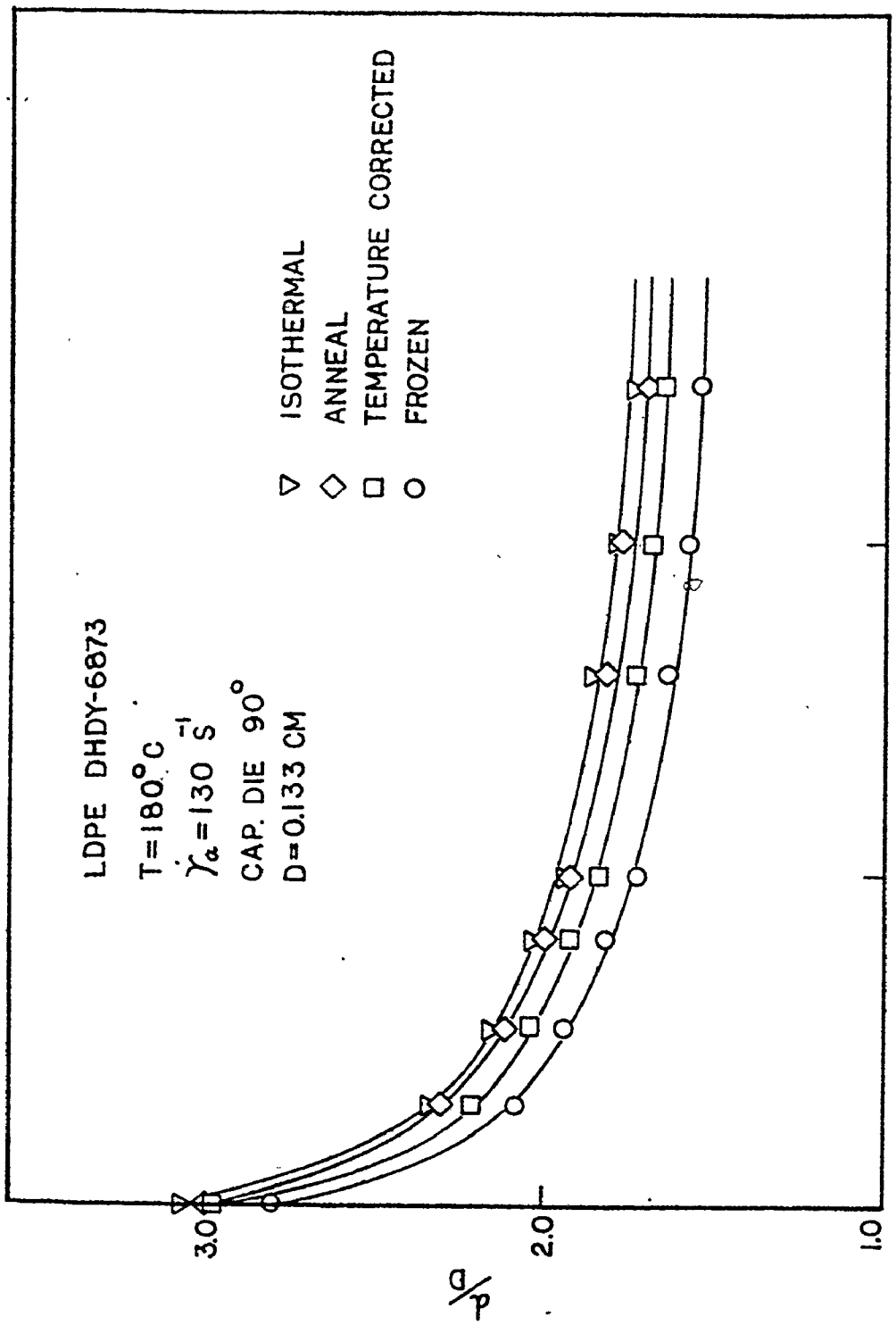

Fig.5.19 Comparison of Methods Measuring Extrudate Swell for Low-density Polyethylene

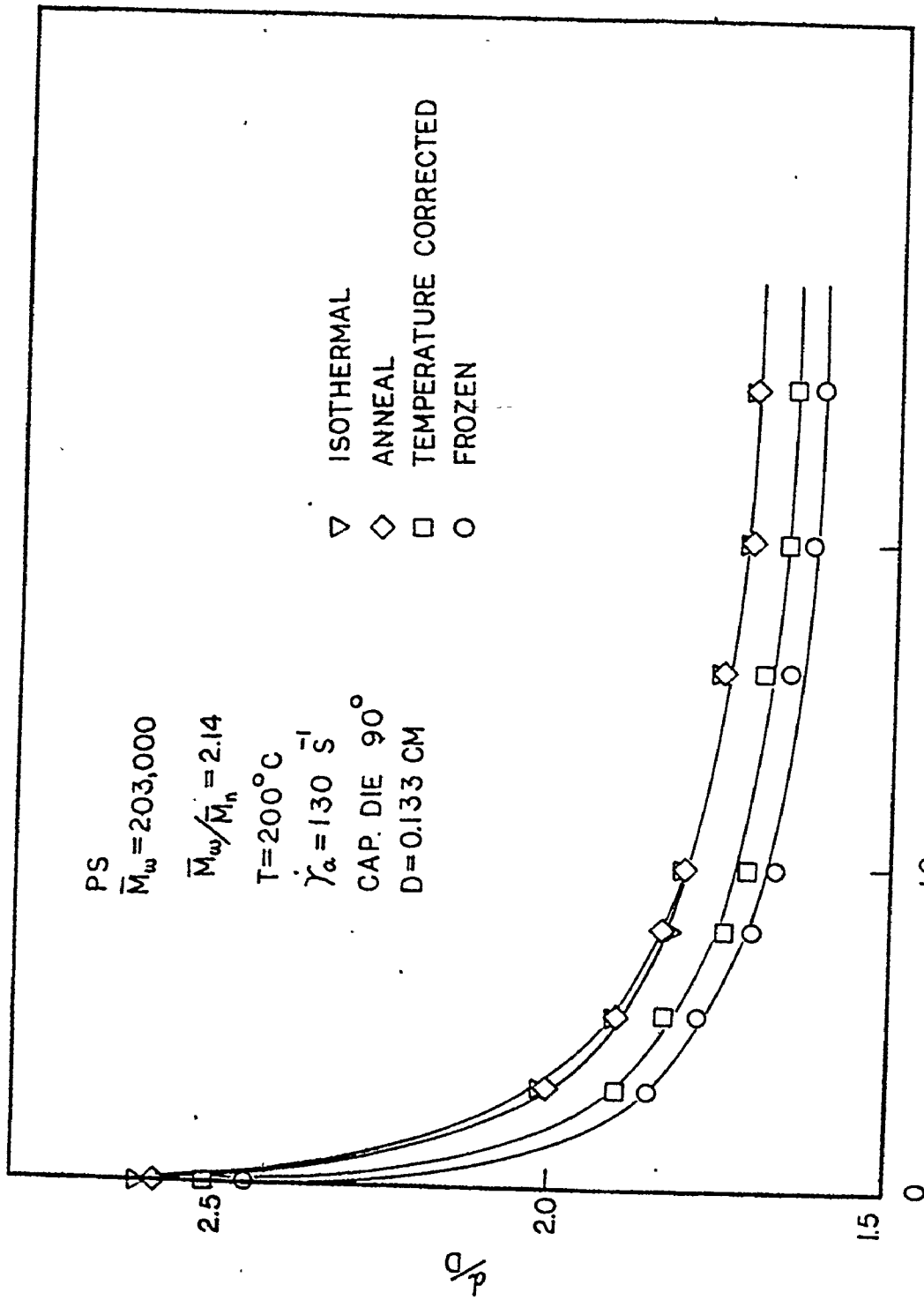

Fig.5.20 Comparison of Methods Measuring Extrudate Swell for Polystyrene

Table 5.2

Comparison of Extrudate Swell Measurements Using Different Techniques

Capillary Die $\theta = 90^{o}$ D = 0.133 cm

L / D	LDPE DHDY- 6873 Test Temperature = 180°C			PS Test Temperaature = 200°C		
	Isothermal %	Anneal In oil %	Temperature corrected %	Isothermal %	Anneal In oil %	Temperature corrected %
24.76	12.79	10.73	6.09	5.81	5.81	2.47
20.00	12.63	11.62	6.09	5.80	5.80	2.47
15.98	12.90	10.96	6.09	6.20	6.20	2.47
9.89	12.55	11.17	6.09	7.53	7.53	2.47
7.96	12.25	9.61	6.09	6.99	7.44	2.47
5.35	11.46	9.39	6.09	6.35	6.35	2.47
2.99	11.43	10.29	6.09	8.28	7.45	2.47
0.00	9.20	7.51	6.09	6.55	5.29	2.47

rene samples, the extrudate swell measurements based on the three techniques show deviation from one to another in the following order:

isothermal > anneal > temperature corrected

2. The deviation in die swell measurement for low-density polyethylene (DHDY-6873) is larger than that for polystyrene in all techniques employed.

Conclusion (1) is in definite agreement with previous work by White and Roman (27), Utracki et al (48), Han and Charles (47) and others (50,51).

Conclusion (2) agrees with Graessley et al (35) for polystyrene and with Mendelson and Finger (52) for low-density polyethylene.

5.6 Effect of Capillary Dimension on Extrudate Swell

5.6.1 Dependence of Extrudate Swell on Die Length

In Figs.5.21 and 5.22 the swelling ratio manifests its exponential dependence on the length-to-diameter (L/D) ratio of the capillary for the polymers studied at different shear rates. The following conclusions can at once be drawn:

1. at fixed temperature and shear rate die swell decays exponentially with increasing L/D ratios of the capillary dies,
2. the swelling index for polystyrene reaches an asymptotic value at a L/D of about 14,
3. the die swell for low-density polyethylene decreases rapidly with increasing L/D ratio up to a L/D of about 20 or longer.

Conclusion (1) is in definite agreement with the bulk of literature (27,37,38,45,46). Confirmation of conclusion (2) is met by Graessley et al (35), Vlachopoulos and his co-workers (41). Conclusion (3) agrees with White and Roman (37) but disagress with Mori and Funatsu (42), and Han and Philipoff (43). The latter researchers observed the die swell of polyethylenes becomes independent of the L/D ratio when a value of about 20 is reached. The reason for this disagreement might have come from the type of polyethylene samples used. Usually the mech-

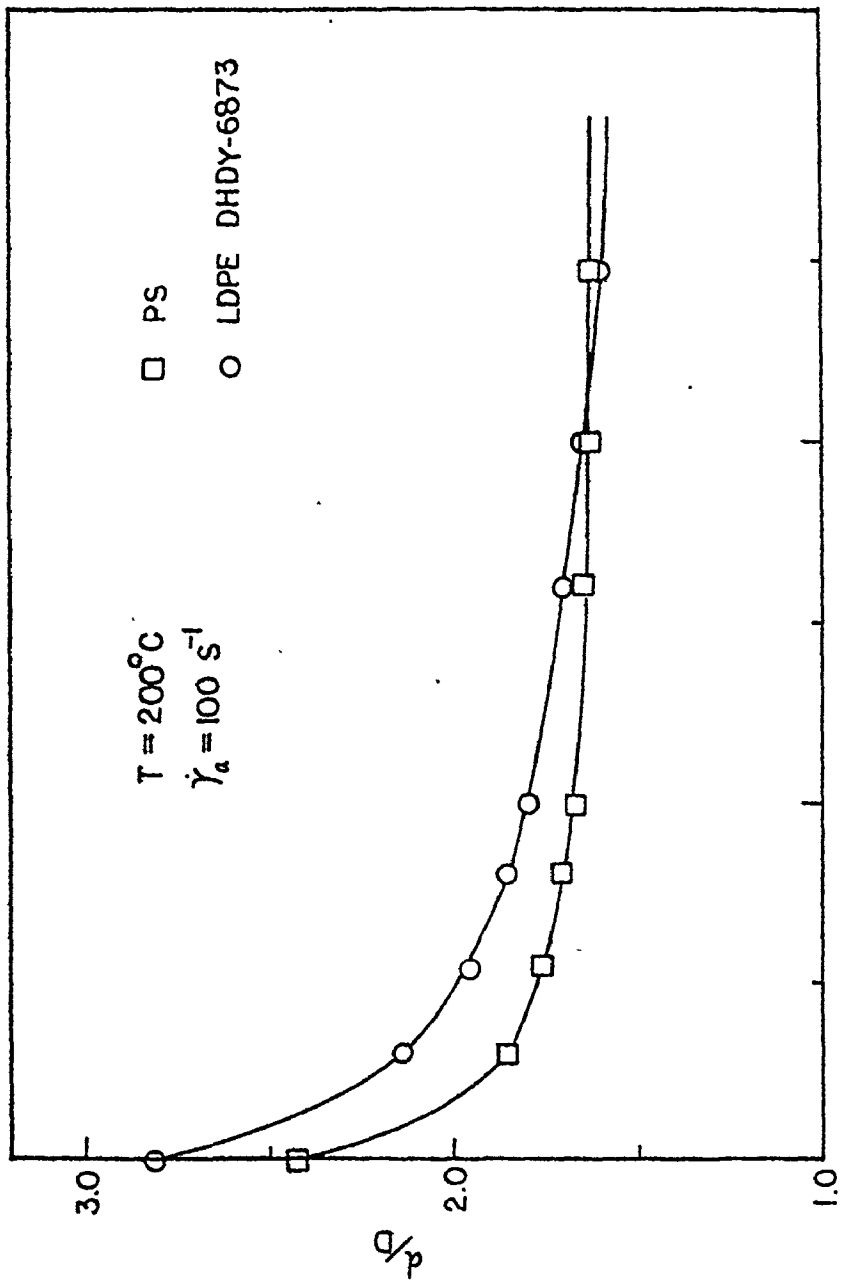

Fig.5.21 Dependence of d/D on Die Length for Low-density Polyethylene and Polystyrene at Pseudo-Shear Rate of 100 1/sec

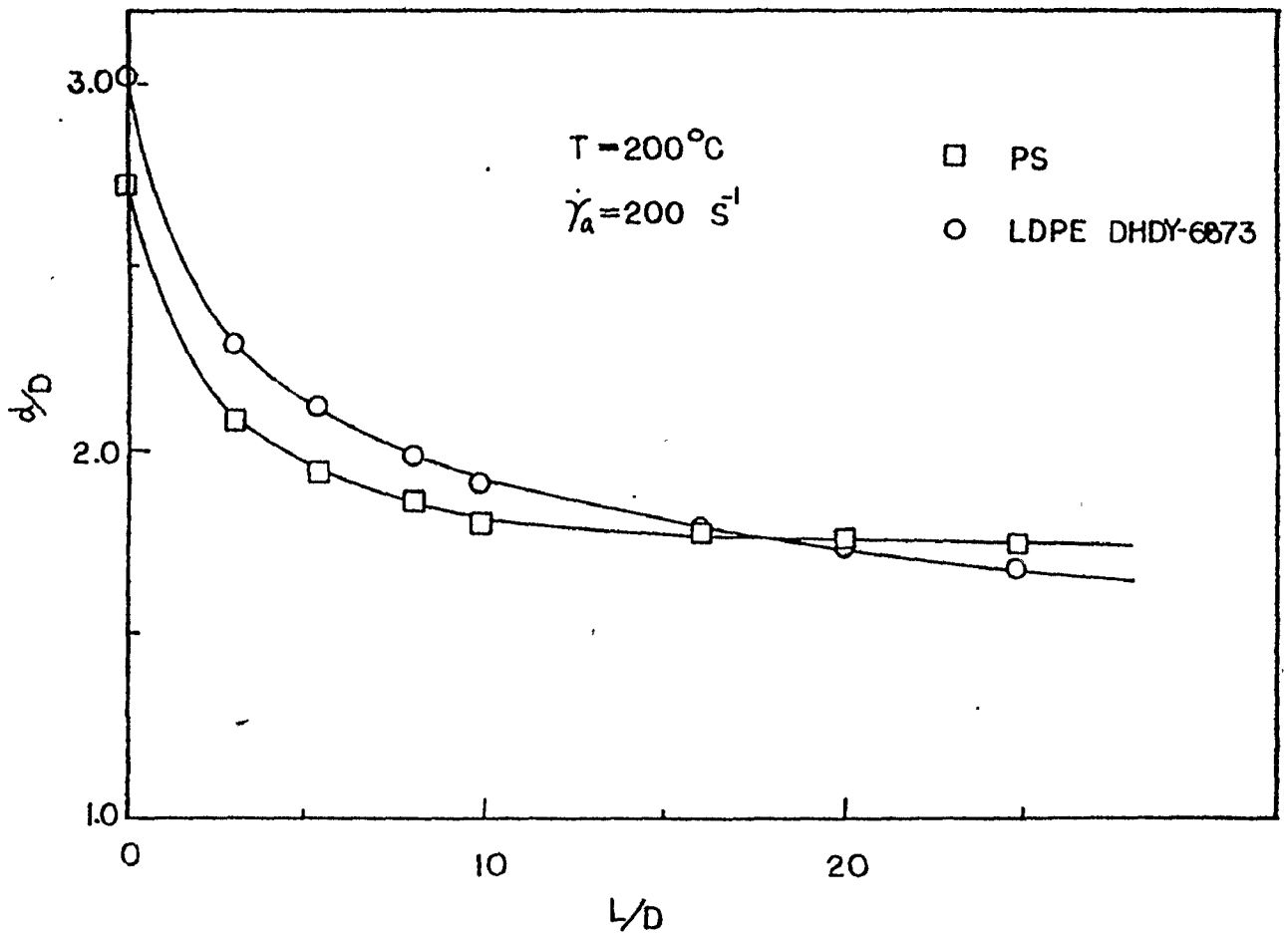

Fig.5.22 Dependence of d/D on Die Length of Low-density Polyethylene and Polystyrene at Pseudo-Shear Rate of 200 1/sec

anism on die swell for polymers with long-chain branching is more complicated than that for linear one.

The reason for this exponential decay can be explained qualitatively as follows. Extrudate swell is related to the ability of polymer melts to undergo "delayed" elastic strain recovery. At the die exit the more strained and more entangled the melt is, the more it will swell. In a long capillary, polymer melts undergo tensile deformation and bring about disentanglement. With large geometric capillary ratio (L/D), viscoelastic fluid is only able to recover from shear strain and the swelling ratios become quite constant. With very short capillaries, the melt is much more entangled and recovers from both shear and tensile strains. As a consequence, extrudate swells increase with decreasing L/D ratio.

5.6.2 Dependence of Swelling Ratio on Die Diameter

The reservoir diameter, D_R, of the Instron model 3211 rheometer used in the present study is 0.953 cm. Figs.5.23 and 5.24 show the swelling index as a function of capillary diameter. At constant shear rate and temperature die swell increases with the reservoir-to-capillary diameter ratio (D_R/D) up to a critical value and decreases thereafter for both polymers. The maximum attainable swelling ratio is found to be at the diameter ratio of 10.3 for low-density polyethyl-

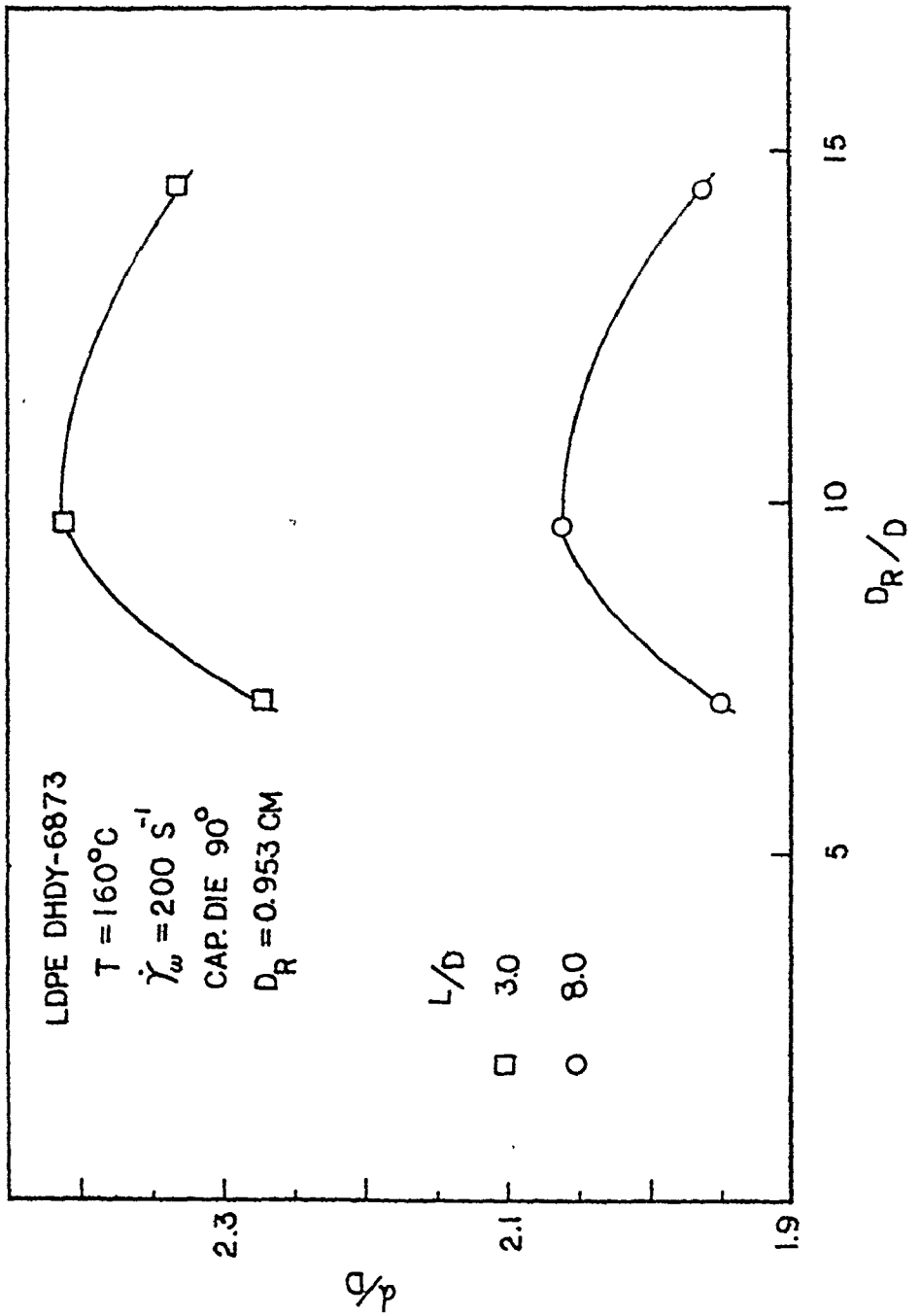

Fig.5.23 Dependence of d/D on Reservoir-to-Capillary Diameter Ratio for Low-density Polyethylene

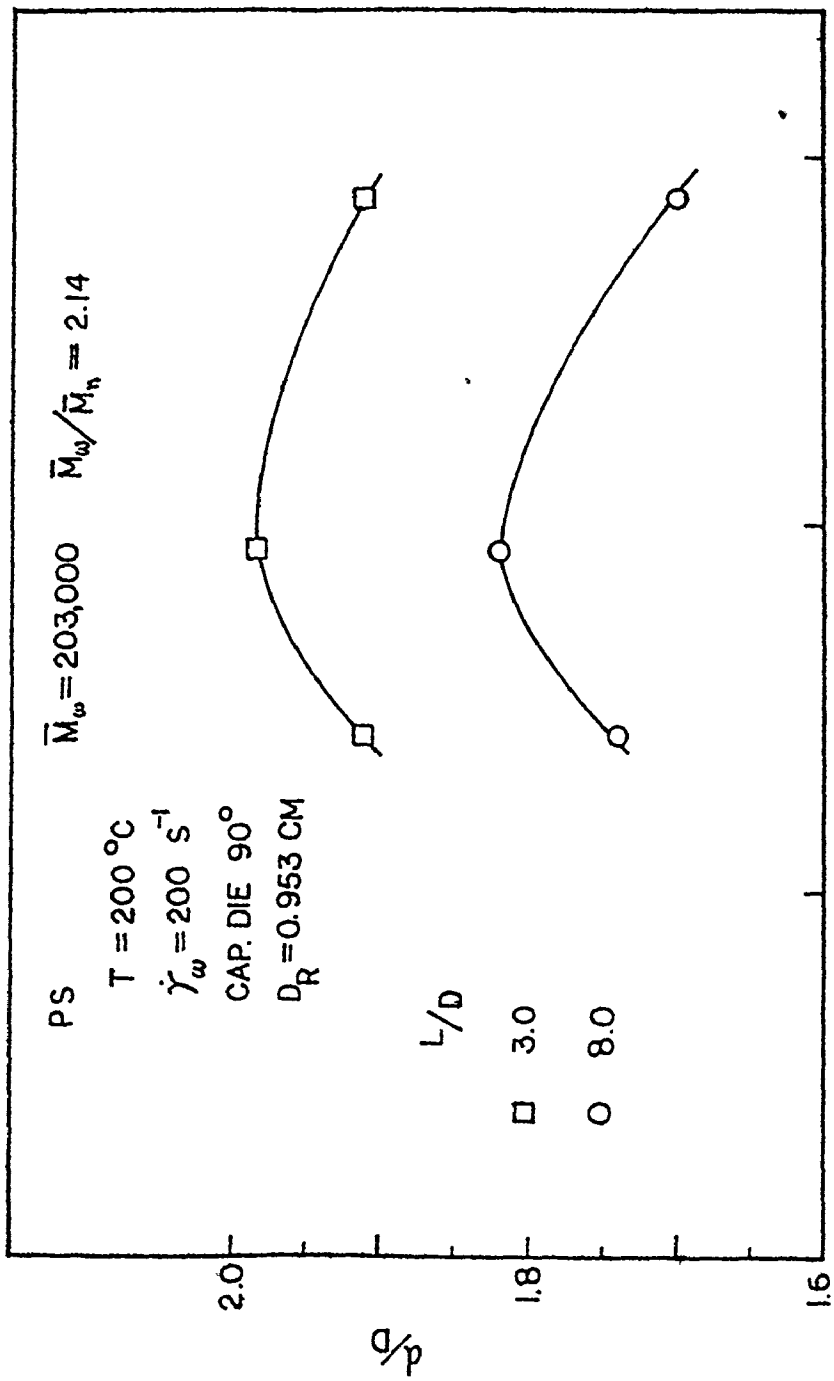

Fig.5.24 Dependence of d/D on Reservoir-to-Capillary Diameter Ratio for Polystyrene

ene and 10.0 for polystyrene.

There is no literature available to date for these polymers for comparison; however, Han et al (85,86) have indicated that for high-density polyethylene, die swell increases with D_R/D up to a value of about 12. But no experimental investigation has been done at larger D_R/D ratios using low-density polyethylene and polystyrene. Their claim that the swelling index levels off at higher diameter ratios becomes plausible. At the critical D_R/D ratio, it can be argued that the conical zone of the converging flow streamlines into the capillary becomes free from the reservoir wall effect resulting in a maximum die swell.

5.6.3. Dependence of Extrudate Swell on Entry Geomety (Entrance Angle)

The effect of entrance angle of the die-orifice on die swell is shown in Figs.5.25 and 5.26. Notably, the swelling ratio increases with increasing entry angle for both polymers up to 150° beyond which value the die swell drops (Figs.5.27 and 5.28). This conclusion is in good agreement with Huang and White (46). However, the argument on this phenomenon is not fully understood.

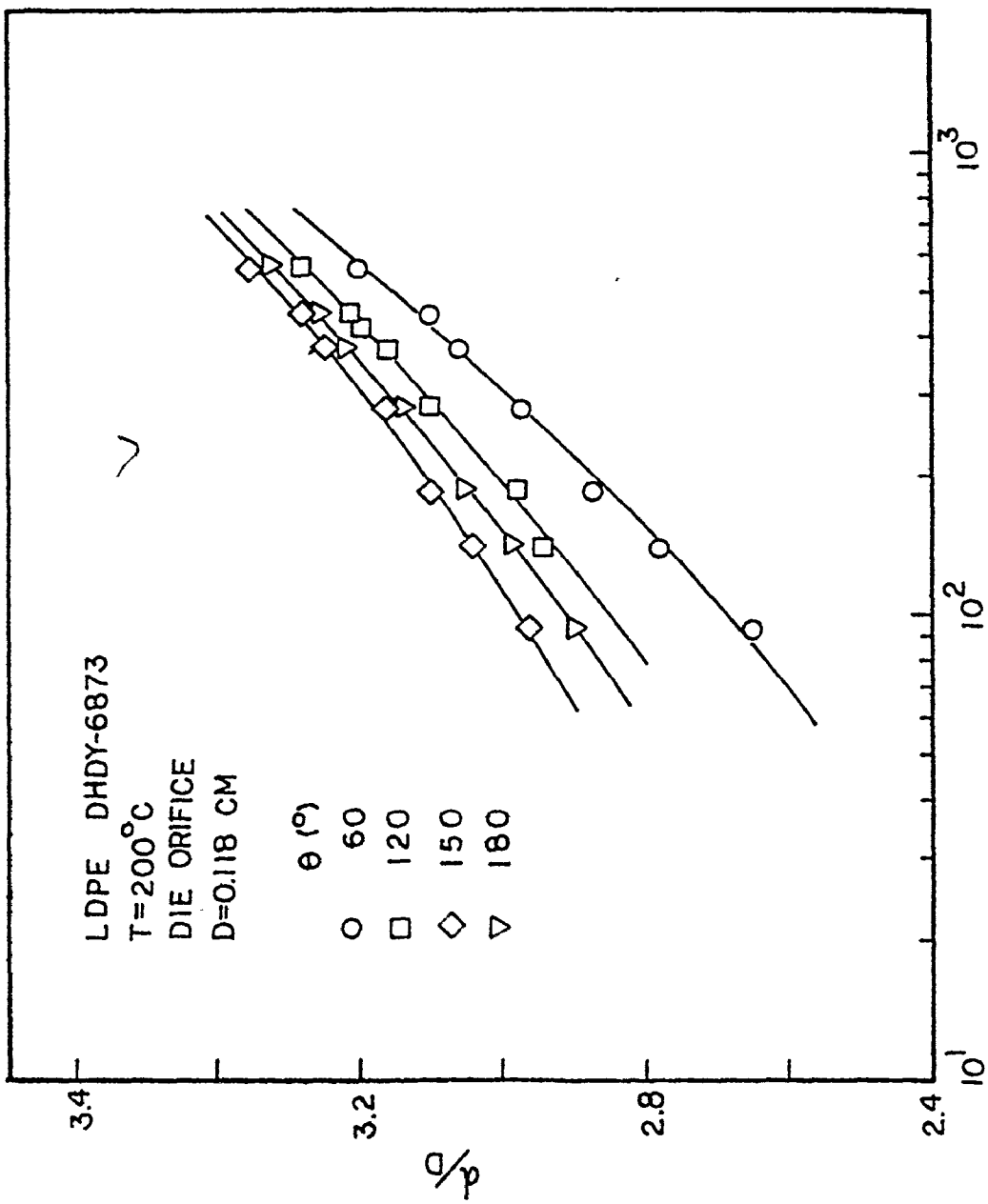

Fig.5.25 Dependence of Extrudate Swell on Capillary Entry Geometry for Low-density Polyethylene

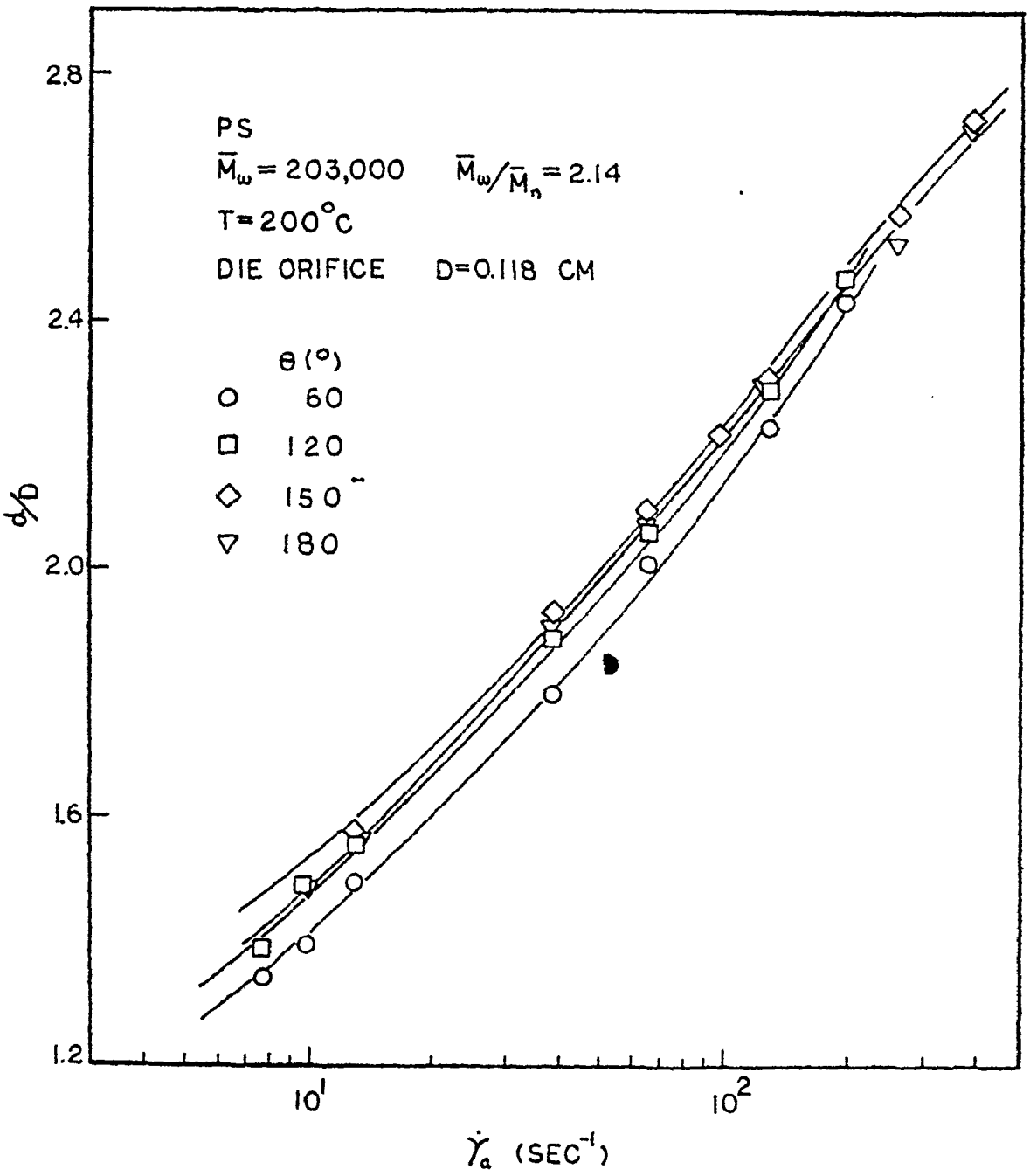

Fig.5.26 Dependence of Estrudate Swell on Capillary Entry Geometry for Polystyrene

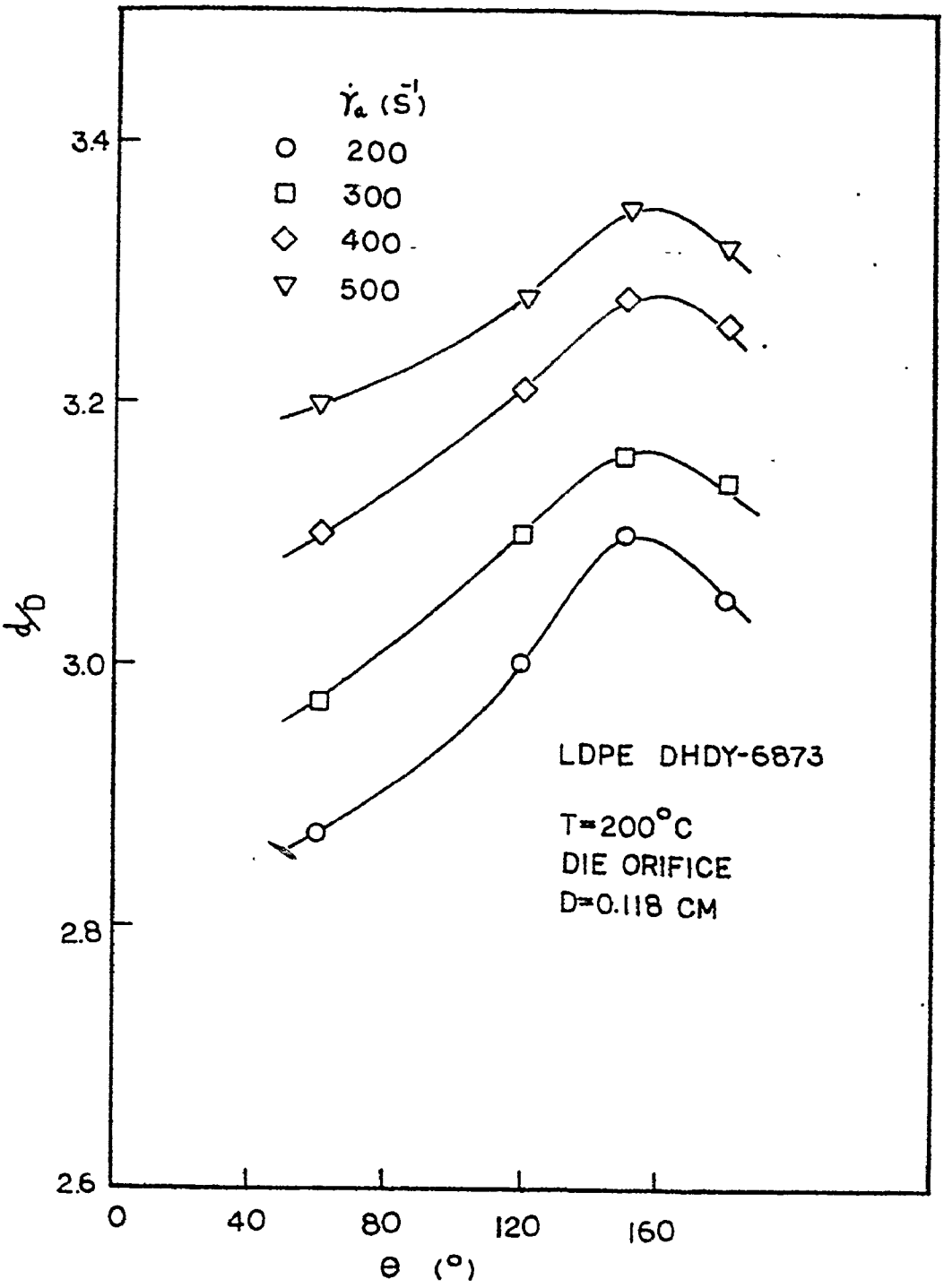

Fig.5.27 Plot of d/D vs. Entrance Angle θ for Low-density Polyethylene

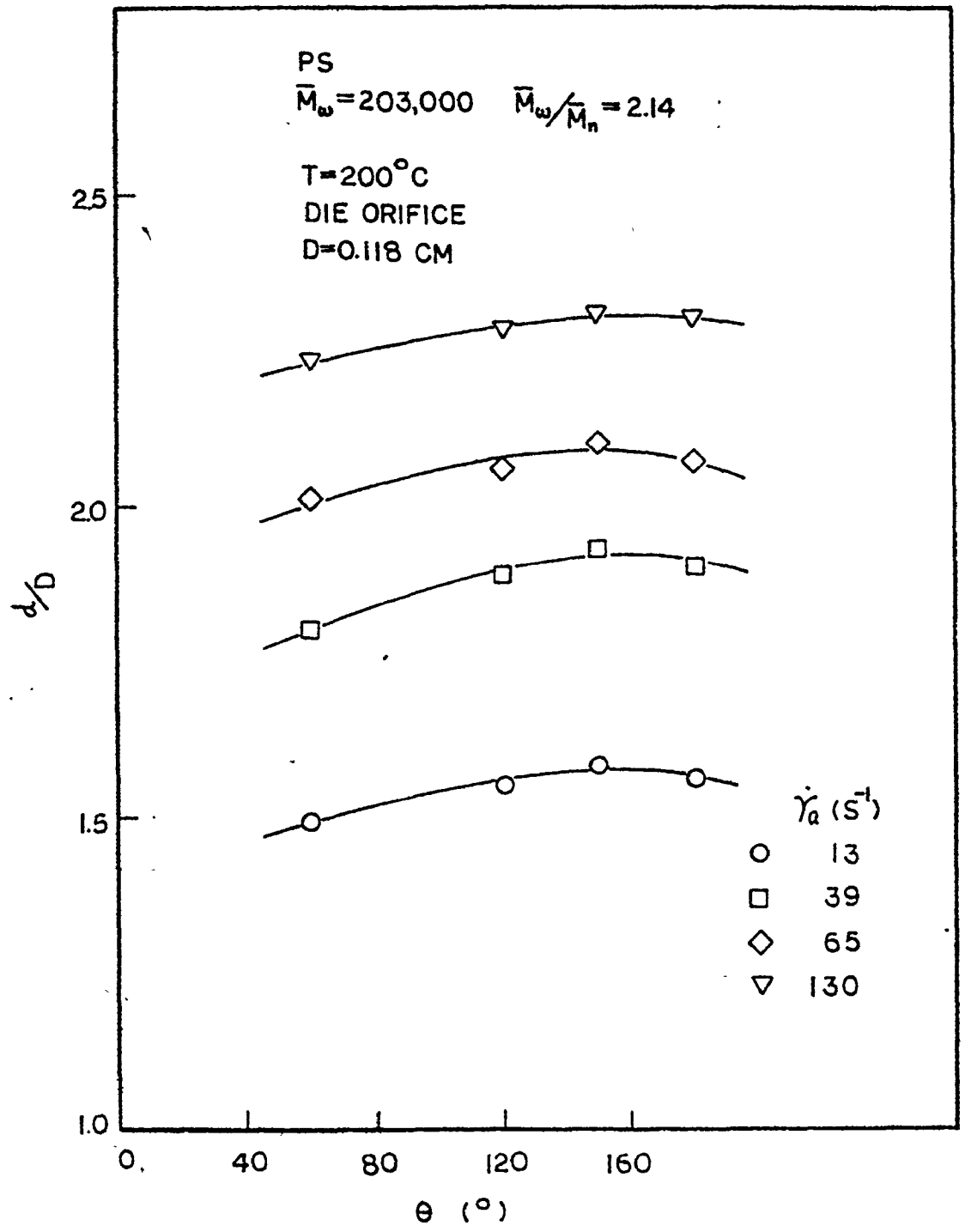

Fig.5.28 Plot of d/D vs. Entrance Angle θ for Polystyrene

Experimental investigations on die entry low in melts has been extensive (61,63,87,88). For low-density polyethylene and polystyrene, it is known that vortex-like flows in the die corners increase in size with extrusion rate. Bagley and Shreiber (89), and White and Kondo (63) have noted a reduction in vortex size with tapering angle at the die entry. The vortices arise as a stress relief mechanism and thus accounts for the experimental observation.

It is interesting to know that not all polymer melts exhibit vortices. However, melts of low-density polyethylene and polystyrene are known to have significant vortices (46, 63).

CHAPTER 6

ANALYSIS

6.1 Investigation on Bagley's Expression (37) Relating Extrudate Swell to L/D Ratio

As discussed in section 5.5, the actual die swell depends on the method of measurement. However, the relative change in die swell measurement for the polymers studied is small so that the effect of frozen-in-stresses can be neglected.

In the evaluation of Bagley's expression all the die swell measurements have been corrected to the extrusion temperature using eq.(2.8).

Bagley's expression (37) takes the following form:

$$(B - B_\infty) = (B_o - B_\infty)\exp[-C(L/R + e)] \qquad (6.1)$$

By taking logarithm on both sides of eq.(6.1) one obtains

$$\ln (B - B_\infty) = \ln (B_o - B_\infty) - C(L/R + e) \qquad (6.2a)$$

Alternatively,

$$\ln (B - B_\infty) = \ln (B_o - B_\infty) - 2C(L/D + N_c) \qquad (6.2b)$$

where $N_c = (e/2)$ = Bagley's end correction factor (72). In the limit when $B \to B_o$ or in case of die-orifice $L/D \to 0$, N_c must vanish so that

$$\lim_{L/D \to 0} \ln (B - B_\infty) = \ln (B_o - B_\infty) \qquad (6.3)$$

Plots of Nc versus pseudo-shear rate are shown in Figs.6.1 and 6.2 for low-density polyethylene and polystyrene. The constant C has been suggested (37) to be independent of shear rate, shear stress and residence time and dependent solely on the kind of polymer used. By means of eq.(6.2), the experimental data for the polymer studied seem to fit reasonable well. Typical results are shown in Figs.6.3 and 6.4 for low-density polyethylene and Fig.6.5 for polystyrene. All the parameters involved in eq.(6.2) are summarized in Tables 6.1 to 6.3 for the polymers investigated at different temperatures.

For the low-density polyethylene DHDY-6873 tested at 160°C, the data at different shear rates as shown in Fig.6.3 collapse to form a single straight line. However, at higher extrusion temperature (e.g.200°C as shown in Fig.6.4) the data fall apart forming a family of straight lines. But the slopes of the straight lines and hence the constant C are found to be almost the same. The value of C is approximately 0.072 and is independent of shear rate and temperature for the three low-density polyethylene samples studied.

The experimental data for polystyrene also from a family of straight lines (Fig.6.5). However, the values of the parameter C are found to decrease with shear rate at three extrusion

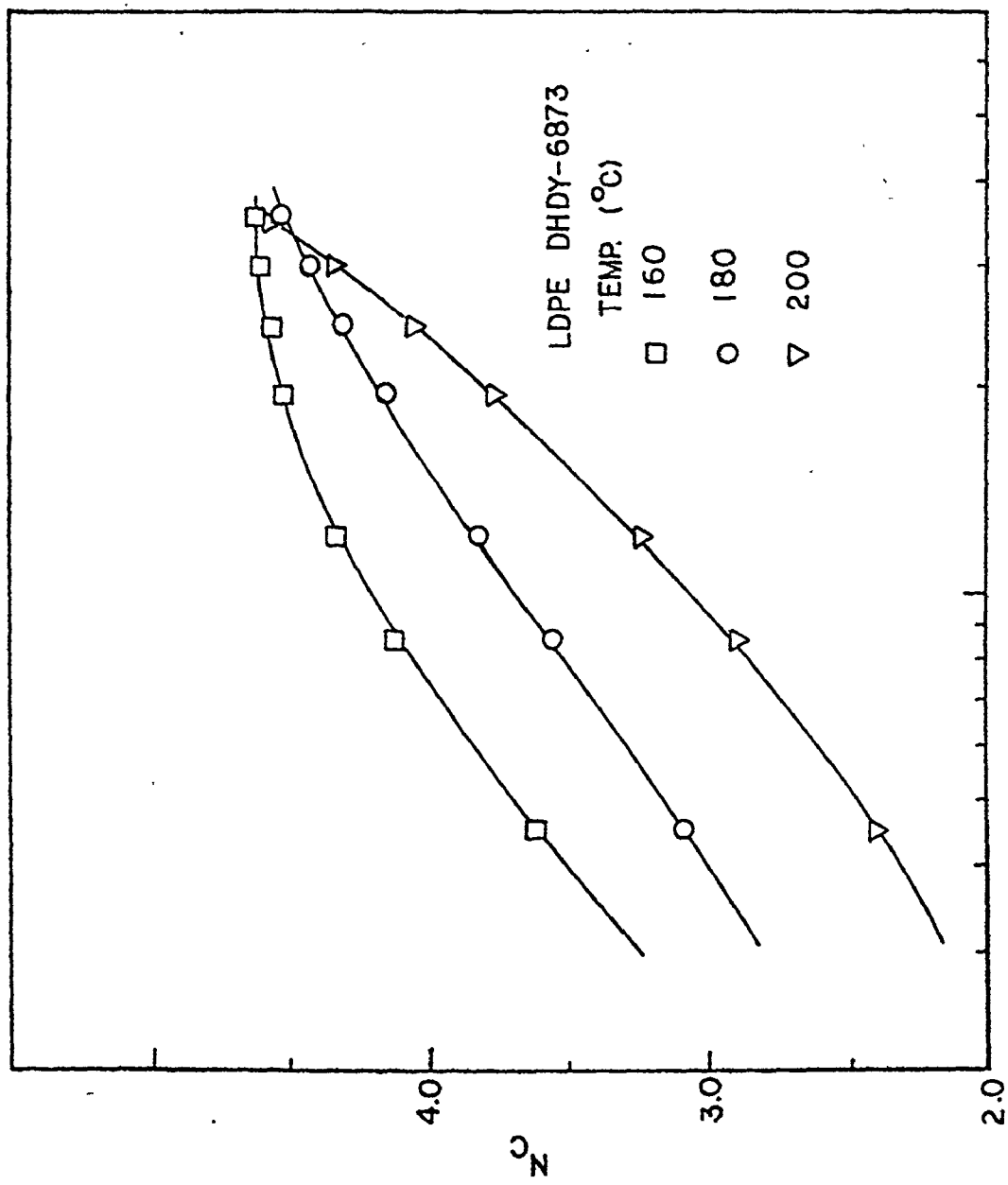

Fig.6.1 Plot of Bagley's End Correction vs. Pseudo-Shear Rate for LDPE

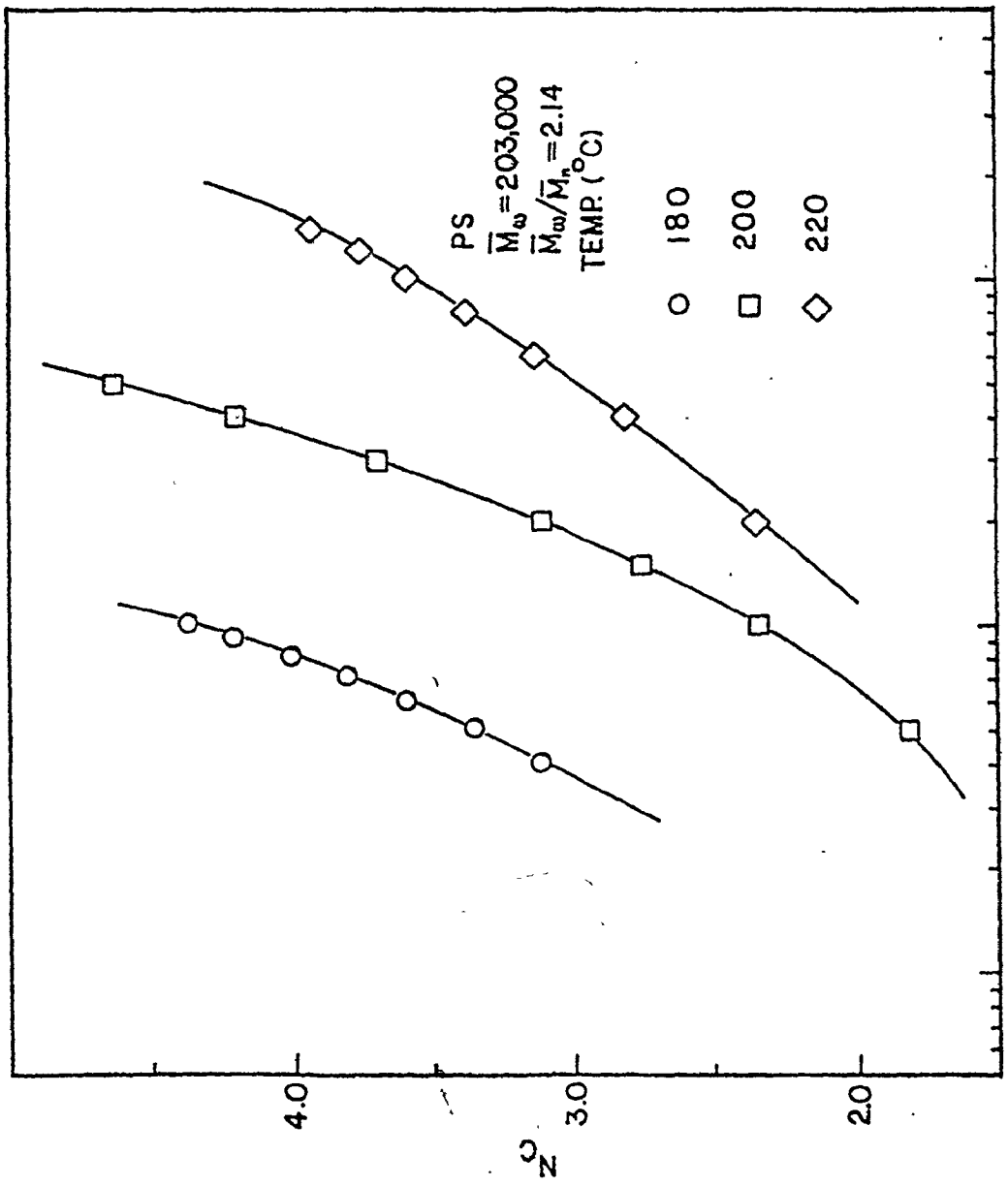

Fig.6.2 Plot of Bagley's End Correction vs. Pseudo-Shear Rate for PS

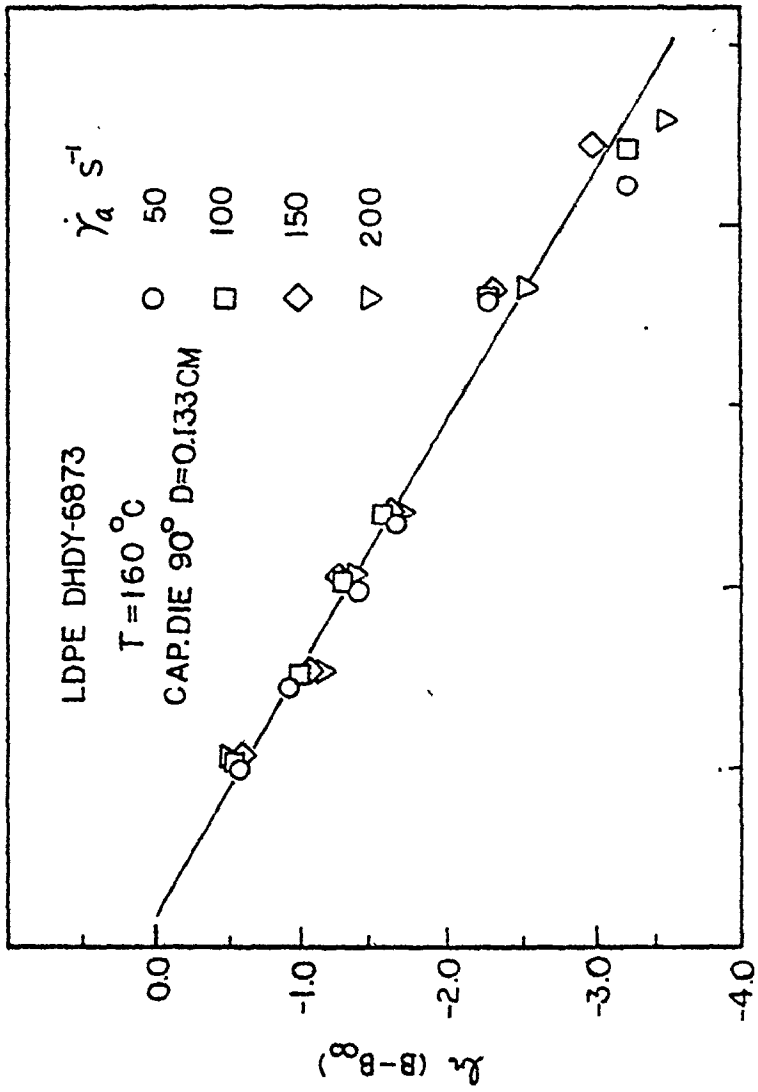

Fig.6.3 Plot of $\ln (B - B_\infty)$ vs. (L/D + Nc) for Low-density Polyethylene at 160°C

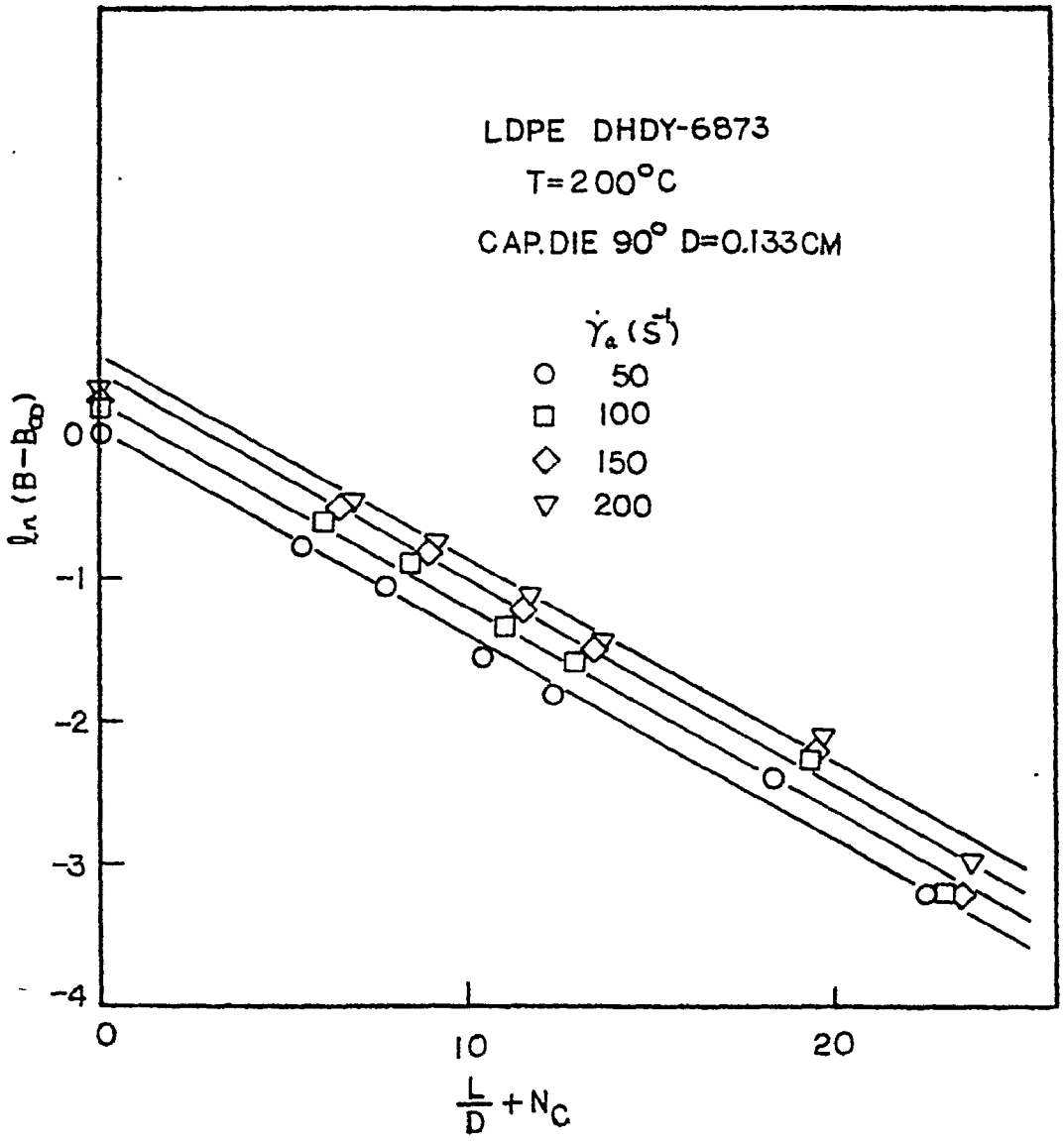

Fig.6.4 Plot of ln (B - B∞) vs. (L/D + Nc) for Low-density Polyethylene at 200°C

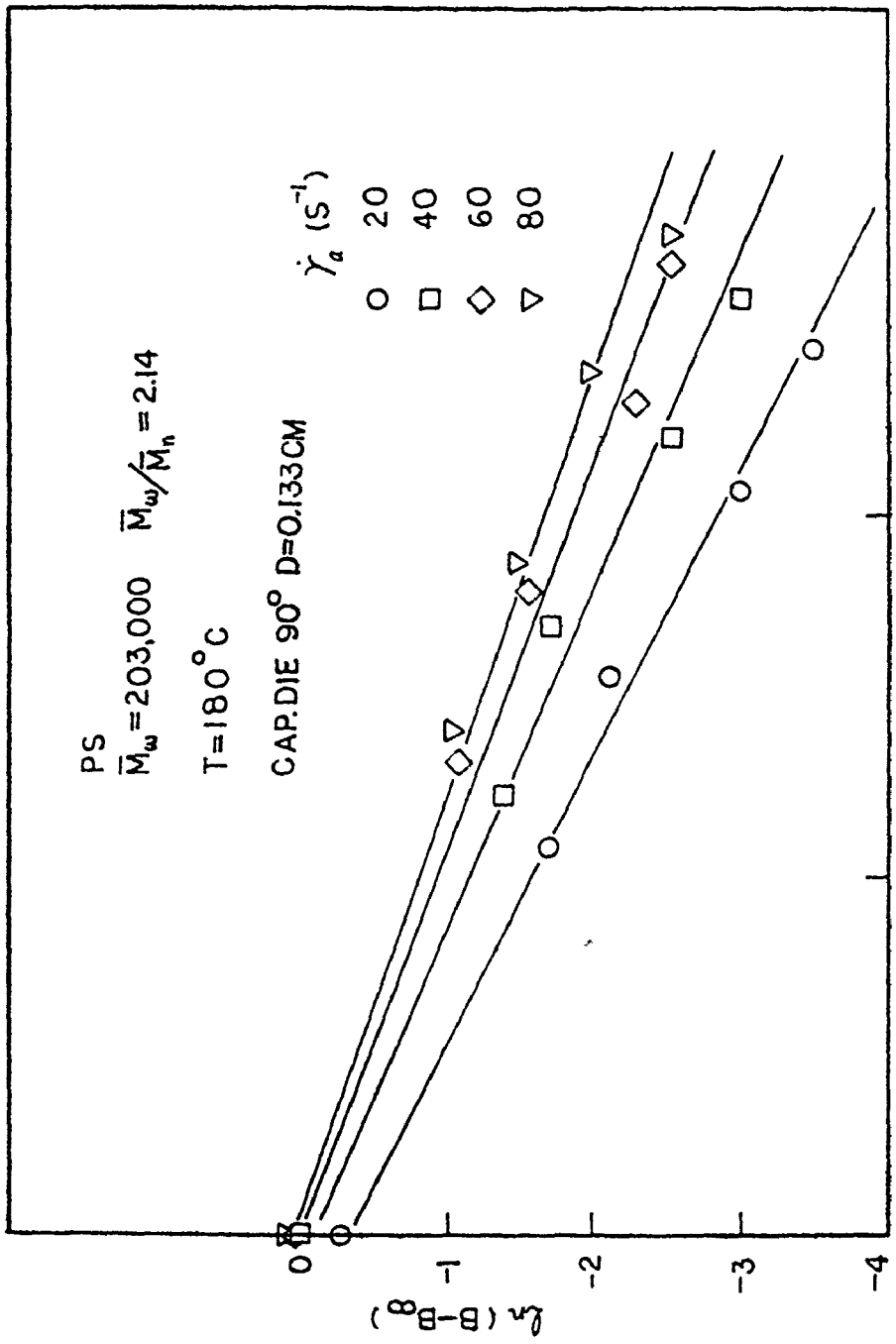

Fig.6.5 Plot of ln (B - B ∞) vs. (L/D + Nc) for Polystyrene at 180°C

Table 6.1

Parameters of Eq.6.2 for LDPE (DHDY-6873) at Different Temperatures

T (^{o}C)	160				180				200			
$\dot{\gamma}_a$ (1/s)	50	100	150	200	50	100	150	200	50	100	150	200
Bo	2.89	3.06	3.16	3.21	2.70	2.92	3.05	3.12	2.58	2.82	2.94	3.02
B_{∞}^{*}	1.55	1.63	1.68	1.72	1.56	1.63	1.67	1.71	1.53	1.60	1.64	1.67
Nc	3.70	4.22	4.44	4.53	3.15	3.66	3.98	4.17	2.45	3.05	3.50	3.80
C	0.073				0.072				0.072			

* die swell at L / D = 24.76 is assumed

Table 6.3

Parameters of Eq.6.2 for LDPE
DFDQ-4400 & DFDY-6600

T (°C)	220				250			
$\dot{\gamma}_a$ (1/s)	30	60	100	150	15	20	30	40
Bo	2.57	2.82	2.97	3.07	2.71	2.80	2.91	2.96
B_∞^*	1.62	1.68	1.72	1.78	1.58	1.61	1.65	1.67
Nc	2.67	2.97	3.80	3.88	3.05	3.60	4.35	4.90
C	0.071				0.070			

* die swell at L / D = 24.76 is assumed

Table 6.2

Parameters of Eq.6.2 for PS at Different Temperatures

$\bar{M}w$ = 203000 $\bar{M}w / \bar{M}n$ = 2.14

T (^{o}C)	180				200				220		
$\dot{\gamma}_a$ (1/s)	20	40	60	80	50	100	200	300	200	400	600
Bo	2.31	2.59	2.75	2.86	2.15	2.42	2.72	2.90	2.17	2.47	2.67
B_{∞}^{*}	1.56	1.66	1.72	1.77	1.54	1.64	1.76	1.85	1.58	1.70	1.75
Nc	2.40	3.10	3.60	4.00	1.83	2.33	3.10	3.70	2.36	2.85	3.15
C x 10	1.26	1.06	0.93	0.86	1.49	1.31	1.16	1.02	1.18	1.14	1.05

* die swell at L / D = 15.98 is assumed

temperatures.

Die swell data for the polyethylenes studied are used to fit Bagley's exponential equation (eq.6.2) and shown in Figs.6.6 to 6.8. However, the actual L/D ratios are replaced by the effective L/D ratios (L/D + Nc) to account for the entrance effect (section 3.2.6). Notably, the data correlate reasonably well with Bagley's expression.

The validity of the value of constant C in Bagley's decaying equation to other low-density polyethylene samples necessitates further investigation. Bagley et al (37) and Rogers (38) have indicated experimental data for the dependence of extrudate swell on L/D ratio of capillaries. However, these data are not sufficient to check the value of the constant C.

Extrudate swell is definitely an exponential decaying function of some sort which can be represented by many types of equation. Apparently, there is no direct correlation based on Bagley's idea. It is possible that a different exponential formulation will be applicable to the polystyrene samples but unfortunately not known to date.

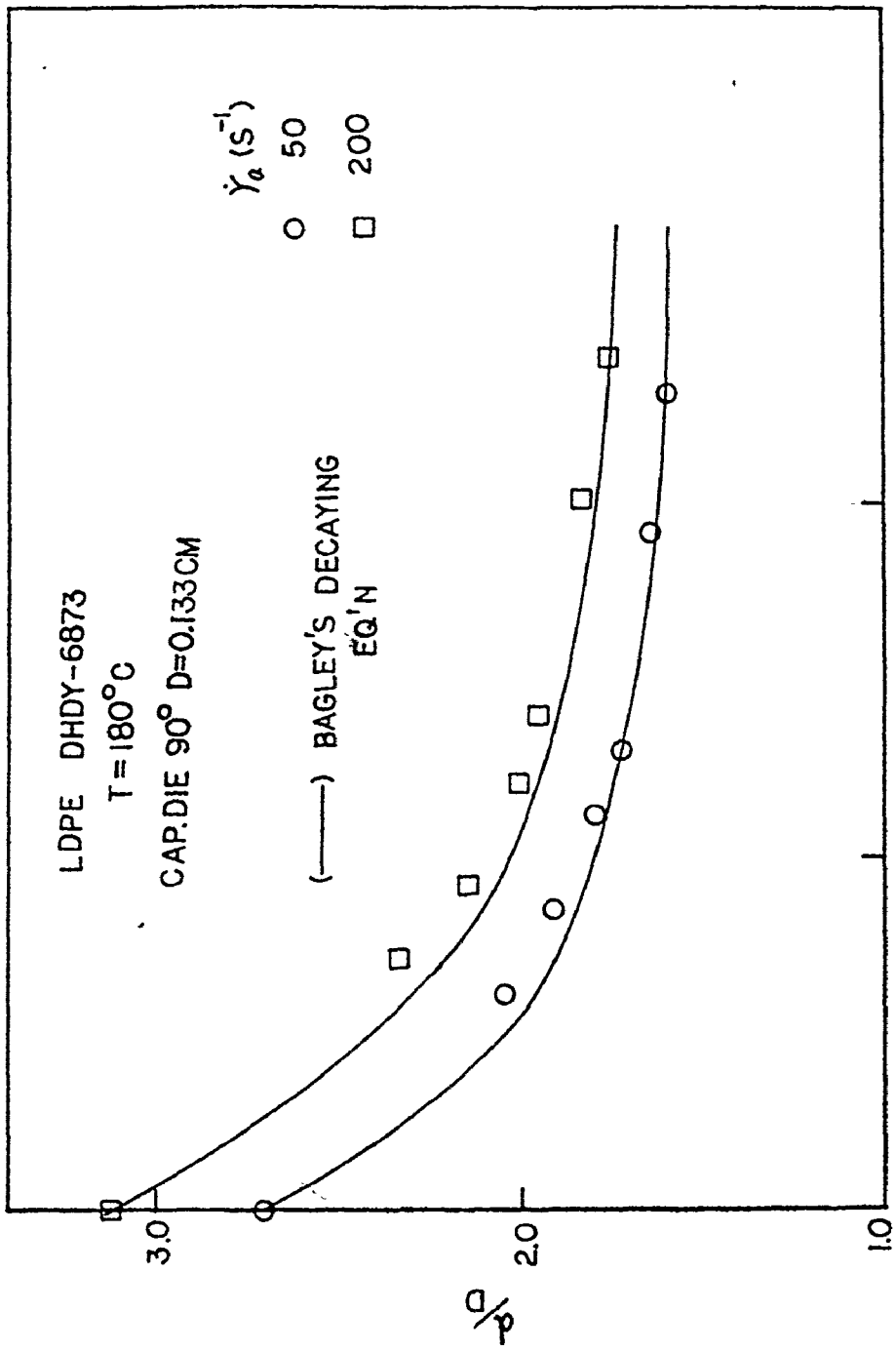

Fig.6.6 Plot of d/D vs. (L/D + Nc) for Low-density Polyethylene DHDY - 6873

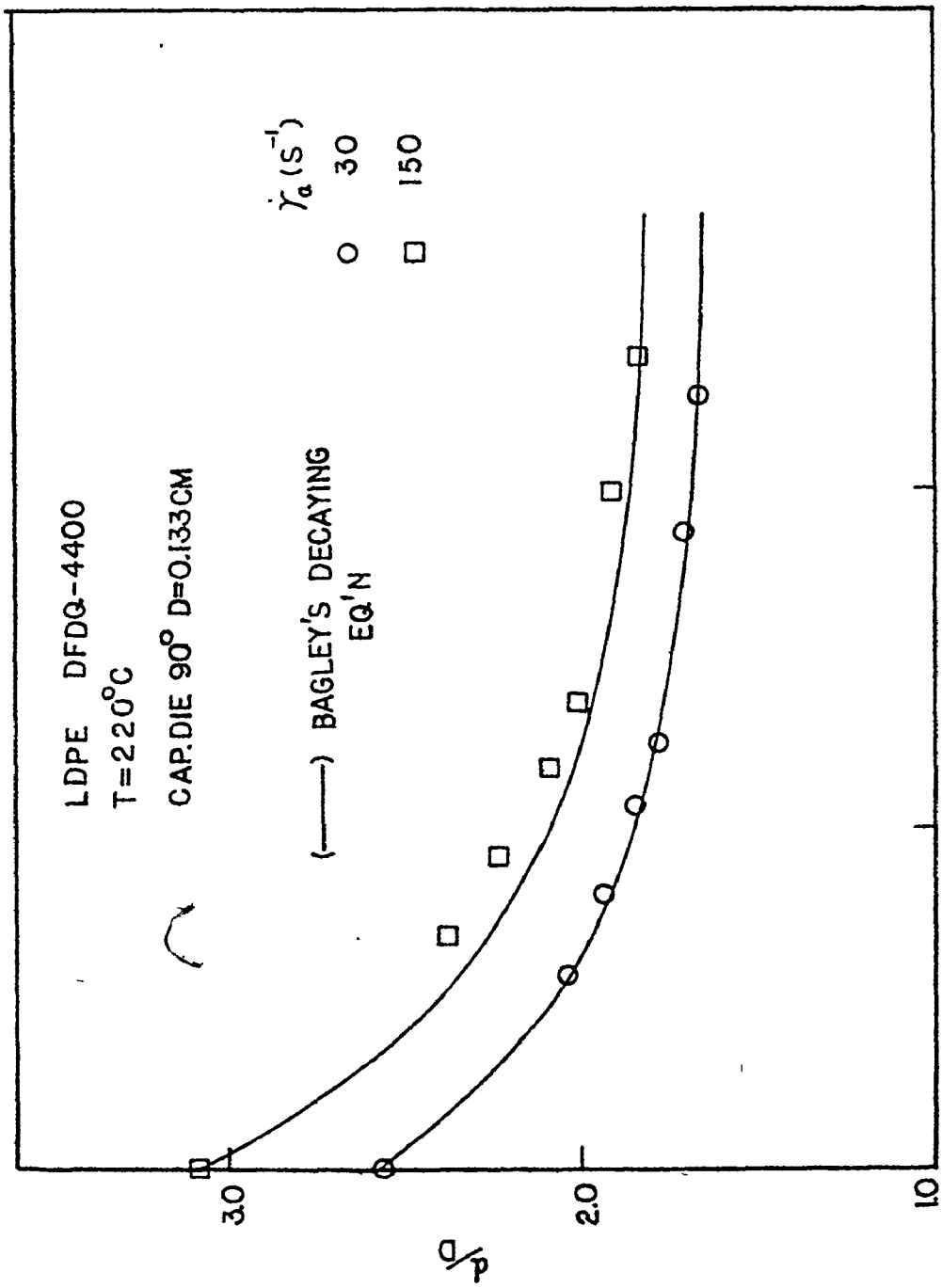

Fig.6.7 Plot of d/D vs. (L/D + Nc) for Low-density Polyethylene DFDQ - 4400

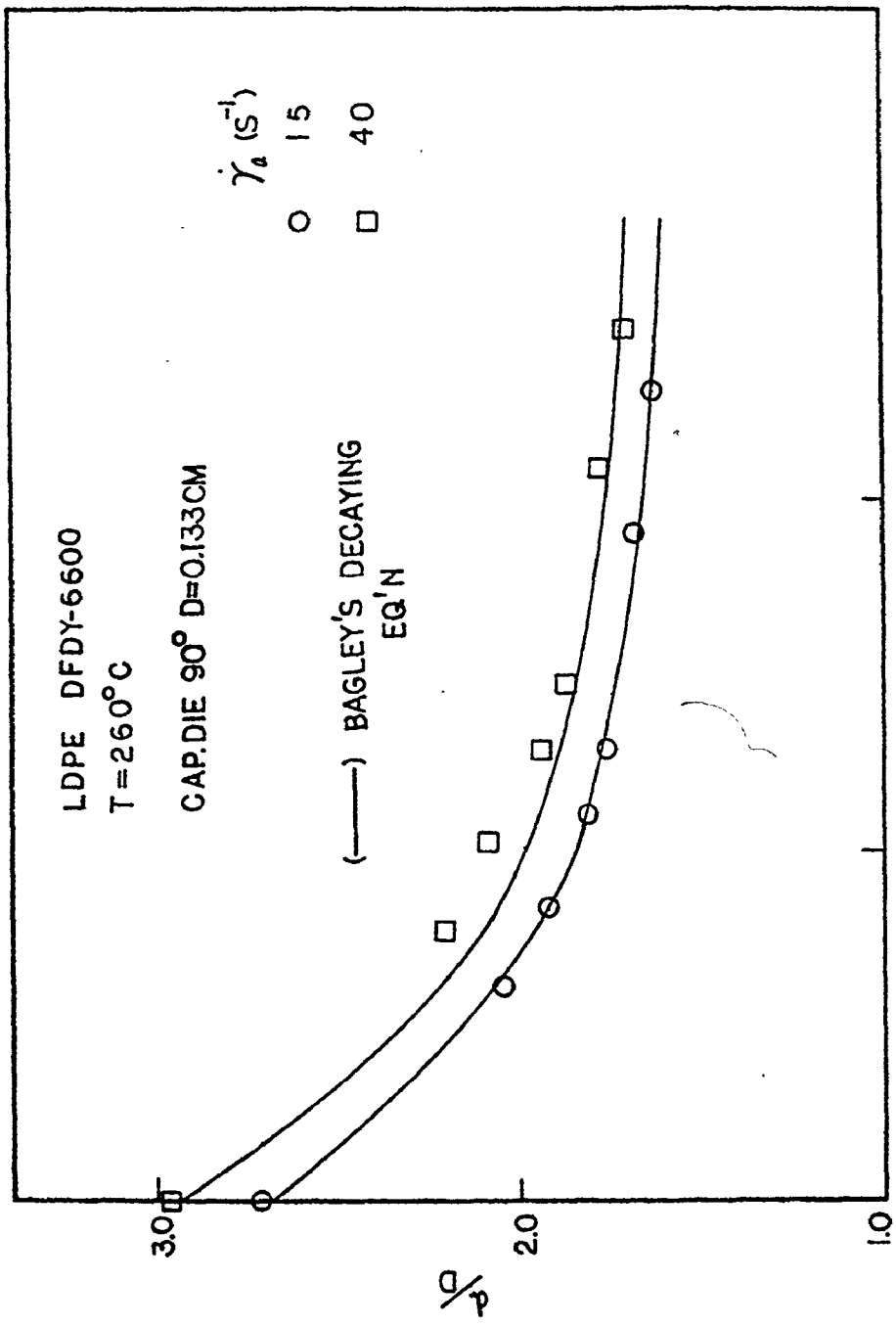

Fig.6.8 Plot of d/D vs. (L/D + Nc) for Low-density Polyethylene DFDY - 6600

6.2 Prediction of Extrudate Swell With Long Dies

Recently Huang and White (45) experimented with polypropylene and polystyrene melts using long slit and capillary dies. They compared the results with the theories of swell based on unconstrained recovery from Poiseuille flow of Tanner (24). They arrived the following expressions:

$$B_\infty = B_{Newt.} + \{ 1 + \frac{1}{8} (\frac{N_{1W}}{\tau_w})^2 \}^{1/6} \qquad \text{for capillary} \qquad (6.4)$$

& $$B_\infty = B_{Newt.} + \{ 1 + \frac{1}{12} (\frac{N_{1W}}{\tau_w})^2 \}^{1/4} \qquad \text{for slit} \qquad (6.5)$$

where $B_{Newt.}$ is the swell in the Newtonian region (section 2.2). $B_{Newt.}$ is 0.13 for capillaries (19,20,90) and 0.19 for slits (90).

Huang and White (45) further employed the empirical power law relation (82)

$$N_1 = A \tau_w^a \qquad (3.47)$$

for commercial polystyrene melts. Oda, White and Clark (82) obtained the values of A and a to be 3.47×10^{-3} $(Pa)^{0.66}$ and 1.6 for moderate molecular weight distribution polystyrenes, 6.48×10^{-6} (Pa) and 2.0 for narrow distribution polystyrenes.

Substitution of eq.(3.47) into eq.(6.4) yields

$$B_\infty = 0.13 + \{ 1 + \frac{1}{8} A^2 (\tau_w)^{2a-1} \}^{1/6} \qquad \text{for capillary} \qquad (6.6)$$

Following the recent discovery of thermal extrudate swell (29,30) (to be discussed in the subsequent section), Vlachopoulos (90) suggested the following:

$$B_\infty = B_{Newt.} + B_{elast.} + B_{inel.} + B_{relax.} \qquad (6.7)$$

which accounts for the mechanisms reponsible for extrudate swell

ing: A Newtonian swelling, a sudden elastic recovery, an inelastic (thermal) swelling and stress relaxation.

Presently, there is no theory to estimate $B_{relax.}$. However, its contribution to extrudate swell is small for polystyrene (35) and low-density polyethylene (52) melts but becomes significant for high-density polyethylene (27). The contribution due to thermal swell requires further investigation. Based on these arguments, Vlachopoulos (90) modified eqs.(6.4) and (6.5) so that

$$B_\infty = 0.13 + \{1 + \frac{1}{8}\left(\frac{N_{1W}}{\tau_w}\right)^2\}^{1/6} + B_{add} \qquad \text{for capillary} \qquad (6.8)$$

$$B_\infty = 0.19 + \{1 + \frac{1}{12}\left(\frac{N_{1W}}{\tau_w}\right)^2\}^{1/4} + B_{add} \qquad \text{for slit} \qquad (6.9)$$

where $B_{add} = B_{inel.} + B_{relax.}$.

In case where B_{add} is relatively small, the above equations become identical to eqs.(6.4) and (6.5) respectively.

The first normal stress difference N_1 is also obtainable through molecular weight measurement. As indicated in section 3.3,

$$\sigma_w = \tau_w J_o \qquad (3.20)$$

& $$\tau_{11} - \tau_{22} = N_1 = 2J_o \tau_w \qquad (3.21)$$

where J_o is the true shear comoliance at zero shear rate, σ_w and τ_w are the recoverable strain and shear stress at the wall respectively. Graessley and Segal (91,92) carried out rheogon-

iometry measurements on concentrated solutions and melts of polystyrene and correlated J_o with the Rouse shear compliance, J_R, at zero shear rate:

$$Jo = \frac{2.2J_R}{1 + 0.347\rho Eo} \qquad (6.10)$$

where $E_o = \bar{M}_w/16500$ and is the entanglement density at zero shear, ρ is the density/concentration for polymer melt/solution, and J_R is given by (57)

$$J_R = \frac{2}{5}\frac{\bar{M}z\,\bar{M}z+1}{\bar{M}w^2}\frac{\bar{M}w}{\rho RgT} \qquad (6.11)$$

where $\bar{M}w$, $\bar{M}z$, and $\bar{M}z+1$ are the weight-, z- and (z+1)-average molecular weights, T is the absolute temperature and Rg is the gas constant.

Thus, N_1 can be determined by means of the above four equations. However, the validity of these equations is restricted to limited ranges. In addition, it is very difficult to accurately measure the higher moment averages because they are sensitive to the presence of minute amount of high molecular tails.

Huang and White's expression for long capillary (eq.6.4) is evaluated using the polystyrene data at L/D=24.76 and compared with the models suggested by Graessley et al (35) and Tanner (24), i.e. eqs.(3.40) and (3.42). Both methods of estimating N_1 are employed. For the polystyrene sample studied, values of A and a

in eq.(3.47) are 3.47×10^{-3} $(Pa)^{0.66}$ and 1.66 respectively.

It is obvious from Fig.6.9 that the values of N_1 obtained from both methods are comparable. The models predicting die swell do not correlate very well with the experimental data. However, Graessly's expression (eq.3.40) gives better approximation. The models also predict a lower value of extrudate swell. This result may have come from the fact that the contribution due to stress relaxation and inelastic swelling, though small, should not be neglected.

Vlachopoulos suggestion (eq.6.7) for the prediction of extrudate swell with long capillary is true for all polymer samples However, there is no theory relating die swell to stress relaxation: it is worthwhile to look into this aspect. The empirical power law which relates N_1 to τ_w may also hold for other polymers other than polystyrene, further investigation on different polymers will be useful for future studies on die swell.

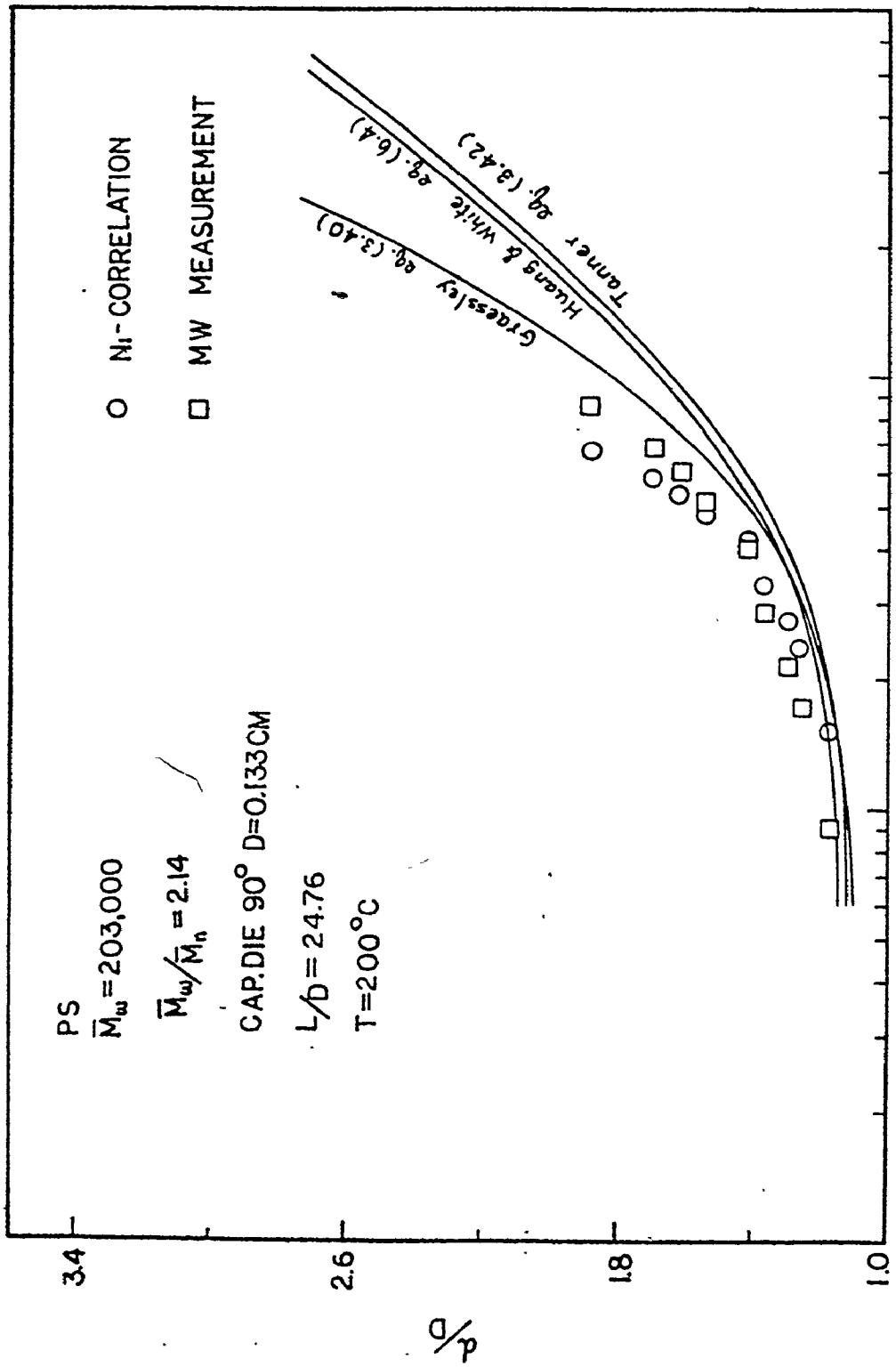

Fig.6.9 Plot of d/D vs. N_1/τ_w for Polystyrene

6.3 Thermal Extrudate Swell

Phuoc and Tanner (29) have recently discovered that Newtonian fluid, whose viscosity is temperature-dependent, exhibits thermal extrudate swell when the temperature difference between the centreline of the die and the wall is large. The variation in viscosity is given by

$$\eta = \bar{\eta} \exp[- \psi (T - Tw)] \qquad (6.12)$$

where $\bar{\eta}$ is the viscosity at wall temperature Tw , and ψ is a material constant. Their finite difference calculations have indicated that for moderate heating

$$B - B_{Newt.} = 0.16 \psi (Tmax - T) \qquad (6.13)$$

For typical low-density polyethylene viscosity values and usual extrusion conditions a swelling of about 70% was estimated (29,30). This additive thermal swell necessitates that the theory on die swell based on elastic recoil mechanism should be amended. Tanner (30) suggested that the thermal extrudate swell is due to the increased resistance to deformation of elongated filaments near the extrudate surface. He also showed that the swelling is predicted for power-law, variable-viscosity Newtonian, second-order and Maxwell fluids.

To investigate the order of magnitude of thermal (inelastic) swell, the viscosity-shear rate data obtained from long

capillary (L/D=24.76) for low-density polyethylene and polystyrene are used (Figs.6.8 and 6.9). Values of the material constant ψ at low and high shear rates at different extrusion temperatures are shown in Tables 6.4 and 6.5. The temperature rise due to viscous heating when operating with Instron's capillary rheometer is usually less than $1^{o}C$ (67). The estimated values of Ψ are small (<0.04) and by means of eq.(6.13) the thermal swell for the polymers studied are found to be negligible (<1%).

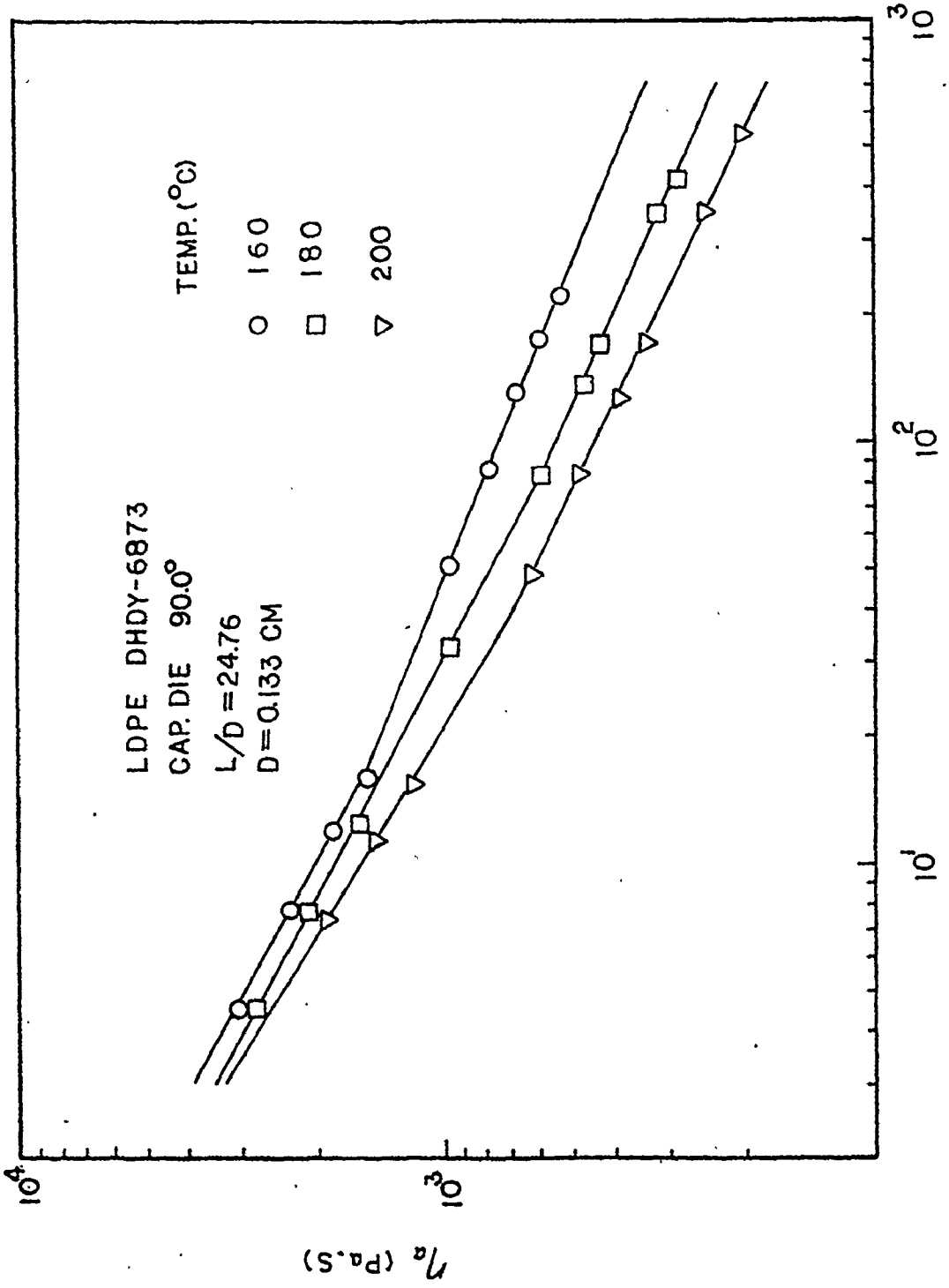

Fig.6.10 Viscosity-Shear Rate Data for Low-density Polyethylene

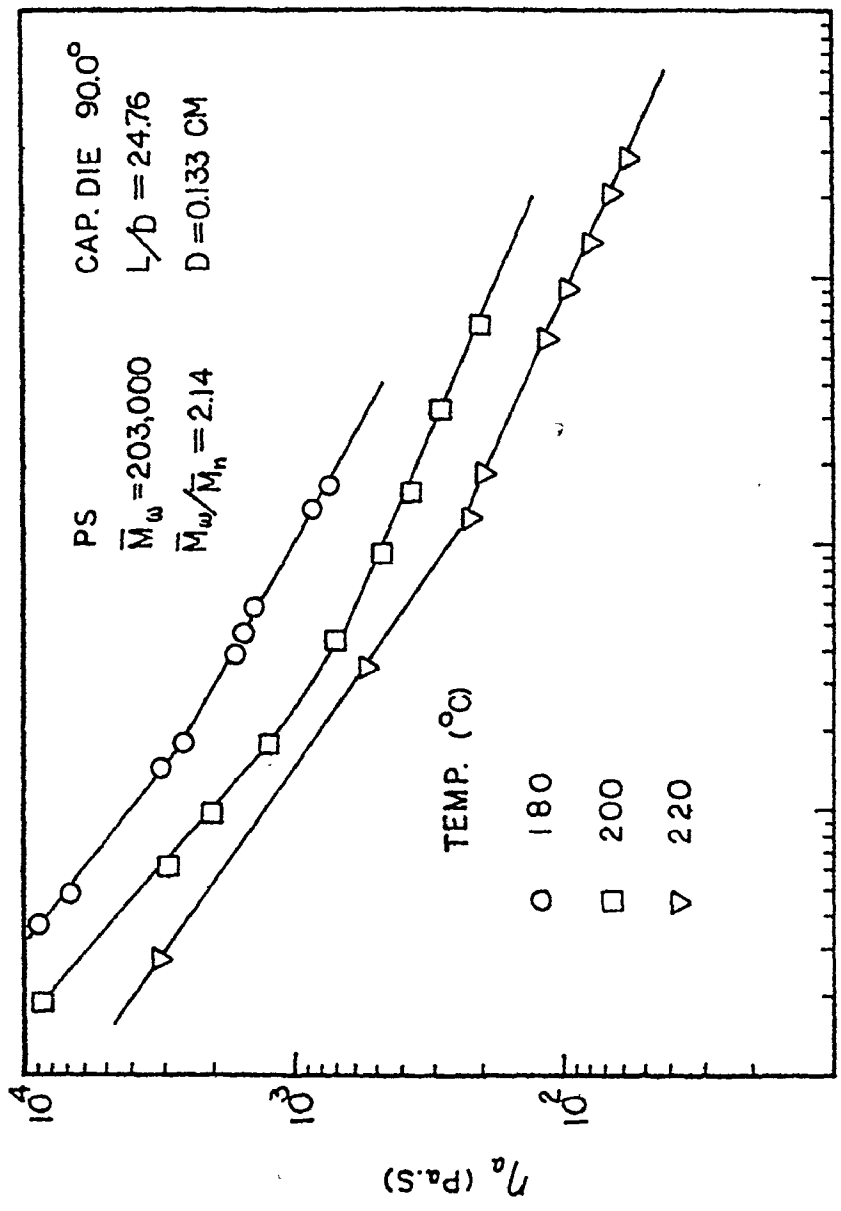

Fig.6.11 Viscosity-Shear Rate Data for Polystyrene

Table 6.4

Parameter ψ Obtained From Eq.6.12 for LDPE

	$\dot{\gamma}_w$ = 4 1/s			$\dot{\gamma}_w$ = 400 1/s		
Temp (^{o}C)	160	180	200	160	180	200
$\bar{\eta} \times 10^{-4}$ Pa.s	0.330	0.295	0.275	0.420	0.300	0.230
ψ at Tw = 160 ^{o}C	-	0.0056	0.0046	-	0.0168	0.0151
ψ at Tw = 180 ^{o}C	0.0056	-	0.0035	0.0168	-	0.0133
ψ at Tw = 200 ^{o}C	0.0046	0.0035	-	0.0150	0.0133	-

Table 6.5

Parameter ψ Obtained From Eq.6.12 for PS

	$\dot{\gamma}_w$ = 4 1/s			$\dot{\gamma}_w$ = 500 1/s		
Temp (^{o}C)	180	200	220	180	200	220
$\bar{\eta} \times 10^{-4}$ Pa.s	0.82	0.44	0.24	0.041	0.023	0.012
ψ at Tw = 180 ^{o}C	-	0.0311	0.0307	-	0.0289	0.0307
ψ at Tw = 200 ^{o}C	0.0311	-	0.0303	0.0289	-	0.0325
ψ at Tw = 220 ^{o}C	0.0307	0.0303	-	0.0307	0.0325	-

6.4 Prediction of Extrudate Swell With Short Dies

Based on dimensional analysis Huang and White (46) have recently developed a new expression to predit extrudate swell of short dies. They suggested that extrudate swell from short capillary and slit dies should be determined from the character of entrance flow since this the only flow history these melts know. They used the Weissenberg number We to represent rheological response so that

$$\lim_{L \to 0} B = B\left(t_{ch}\frac{Vch}{Lch} \text{ , } \begin{matrix}\text{dimensionless ratio of} \\ \text{viscoelastic constitutive,} \\ \text{parameters}\end{matrix} \text{ } \theta \right) \tag{6.14}$$

where $$We = \frac{t_{ch}\, Vch}{Lch} = t\dot{\gamma}_w = \frac{N_{1w}}{2\tau_w \dot{\gamma}_w}\dot{\gamma}_w = \frac{N_{1w}}{2\tau_w} \tag{3.49}$$

The parameters in eq.(3.49) are described in section 3.3.

By assuming $t_{ch} = \bar{t}$, one obtains

$$\bar{t} = \frac{N_{1w}}{2\tau_w \dot{\gamma}_w} \tag{6.15}$$

Next, they argued that the ratio Vch/Lch should be given by the elongation rate $\dot{\gamma}_{E1}$,i.e.

$$\left(\frac{Vch}{Lch}\right)_c = \dot{\gamma}_{E1c} \tag{6.16}$$

where the subscript "c" refers to capillary. The elongation rate for capillary is related to shear rate by

$$\dot{\gamma}_w = \sqrt{3}\dot{\gamma}_{E1c} \tag{6.17}$$

Previous studies on polystyrene (82) yield an empirical power law so that

$$N_1 = A(\tau_w)^a \tag{3.47}$$

From eqs.(6.15) and (3.47), one obtains

$$\bar{t} = \tfrac{1}{2} A \left(\tau_w \right)^{a-1} \dot{\gamma}_w^{-1} \qquad (6.18)$$

By assuming that the flow in the die entry region to be elongational in character and shear flow contribution is small (see Fig.3.4) and that $\bar{t}$ can be equared to effective relaxation time t_{eff} for Maxwellian fluids, the unconstrained recovery in the melt emerging from the die entry region is, after a minor correction,

$$B = \left[\frac{1 + 0.5\, t_{eff}\, \dot{\gamma}_{Elc}}{1 - t_{eff}\, \dot{\gamma}_{Elc}} \right]^{1/6} \qquad (3.53)$$

Since one never has an infinite swelling, the condition for the above equation to hold is that

$$t_{eff}\, \dot{\gamma}_{Elc} < 1 \qquad (6.19)$$

Under the above constraint, eq.(3.53) was found to be valid only at low shear rate region (<20 1/sec) for the polystyrene sample studied. This argument can also be confirmed by comparing their theoretical and experimental swelling ratios at higher rates as indicated in their paper (46).

By means of eqs.(6.15),(6.17) and (6.18), the new model for short dies is tested with the present polystyrene data and is shown in Fig.6.10. The data correlate well at low shear rates (<20 1/sec) but deviate considerably at higher shear rates (>35 1/sec). The reason the latter phenomenon may have come

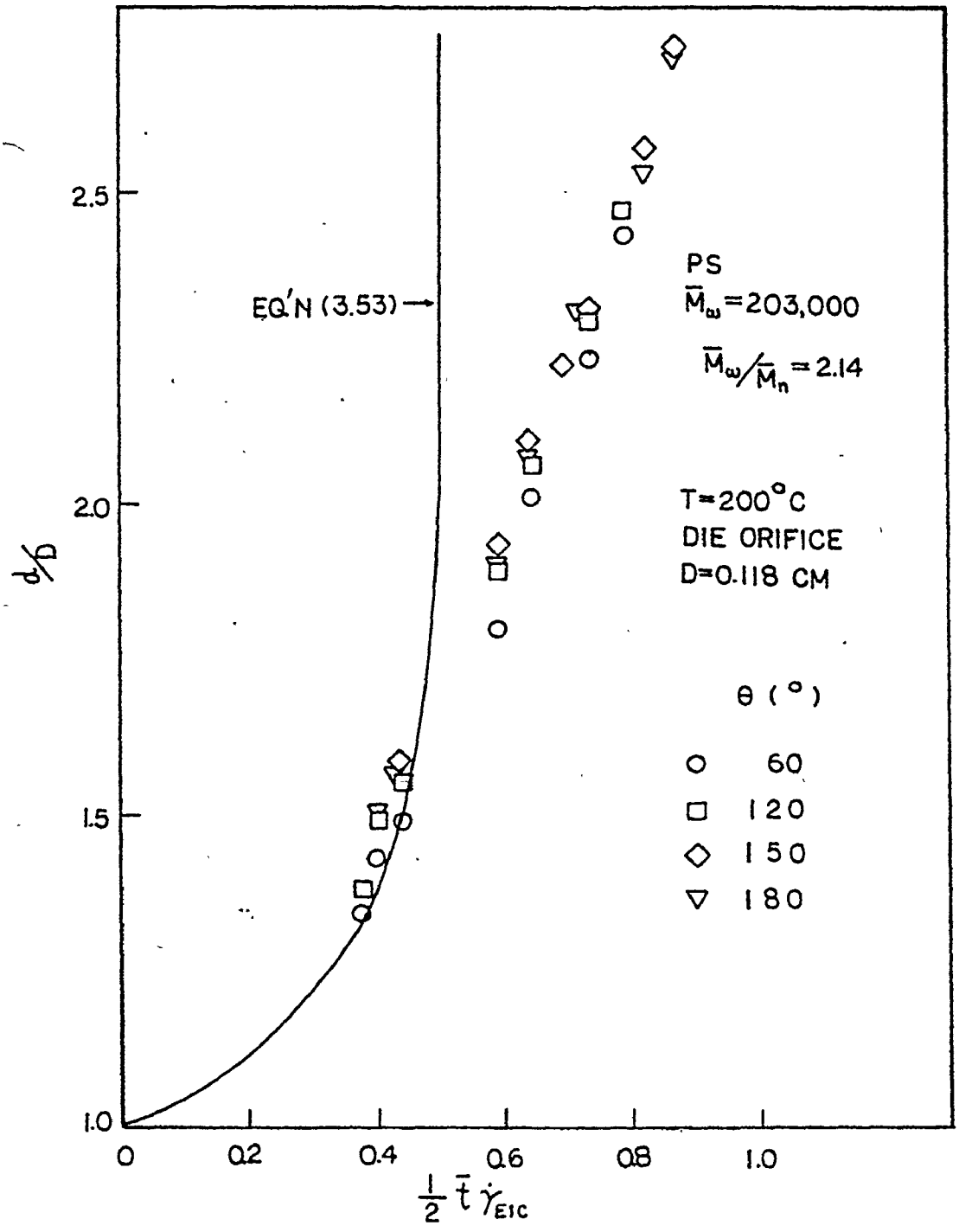

Fig.6.12 Plot of d/D vs. $\frac{1}{2}\bar{t}\,\dot{\gamma}_{E1c}$

from the fact that the flow in the entry region is actually elongational and shear in character. Flow of this kind is complex and there is no reliable theory, which is based on the analysis of this combination of flow in the entry region, to predict extrudate swell.

CHAPTER 7

CONCLUSIONS

For the low-density polyethylene and polystyrene samples studied, the following conclusion can be drawn:

1. extrudate swell increases with shear rate,
2. extrudate swell increases with shear stress,
3. at constant shear rate extrudate swell decreases with temperature but the maximum attainable swell, before the onset of melt fracture, increases with temperature,
4. the effect of "frozen-in-stress" on extrudate swell is not pronounced,
5. extrudate swell decays exponentially with the L/D ratio of the capillary dies,
6. extrudate swell increases with the reservoir-to-capillary diameter ratio up to a certain value and decreases thereafter,
7. swelling ratio increases with increasing entry angle of die-orifice up to 150° beyond which value extrudate swell decreases,
8. the parameter C in Bagley's decaying equation is found to be about 0.072 and is independent both of shear rate and

temperature for low-density polyethylene, but decreases with shear rate at constant temperature and increases with temperature at constant shear rate for polystyrene,

9. the inelastic (thermal) extrudate swell is insignificant for capillary dies,

10. for long capillary dies, expressions predicting extrudate swell as suggested by Graessley and Tanner together with Huang and White's new model are used to correlate the polystyrene data. This new expression predicts slightly better die swell than Tanner's expression. However, Graessley's equation gives better approximation,

11. Huang and White's new expression for short capillary dies is applicable only in the low shear rate region. It is found that at shear rate higher than 30 1/sec for the polystyrene studied, the model does not correlate well with the data.

CHAPTER 8

RECOMMENDATIONS

The mechanism of swelling process is complicated both with short and long dies. The available expressions predict extrudate swell reasonably well at low shear rate regions only. At higher shear rates they do not correlate well with experimental results. The development of these expressions neglect the contribution of swelling due to thermal swell and stress relaxation. Though thermal swell is found to be insignificant for the polymers studied at low shear rate, it has not been justified with other polymer samples at higher shear rates. Further work in this aspect would be worthwhile. At present, there is no reliable theory relating stress relaxation to extrudate swell. Extrudate swell due to stress relaxation should not be neglected at high shear rate. Additional study in this aspect would be useful.

Besides polystyrene samples no empirical power law, which relates the first normal stress difference to shear stress, is available for other polymers. To obtain a similar correlation, experimental study on standard polymers such as polypropylene, low- and high-density polyethylenes will be necessary. Al-

though Bagley's decaying equation, which relates die swell to L/D ratio of capillary dies, could only be used for curve fitting purpose, it would be interesting to know how the parameter C in his expression varies with different polymers, and hence with molecular weight and molecular weight distribution.

More work on extrudate swell with short dies would be of practical importance for polymer processing. In addition, investigation of extrudate swell using different die geometry, such as slit (rectangular) and polygonal dies, would be useful in the design of extrusion dies.

NOMENCLATURE

A, a	constants defined by eq.(3.47)
Ao	cross-sectional area of the capillary
B	swelling ratio
Bo, B_∞	values of B at zero and infinite transit times
b_1, b_2	constants defined by eq.(5.3)
C	parameter in Bagley's decaying eq.(6.1)
C_1	constant defined by eq.(3.29)
c	Boltzman's constant
D	diameter of capillary
Dp	diameter of plunger
d	extrudate diameter corrected to extrusion temperature
d_o	diameter of frozen extrudate
E	constant defined by eq.(5.1b)
$\bar{F}$	force field
Fp	force on the plunger
f_b	force acting along the axis of the capillary
G	shear modulus
G_2	relaxation modulus of the Voigt element
I_1, I_2, I_3	first, second and third strain invariant
Jo	shear compliance

K	consistency index
k	decay rate constant
L	length of capillary
Lch	characteristic length
MW	molecular weight
Mn	number-average MW
Mw	weight-average MW
Mz	z-average MW
Mz	(z+1)-average MW
m	constant defined by eq.(5.1b)
N_1	first normal stress difference
Na	number of chains per unit volume
Nc	Bagley's end correction factor
n	flow index
P	pressure
Q	volumetric flow rate
R	radius of capillary
Re	Reynolds number
r,θ,z	cylindrical co-ordinates
r_o	radius vector defined by eq.(3.51)
T	absolute temperature
t_{ch}	characterisitc time

t	average time of transit through the die
t_a	volume-average transit or residence time
t_{zz}	tensile stress acting along the capillary axis
$\bar{V}$	velocity vector
Vch	characteristic velocity
Vp	plunger speed
W	stored energy function
We	Weissenberg number

Greek Letters

α	natural flow angle
β	parameter in eq.(2.7)
$\dot{\gamma}$	shear rate
$\dot{\gamma}_a$	pseudo-shear rate
$\dot{\gamma}_{Ez}$	elongation rate
$\dot{\gamma}_w$	true shear rate
Δ	parameter in eq.(2.7)
η ,$\bar{\eta}$	viscosities of temperature-dependent Newtonian fluids related by eq.(6.12)
η_a	apparent viscosity
θ	entrance angle of capillary die
λ	square of swelling ratio

$\lambda_1, \lambda_2, \lambda_3$	principal extension ratios
μ_1	dynamic viscosity of the dash-pot
μ_2	dynamic viscosity of the Voigt element
ρ	density of polymer melt at extrusion temperature
ρ_o	density of frozen polymer at room temperature
σ	recoverable shear strain
$\bar{\sigma}$	average recoverable shear
σ_w	recoverable shear strain at the wall
$\tau, \tau_{rz}, \tau_{12}$	shear stress
$\bar{\bar{\tau}}$	stress tensor
$\tau_{11}, \tau_{22}, \tau_{33}$	normal stresses
τ_t	tensile stress
τ_w	true shear stress
ψ	material constant defined by eq.(6.12)

Subscripts

c	capillary
s	slit
w	wall

REFERENCES

1. Dillon, J.H. and N. Johnston, Physics, 4, 225 (1933).
2. Dillon, J.H. and N. Johnston, Rubber Chem. Technol., 7, 248 (1934).
3. Brydson, J.A., "Flow Properties of Polymer Melts", Van Nostrand Rheinold Co., New York (1970).
4. Holmes-Walker, W.A., "Polymer Conversion", Halsted Press, Wiley (1975).
5. Wechsler, R.L. and T.H. Baylis, Mod. Plast., 36, 107 (1959).
6. Wilson, W.R.K., International Congress Technol., Plastic Process, Proc. Discuss., Amsterdam (1960).
7. Beynon, D.L.T. and B.S. Glyde, Br. Plast., 33, 416 (1960).
8. Burgess, H. and H.I. Lewis, Br. Plast., 34(3), 177 (1961).
9. Kaltenbacher, E.J., J.K. Lund and R.A. Mendelson, S.P.E. Jl., 23(11),55 (Nov 1967).
10. Edwards, R., TAPPI, 49(4), 55A (1966).
11. White, C.E., Plast. Technol., 12, 41 (1966).
12. Hall, D.A. and W.B.I. Small, Plastics (London), 31, 269 (1966).
13. Spencer, R.S. and R.E. Dillon, J. Colloid Sci., 3, 163 (1948).

14. Spencer, R.S. and R.E. Dillon, J. Colloid Sci., 4, 241 (1949).

15. Brau, I. and M. Reiner, Quart. J. Mech. Appl. Math., 5, 12 (1952).

16. Goren, S.L., S. Middleman and J. Gavis, J. Appl. Polym. Sci., 3(9), 367 (1960).

17. Gavis, J. and S. Middleman, J. Appl. Polym. Sci., 7, 493 (1963).

18. Gavis, J. and M. Modan, Phys. Fluids, 10, 487 (1967).

19. Batchelor, J. and F. Horsfall, Rub. Plast. Res. Assoc. G.B. Res. Rep. 189 (1971).

20. Tanner, R.I., Appl. Polym. Symp., No.20, 201 (1973).

21. Nakajima, N. and M. Shida, Trans. Soc. Rheol., 10, 299 (1966).

22. Lodge, A.S., "Elastic Liquids", Academic Press, New York (1964).

23. Bernstein, B., E. Kearsley and L. Zapas, Trans. Soc. Rheol., 7, 391 (1963).

24. Tanner, R.I., J. Polym. Sci., A2, 8, 2067 (1970).

25. White, J.L., Trans. Soc. Rheol., 19, 271 (1975).

26. Huilgol, R.R., "Continuum Mechanics of Viscoelastic Liquids", Halsted Press, New York (1975).

27. White, J.L. and J.F. Roman, J. Appl. Polym. Sci., 20, 1005 (1976).

28. Pearson, J.R.A. and R. Trottnow, J. Non-Newt. Fluid Mech., 4, 195 (1978).

29. Phuoc, H.B. and R.I. Tanner, Thermally-induced Extrudate Swell, J. Fluid Mech. (1980) to appear.

30. Tanner, R.I., J. Non-Newt. Fluid Mech., 6, 289 (1980).

31. Kiselev, A.P. and I.F. Kanavets, Soviet Plastics, 34 (Oct. 1967).

32. Mendelson, R.A., F.L. Finger and E.B. Bagley, J. Polym. Sci., 35(Pt.C), 177 (1971).

33. Chapoy, L.L. and S. Pedersen, Polym. Eng. Sci., 17(10), 724 (1977).

34. Rokudai, M., Kobunshi Ronbunshu, 36(1), 21 (1979).

35. Graessley, W.W., S.D. Glasscock and R.L. Crawley, Trans. Soc. Rheol., 14, 519 (1970).

36. Mooney, M., "Rheology", Academic Press, vol.2, p.196, New York (1958).

37. Bagley, E.B., S.H. Storey and D.C. West, J. Appl. Polym. Sci., 7, 1661 (1963).

38. Rogers, M.G., J. Appl. Polym. Sci., 14, 1679 (1970).

39. Kawasaki, N., Tatsusaka and Ono, Kobunshi Kagaku, 30

(338), 326 (1973).

40. Kamide, K., Y. Inamoto and K. Ohno, Kobunshi Kagaku, 22(244), 505 (1965).

41. Vlachopoulos, J., M. Horie and S. Lidorikis, Trans. Soc. Rheol., 16, 669 (1972).

42. Mori, Y. and K. Funatsu, J. Appl. Polym. Sci., 20, 209 (1973).

43. Han, C.D. and W. Philipoff, Trans. Soc. Rheol., 14, 393 (1970).

44. Arai, T. and H. Aoyama, Trans. Soc. Rheol., 7, 333 (1963).

45. Huang, D.C. and J.L. White, Polym. Eng. Sci., 19, 609 (1979).

46. Huang, D.C. and J.L. White, Polym. Eng. Sci., 20, 182 (1980).

47. Han, C.D. and M. Charles, Trans. Soc. Rheol., 14, 213 (1970).

48. Utracki, L.A., Z. Bakerdjian and M.R. Kamal, J. Appl. Polym. Sci., 19, 481 (1975).

49. Cogswell, F.N., Plastics and Polymers, 391 (Dec 1970).

50. Petraglia, G. and A. Coen, Polym. Eng. Sci., 10, 79 (1970).

51. Han, C.D. and T.C. Yu, AIChE J., 17, 1512 (1971).

52. Mendelson, R.A. and F.L. Finger, J. Appl. Polym. Sci., 17, 797 (1973).

53. McCord, R.A. and B. Maxwell, Mod. Plast., 39, 116 (Sept 1961).

54. Sieglaff, C.L., Soc. Plastics Engrs. Trans., 4(2), 129 (1964).

55. Racin, R. and D.C. Bogue, J. Rheol., 23, 263 (1979).

56. Horie, M., M. Eng. Thesis, McMaster University, Hamilton, Ontario, Canada (1972).

57. Vlachopoulos, J. and M. Alam, Polym. Eng. Sci., 12(3), 184 (1972).

58. Vlachopoulos, J. and T.W. Chan, J. Appl. Polym. Sci., 21, 1177 (1977).

59. Vlachopoulos, J. and S. Lidorikis, Polym. Eng. Sci., 11(1), 1 (1971).

60. Chan, T.W., M. Eng. Thesis, McMaster University, Hamilton, Ontario, Canada (1975).

61. Ballenger, T.F. and J.L. White, J. Appl. Polym. Sci., 15, 1949 (1971).

62. Ballenger, T.F., I.J. Chen, J.W. Crowder, G.E. Hagler, D.C. Bogue and J.L. White, Trans. Soc. Rheol., 15, 195 (1971).

63. White, J.L. and A. Kondo, J. Non-Newt. Fluid Mech., 3,

77 (1977).

64. Rabinowitsch, B., Z. Phys. Chem., A145, 1 (1929).

65. Van Wazer, J.R., J.W. Lyons, K.Y. Kim and R.E. Colwell, "Viscosity and Flow Measurement", Interscience, New York (1963)

66. Brodkey, R.S., "The Phenomena of Fluid Motions", Addison-Wesley Publishing Co. (1967).

67. Middleman, S., "The Flow of High Polymers", Wiley, New York (1968).

68. Dodge, D.W. and A.M. Metzner, AIChE J., 5, 2, 189 (1959).

69. Lupton, J.M. and J.W. Regester, Polym. Eng. Sci., 5, 235 (1965).

70. Spencer, R.S. and G.D. Gilmore, J. Appl. Phys., 20, 502 (1949).

71. Pezzin, G., Instron Application Series, PC-12 (1972).

72. Bagley, E.B., J. Appl. Phys., 28, 624 (1957).

73. Merz, E.H. and R.E. Colwell, ASTM Bulletin, No.232 (1958).

74. Shroff, R.N., L.V. Cancio and M. Shida, Trans. Soc. Rheol., 21, 429 (1977).

75. Metzger, A.P. and J.R. Knox, Trans. Soc. Rheol., 9, 13 (1965).

76. Colbert, G.P. and K.D, Ziegel, Paper presented at the Con-

ference of Society of Rheology at Boston, Mass., Oct 28 - Nov 1 (1979).

77. Coleman, B.D. and H. Markovitz, J. Appl. Phys., 35, 1 (1964).

78. Treloar, L.R.G., "The Physics of Rubber Elasticity", Oxford University Press (1967).

79. Bagley, E.B. and H.J. Duffey, Trans. Soc. Rheol., 14, 545 (1970).

80. LaNieve, H. and D.C. Bogue, J. Appl. Polym. Sci., 12, 353 (1968).

81. Rivlin, R.S., "Rheology", F.R. Eirich Ed., vol.1, ch.10, Interscience, New York (1956).

82. Oda, K., J.L White and E.S. Clark, Polym, Eng. Sci., 18, 25 (1978).

83. McKelvey, J.M., "Polymer Processing", Wiley (1962).

84. Smelkov, R.E. and N.A. Kozulin, Zh. Prikl. Khim., 35(12), 2693 (1962).

85. Han, C.D. and K.U. Kim, Polym. Eng. Sci., 11, 395 (1971).

86. Han, C.D., "Rheology in Polymer Processing", Academic Press, (1976).

87. Bagley, E.B. and A.M. Birks, J. Appl. Phys., 31, 556 (1960).

88. Cable, P.J. and D.V. Boger, AIChE J., 24(5), 869 (1978).

89. Bagley, E.B. and H.P. Shreiber, Trans. Soc. Rheol., 5, 341 (1961).

90. Vlachopoulos, J., Extrudate Swell in Polymer Rheology, Rev. Deform. Behav. Mat. (1980) to appear.

91. Graessley, W.W. and L. Segal, Macromol., 2, 49 (1969).

92. Graessley, W.W. and L. Segal, AIChE J., 16, 261 (1970).

APPENDIX

EXPERIMENTAL RESULTS

LDPE DHDY-6873

TEST TEMPERATURE = 160.0 DEG C

DIAMETER OF CAPILLARY = .133 CM

ENTRANCE ANGLE = 90.0 DEG

L/D	$\Delta P \times 10^{-6}$	$\dot{\gamma}_a$	$\tau_\omega \times 10^{-4}$	$\dot{\gamma}_\omega$	B	B+	t_a
-	PASCAL	1/SEC	PASCAL	1/SEC	-	-	SEC
	1.75	3.89	1.55	4.51	1.29	1.36	50.96
	2.34	6.48	2.08	7.73	1.32	1.39	30.58
	2.98	9.72	2.64	11.86	1.35	1.43	20.38
	3.42	12.96	3.03	16.01	1.37	1.45	15.29
24.76	5.90	38.87	5.19	50.37	1.45	1.53	5.10
	7.49	64.79	6.54	85.63	1.49	1.58	3.06
	8.80	97.18	7.63	130.12	1.54	1.62	2.04
	10.11	129.58	8.71	175.42	1.57	1.66	1.53
	11.28	161.97	9.66	221.16	1.60	1.69	1.22
	2.20	7.77	2.35	9.35	1.36	1.44	20.58
	2.55	10.37	2.72	12.64	1.39	1.46	15.44
	2.84	12.96	3.03	15.96	1.39	1.47	12.35
	4.09	25.92	4.34	33.02	1.45	1.53	6.17
20.00	4.93	38.87	5.21	50.37	1.48	1.57	4.12
	5.68	51.83	5.97	67.99	1.51	1.60	3.09
	6.93	77.75	7.23	103.74	1.56	1.65	2.06
	7.62	103.66	7.89	139.38	1.59	1.68	1.54
	8.55	129.58	8.81	175.91	1.62	1.71	1.23

+ TEMPERATURE CORRECTED SWELLING RATIOS

LAST SET OF VALUES REFERS TO ONSET OF MELT FRACTURE

LDPE DHDY-6873

TEST TEMPERATURE = 160.0 DEG C

DIAMETER OF CAPILLARY = .133 CM

ENTRANCE ANGLE = 90.0 DEG

L/D	$\Delta P \times 10^{-6}$	$\dot{\gamma}_a$	$\tau_\omega \times 10^{-4}$	$\dot{\gamma}_\omega$	B	B+	t_a
-	PASCAL	1/SEC	PASCAL	1/SEC	-	-	SEC
15.98	1.27	3.89	1.64	4.75	1.36	1.44	32.89
	1.64	6.48	2.12	7.99	1.39	1.46	19.73
	2.02	9.72	2.60	12.07	1.42	1.50	13.16
	2.39	12.96	3.07	16.19	1.43	1.51	9.87
	3.34	25.92	4.27	32.76	1.48	1.57	4.93
	4.71	51.83	5.96	66.29	1.57	1.65	2.47
	5.79	77.75	7.25	100.12	1.61	1.70	1.64
	6.62	103.66	8.22	134.07	1.63	1.73	1.23
	7.37	129.58	9.09	168.17	1.67	1.77	.99
9.89	.93	5.18	1.75	5.98	1.40	1.48	15.26
	1.18	7.77	2.22	9.15	1.45	1.53	10.17
	1.39	10.37	2.60	12.36	1.48	1.56	7.63
	1.62	12.96	3.04	15.64	1.49	1.58	6.10
	2.28	25.92	4.23	32.10	1.57	1.65	3.05
	3.30	51.83	6.03	65.94	1.65	1.74	1.53
	4.12	77.75	7.43	100.46	1.71	1.81	1.02
	4.68	103.66	8.35	135.09	1.73	1.83	.76
	5.18	129.58	9.15	169.99	1.77	1.87	.61

\+ TEMPERATURE COFRECTED SWELLING RATIOS

LAST SET OF VALUES REFERS TO ONSET OF MELT FRACTURE

LDPE DHDY-6873

TEST TEMPERATURE = 160.0 DEG C

DIAMETER OF CAPILLARY = .133 CM

ENTRANCE ANGLE = 90.0 DEG

L/D	$\Delta P \times 10^{-6}$	$\dot{\gamma}_a$	$\tau_\omega \times 10^{-4}$	$\dot{\gamma}_\omega$	B	B+	t_a
-	PASCAL	1/SEC	PASCAL	1/SEC	-	-	SEC
	.66	3.89	1.46	4.47	1.41	1.49	16.39
	.90	6.48	1.98	7.63	1.45	1.54	9.83
	1.15	9.72	2.53	11.65	1.51	1.59	6.55
	1.36	12.96	2.98	15.72	1.54	1.62	4.92
7.96	1.90	25.92	4.13	32.20	1.62	1.71	2.46
	2.80	51.83	5.97	66.09	1.72	1.81	1.23
	3.41	77.75	7.15	100.39	1.77	1.87	.82
	4.00	103.66	8.26	135.17	1.81	1.91	.61
	4.40	129.58	8.99	169.95	1.84	1.94	.49
	.39	3.89	1.11	3.89	1.46	1.54	11.02
	.47	5.18	1.34	5.35	1.51	1.59	8.26
	.58	6.48	1.66	6.92	1.54	1.62	6.61
	.75	8.68	2.13	9.63	1.58	1.67	4.93
5.35	.83	10.37	2.36	11.68	1.60	1.69	4.13
	.96	12.96	2.73	14.91	1.65	1.74	3.30
	1.80	38.87	4.98	48.60	1.81	1.91	1.10
	2.36	64.79	6.39	83.68	1.87	1.98	.66
	2.90	97.18	7.68	128.49	1.93	2.04	.44

+ TEMPERATURE CORRECTED SWELLING RATIOS

LAST SET OF VALUES REFERS TO ONSET OF MELT FRACTURE

LDPE DHDY-6873

TEST TEMPERATURE = 160.0 DEG C

DIAMETER OF CAPILLARY = .133 CM

ENTRANCE ANGLE = 90.0 DEG

L/D	$\Delta P \times 10^{-4}$ PASCAL	γ_a 1/SEC	$\tau_w \times 10^{-4}$ PASCAL	γ_w 1/SEC	B -	B+ -	t_a SEC
	.26	3.89	1.03	3.94	1.52	1.61	6.15
	.45	7.77	1.75	8.42	1.65	1.74	3.08
	.66	12.96	2.54	14.67	1.75	1.85	1.85
	1.32	38.87	4.94	47.41	1.95	2.06	.62
2.99	1.54	51.83	5.69	64.18	2.00	2.11	.46
	1.78	64.79	6.47	81.33	2.04	2.15	.37
	2.20	97.18	7.77	124.34	2.10	2.22	.25
	2.62	129.58	9.02	168.33	2.13	2.25	.18
	2.81	161.97	9.47	211.46	2.15	2.27	.15

+ TEMPERATURE CORRECTED SWELLING RATIOS

LAST SET OF VALUES REFERS TO ONSET OF MELT FRACTURE

LDPE DHDY-6873

TEST TEMPERATURE = 160.0 DEG C

DIAMETER OF DIE ORIFICE = .133 CM

θ	V_p	$\Delta P \times 10^{-5}$	$\dot{\gamma}_a$	B	B+
DEG	CM/MIN	PASCAL	1/SEC	-	-
90.0	.25	2.12	12.96	2.34	2.47
	.51	4.06	25.92	2.56	2.70
	.76	5.31	38.87	2.68	2.83
	1.27	7.99	64.79	2.80	2.95
	1.52	9.30	77.75	2.84	3.00
	1.91	10.80	97.18	2.89	3.06
	2.54	14.17	129.58	2.95	3.13
	3.81	17.67	194.36	3.04	3.21
	5.08	21.04	259.15	3.08	3.25

+ TEMPERATURE CORRECTED SWELLING RATIOS

LDPE DHDY-6873

TEST TEMPERATURE = 180.0 DEG C

DIAMETER OF CAPILLARY = .133 CM

ENTRANCE ANGLE = 90.0 DEG

L/D	$\Delta P \times 10^{-6}$	$\dot{\gamma}_a$	$\tau_w \times 10^{-4}$	$\dot{\gamma}_w$	B	B+	t_a
-	PASCAL	1/SEC	PASCAL	1/SEC	-	-	SEC
	1.32	3.89	1.20	4.56	1.31	1.39	50.96
	1.71	6.48	1.55	7.72	1.33	1.42	30.58
	2.25	10.37	2.04	12.57	1.36	1.45	19.11
	3.64	25.92	3.28	32.35	1.42	1.50	7.64
24.76	5.89	64.79	5.24	83.18	1.49	1.58	3.06
	7.40	103.66	6.51	134.79	1.54	1.64	1.91
	7.97	129.58	6.97	169.16	1.57	1.66	1.53
	11.05	259.15	9.47	344.33	1.65	1.75	.76
	12.24	310.98	10.46	415.53	1.68	1.78	.64
	1.06	3.89	1.17	4.35	1.33	1.41	41.16
	1.43	6.48	1.57	7.48	1.36	1.44	24.70
	1.85	9.72	2.03	11.50	1.38	1.46	16.46
	3.88	38.87	4.20	49.27	1.48	1.58	4.12
20.00	5.01	64.79	5.38	83.96	1.53	1.62	2.47
	6.11	97.18	6.47	128.01	1.57	1.67	1.65
	6.99	129.58	7.34	172.56	1.61	1.71	1.23
	9.44	259.15	9.68	353.36	1.70	1.81	.62
	10.24	310.98	10.45	426.79	1.73	1.84	.51

+ TEMPERATURE CORRECTED SWELLING RATIOS

LAST SET OF VALUES REFERS TO ONSET OF MELT FRACTURE

LDPE DHDY-6873

TEST TEMPERATURE = 180.0 DEG C

DIAMETER OF CAPILLARY = .133 CM

ENTRANCE ANGLE = 90.0 DEG

L/D	$\Delta P \times 10^{-6}$	$\dot{\gamma}_a$	$\tau_\omega \times 10^{-4}$	$\dot{\gamma}_\omega$	B	B+	t_a
-	PASCAL	1/SEC	PASCAL	1/SEC	-	-	SEC
	.87	3.89	1.17	4.32	1.34	1.42	32.89
	1.32	7.77	1.76	9.04	1.39	1.48	16.44
	1.54	10.37	2.05	12.25	1.42	1.51	12.33
	1.78	12.96	2.37	15.53	1.43	1.52	9.87
15.98	3.21	38.87	4.22	49.36	1.52	1.62	3.29
	4.19	64.79	5.44	84.29	1.58	1.68	1.97
	5.29	103.66	6.75	137.62	1.63	1.73	1.23
	5.81	129.58	7.33	173.35	1.66	1.77	.99
	7.68	259.15	9.42	354.68	1.75	1.86	.49
	.56	3.89	1.10	4.28	1.36	1.45	20.34
	.88	7.77	1.74	8.95	1.43	1.52	10.17
	1.20	12.96	2.37	15.37	1.48	1.57	6.10
	2.20	38.87	4.25	48.68	1.60	1.69	2.03
9.89	2.86	64.79	5.42	82.89	1.64	1.74	1.22
	3.17	77.75	5.96	100.31	1.69	1.79	1.02
	3.63	103.66	6.72	135.15	1.72	1.83	.76
	4.11	129.58	7.50	170.53	1.77	1.88	.61
	5.74	259.15	10.04	349.58	1.85	1.97	.31

+ TEMPERATURE CORRECTED SWELLING RATIOS

LAST SET OF VALUES REFERS TO ONSET OF MELT FRACTURE

LDPE DHDY-6873

TEST TEMPERATURE = 180.0 DEG C

DIAMETER OF CAPILLARY = .133 CM

ENTRANCE ANGLE = 90.0 DEG

L/D	$\Delta P \times 10^{-6}$	$\dot{\gamma}_a$	$\tau_\omega \times 10^{-4}$	$\dot{\gamma}_\omega$	B	B+	t_a
-	PASCAL	1/SEC	PASCAL	1/SEC	-	-	SEC
7.96	.46	3.89	1.07	4.29	1.39	1.48	16.39
	.67	7.77	1.57	8.91	1.45	1.54	8.19
	.86	10.37	2.00	12.16	1.48	1.58	6.14
	.97	12.96	2.24	15.36	1.51	1.61	4.92
	1.44	25.92	3.29	31.79	1.60	1.69	2.46
	2.32	64.79	5.15	82.64	1.72	1.83	.98
	2.90	97.18	6.29	126.08	1.79	1.90	.66
	3.37	129.58	7.16	169.94	1.84	1.95	.49
	4.71	259.15	9.53	347.95	1.93	2.05	.25
5.35	.69	12.96	2.10	14.40	1.60	1.69	3.30
	1.05	25.92	3.18	30.61	1.70	1.81	1.65
	1.35	38.87	4.02	47.94	1.77	1.88	1.10
	1.56	51.83	4.56	65.17	1.80	1.91	.83
	1.79	64.79	5.15	82.94	1.85	1.97	.66
	1.98	77.75	5.64	100.86	1.89	2.00	.55
	2.33	103.66	6.50	137.26	1.93	2.05	.41
	2.58	129.58	7.04	173.51	1.97	2.09	.33
	3.12	194.36	8.19	265.85	2.02	2.15	.22

\+ TEMPERATURE CORRECTED SWELLING RATIOS

LAST SET OF VALUES REFERS TO ONSET OF MELT FRACTURE

LDPE DHDY-6873

TEST TEMPERATURE = 180.0 DEG C

DIAMETER OF CAPILLARY = .133 CM

ENTRANCE ANGLE = 90.0 DEG

L/D	$\Delta P \times 10^{-6}$	$\dot{\gamma}_a$	$\tau_\omega \times 10^{-4}$	$\dot{\gamma}_\omega$	B	B+	t_a
-	PASCAL	1/SEC	PASCAL	1/SEC	-	-	SEC
	.46	12.96	1.99	14.47	1.66	1.76	1.85
	.95	38.87	3.91	46.84	1.88	2.00	.62
	1.29	64.79	5.10	80.31	1.99	2.12	.37
	1.44	77.75	5.60	97.32	2.02	2.15	.31
2.99	1.69	103.66	6.39	131.55	2.09	2.22	.23
	1.97	129.58	7.23	166.52	2.13	2.26	.18
	2.43	194.36	8.48	253.82	2.19	2.32	.12
	2.88	259.15	9.74	343.10	2.23	2.36	.09
	3.20	310.98	10.69	415.51	2.25	2.39	.08

+ TEMPERATURE CORRECTED SWELLING RATIOS

LAST SET OF VALUES REFERS TO ONSET OF MELT FRACTURE

LDPE DHDY-6873

TEST TEMPERATURE = 180.0 DEG C

DIAMETER OF DIE ORIFICE = .133 CM

θ	V_p	$\Delta P \times 10^{-5}$	$\dot{\gamma}_a$	B	B+
DEG	CM/MIN	PASCAL	1/SEC	-	-
90.0	.76	3.87	38.87	2.48	2.63
	1.02	4.68	51.83	2.56	2.71
	1.27	5.81	64.79	2.62	2.78
	1.91	7.49	97.18	2.74	2.91
	2.54	9.68	129.58	2.83	3.00
	3.81	12.92	194.36	2.93	3.11
	5.08	14.98	259.15	3.01	3.20
	6.10	16.73	310.98	3.03	3.21

+ TEMPERATURE CORRECTED SWELLING RATIOS

LDPE DHDY-6873

TEST TEMPERATURE = 200.0 DEG C

DIAMETER OF CAPILLARY = .133 CM

ENTRANCE ANGLE = 90.0 DEG

L/D	$\Delta P \times 10^{-6}$	$\dot{\gamma}_a$	$\tau_\omega \times 10^{-4}$	$\dot{\gamma}_\omega$	B	B+	t_a
-	PASCAL	1/SEC	PASCAL	1/SEC	-	-	SEC
	1.27	6.48	1.19	7.32	1.30	1.39	30.58
	1.63	9.72	1.52	11.26	1.33	1.42	20.38
	1.97	12.96	1.84	15.30	1.35	1.44	15.29
	3.59	38.87	3.31	48.56	1.42	1.51	5.10
24.76	4.65	64.79	4.24	82.81	1.46	1.56	3.08
	5.65	97.18	5.09	126.29	1.50	1.60	2.04
	6.49	129.58	5.79	170.33	1.52	1.62	1.53
	8.86	259.15	7.66	349.11	1.60	1.71	.76
	10.99	388.73	9.35	532.68	1.66	1.77	.51
	.77	3.89	.88	4.22	1.30	1.38	41.16
	1.20	7.77	1.37	8.88	1.33	1.42	20.58
-	1.64	12.96	1.86	15.30	1.37	1.46	12.35
	2.99	38.87	3.34	48.76	1.45	1.54	4.12
20.00	3.96	64.79	4.37	83.46	1.50	1.60	2.47
	4.89	97.18	5.32	127.57	1.54	1.64	1.65
	5.65	129.58	6.07	172.25	1.57	1.67	1.23
	7.49	259.15	7.75	352.46	1.66	1.77	.62
	9.11	388.73	9.26	537.35	1.71	1.82	.41

+ TEMPERATURE CORRECTED SWELLING RATIOS

LAST SET OF VALUES REFERS TO ONSET OF MELT FRACTURE

LDPE DHDY-6873

TEST TEMPERATURE = 200.0 DEG C

DIAMETER OF CAPILLARY = .133 CM

ENTRANCE ANGLE = 90.0 DEG

L/D	$\Delta P \times 10^{-6}$ PASCAL	$\dot{\gamma}_a$ 1/SEC	$\tau_w \times 10^{-4}$ PASCAL	$\dot{\gamma}_w$ 1/SEC	B -	B+ -	t_a SEC
15.98	.87	6.48	1.21	7.26	1.36	1.45	19.73
	1.14	9.72	1.58	11.21	1.39	1.48	13.16
	1.34	12.96	1.86	15.22	1.41	1.50	9.87
	2.45	38.87	3.33	48.68	1.49	1.59	3.29
	3.21	64.79	4.31	83.16	1.55	1.65	1.97
	3.97	97.18	5.24	127.16	1.59	1.69	1.32
	4.59	129.58	5.96	171.71	1.63	1.73	.99
	6.49	259.15	8.06	353.49	1.73	1.85	.49
	7.52	388.73	9.13	536.48	1.78	1.89	.33
9.89	.68	7.77	1.43	8.85	1.39	1.49	10.17
	.87	12.96	1.82	15.12	1.45	1.54	6.10
	1.70	38.87	3.46	48.27	1.55	1.65	2.03
	1.99	51.83	4.00	65.24	1.60	1.70	1.53
	2.47	77.75	4.88	99.66	1.65	1.76	1.02
	2.92	103.66	5.64	134.64	1.69	1.81	.76
	3.23	129.58	6.13	169.57	1.72	1.83	.61
	4.67	259.15	8.31	348.32	1.82	1.94	.31
	5.65	388.73	9.74	529.67	1.89	2.01	.20

\+ TEMPERATURE CORRECTED SWELLING RATIOS

LAST SET OF VALUES REFERS TO ONSET OF MELT FRACTURE

LDPE DHDY-6873

TEST TEMPERATURE = 200.0 DEG C

DIAMETER OF CAPILLARY = .133 CM

ENTRANCE ANGLE = 90.0 DEG

L/D	$\Delta P \times 10^{-6}$	$\dot{\gamma}_a$	$\tau_w \times 10^{-4}$	$\dot{\gamma}_w$	B	B+	t_a
-	PASCAL	1/SEC	PASCAL	1/SEC	-	-	SEC
7.96	.52	7.77	1.30	8.57	1.41	1.50	8.19
	.62	10.37	1.56	11.70	1.44	1.53	6.14
	.71	12.96	1.75	14.85	1.47	1.57	4.92
	1.35	38.87	3.27	48.08	1.60	1.70	1.64
	1.84	64.79	4.32	82.75	1.68	1.79	.98
	2.30	97.18	5.25	126.89	1.74	1.85	.66
	2.63	129.58	5.86	171.27	1.78	1.90	.49
	3.81	259.15	7.85	353.56	1.90	2.02	.25
	4.62	388.73	9.18	539.19	1.96	2.09	.16
5.35	.50	12.96	1.68	14.55	1.54	1.64	3.30
	.97	38.87	3.13	47.39	1.71	1.82	1.10
	1.17	51.83	3.73	64.59	1.75	1.87	.83
	1.33	64.79	4.15	81.82	1.79	1.91	.66
	1.49	77.75	4.58	99.37	1.83	1.95	.55
	1.73	103.66	5.15	134.38	1.87	2.00	.41
	1.98	129.58	5.74	170.13	1.91	2.04	.33
	2.92	259.15	7.68	351.93	2.04	2.17	.17
	3.60	388.73	9.03	537.66	2.10	2.24	.11

\+ TEMPERATURE COFRECTED SWELLING RATIOS

LAST SET OF VALUES REFERS TO ONSET OF MELT FRACTURE

LDPE DHDY-6873

TEST TEMPERATURE = 200.0 DEG C

DIAMETER OF CAPILLARY = .133 CM

ENTRANCE ANGLE = 90.0 DEG

L/D	$\Delta P \times 10^{-6}$ PASCAL	$\dot{\gamma}_a$ 1/SEC	$\tau_\omega \times 10^{-4}$ PASCAL	$\dot{\gamma}_\omega$ 1/SEC	B -	B+ -	t_a SEC
	.34	12.96	1.69	14.34	1.58	1.69	1.85
	.72	38.87	3.34	47.81	1.80	1.92	.62
	.82	51.83	3.74	64.80	1.87	1.99	.46
	.88	64.79	3.90	81.48	1.91	2.04	.37
2.99	1.06	77.75	4.59	100.09	1.95	2.08	.31
	1.27	103.66	5.28	136.07	2.01	2.14	.23
	1.53	129.58	6.11	173.50	2.06	2.20	.18
	2.15	259.15	7.53	356.77	2.19	2.33	.09
	2.70	388.73	8.86	546.61	2.26	2.41	.06

+ TEMPERATURE CORRECTED SWELLING RATIOS

LAST SET OF VALUES REFERS TO ONSET OF MELT FRACTURE

LDPE DHDY-6873

TEST TEMPERATURE = 200.0 DEG C

DIAMETER OF DIE ORIFICE = .133 CM

θ DEG	V_p CM/MIN	$\Delta P \times 10^{-5}$ PASCAL	$\dot{\gamma}_a$ 1/SEC	B -	B+ -
90.0	.76	2.50	38.87	2.34	2.49
	1.27	3.43	64.79	2.50	2.67
	1.52	4.06	77.75	2.55	2.72
	2.03	5.18	103.66	2.66	2.84
	2.54	6.30	129.58	2.73	2.91
	3.81	8.43	194.36	2.83	3.01
	5.08	10.61	259.15	2.89	3.09
	7.62	14.48	388.73	3.01	3.21
	10.16	17.54	518.30	3.07	3.27

* TEMPERATURE CORRECTED SWELLING RATIOS

LDPE DHDY-6873

TEST TEMPERATURE = 160.0 DEG C

DIAMETER OF CAPILLARY = .099 CM

ENTRANCE ANGLE = 90.0 DEG

L/D	$\Delta P \times 10^{-6}$	$\dot{\gamma}_a$	$\tau_\omega \times 10^{-4}$	$\dot{\gamma}_\omega$	B	B+	t_a
-	PASCAL	1/SEC	PASCAL	1/SEC	-	-	SEC
	.42	9.48	1.90	10.24	1.78	1.88	2.53
	.62	15.80	2.75	17.99	1.87	1.97	1.52
	.78	23.71	3.38	27.76	1.96	2.07	1.01
	.96	31.61	4.09	37.98	2.02	2.13	.76
3.00	1.25	47.41	5.15	58.71	2.09	2.21	.51
	1.49	63.22	5.96	79.74	2.15	2.27	.38
	1.84	94.83	7.02	122.10	2.22	2.35	.25
	2.22	126.44	8.10	165.67	2.26	2.39	.19
	2.54	158.04	8.97	209.65	2.29	2.42	.15
	.64	9.48	1.98	10.42	1.65	1.74	4.65
	.93	15.80	2.84	18.33	1.72	1.81	2.79
	1.15	23.71	3.46	28.28	1.79	1.89	1.86
	1.37	31.61	4.09	38.60	1.84	1.94	1.40
5.51	2.63	94.83	7.24	124.89	2.01	2.12	.47
	2.95	126.44	7.88	168.30	2.04	2.15	.35
	3.35	158.04	8.74	213.13	2.07	2.19	.28
	3.84	211.78	9.68	289.26	2.09	2.21	.21
	4.31	252.87	10.69	349.57	2.10	2.22	.17

\+ TEMPERATURE CORRECTED SWELLING RATIOS

LAST SET OF VALUES REFERS TO ONSET OF MELT FRACTURE

LOPE DHDY-6873

TEST TEMPERATURE = 160.0 DEG C

DIAMETER OF CAPILLARY = .099 CM

ENTRANCE ANGLE = 90.0 DEG

L/D	$\Delta P \times 10^{-6}$	$\dot{\gamma}_a$	$\tau_w \times 10^{-4}$	$\dot{\gamma}_w$	B	B+	t_a
-	PASCAL	1/SEC	PASCAL	1/SEC	-	-	SEC
	.91	9.48	2.14	10.81	1.59	1.68	6.75
	1.20	15.80	2.82	18.71	1.66	1.75	4.05
	1.40	18.97	3.28	22.90	1.68	1.77	3.37
	1.64	25.29	3.80	31.12	1.73	1.82	2.53
8.00	1.80	31.61	4.15	39.32	1.76	1.85	2.02
	2.23	47.41	5.05	60.45	1.81	1.91	1.35
	3.26	94.33	7.05	125.84	1.90	2.00	.67
	4.19	158.04	8.68	214.88	1.96	2.07	.40
	5.11	237.07	10.21	328.31	1.99	2.10	.27
	1.57	12.64	2.59	15.09	1.57	1.66	7.92
	1.98	18.97	3.25	23.14	1.61	1.69	5.28
	2.31	25.29	3.77	31.29	1.64	1.73	3.96
	2.57	31.61	4.18	39.50	1.67	1.76	3.17
12.51	3.28	47.41	5.26	60.52	1.71	1.80	2.11
	3.67	63.22	5.83	81.46	1.75	1.84	1.58
	4.49	94.83	6.99	124.22	1.80	1.90	1.06
	5.19	126.44	7.94	167.51	1.85	1.95	.79
	5.93	158.04	8.94	211.57	1.87	1.97	.63

+ TEMPERATURE CORRECTED SWELLING RATIOS

LAST SET OF VALUES REFERS TO ONSET OF MELT FRACTURE

LDPE DHDY-6873

TEST TEMPERATURE = 160.0 DEG C

DIAMETER OF DIE ORIFICE = .099 CM

θ	V_p	$\Delta P \times 10^{-5}$	$\dot{\gamma}_a$	B	B+
DEG	CM/MIN	PASCAL	1/SEC	-	-
90.0	.51	4.62	63.22	3.37	3.56
	.76	6.30	94.83	3.52	3.72
	1.02	7.80	126.44	3.62	3.83
	1.27	8.74	158.04	3.73	3.93
	1.52	10.67	189.65	3.77	3.98
	2.03	12.55	252.87	3.85	4.06
	2.54	14.55	316.09	3.92	4.14
	3.81	18.73	474.13	4.04	4.26
	5.08	22.22	632.18	4.09	4.32

+ TEMPERATURE CORRECTED SWELLING RATIOS

LDPE DHDY-6873

TEST TEMPERATURE = 160.0 DEG C

DIAMETER OF CAPILLARY = .066 CM

ENTRANCE ANGLE = 90.0 DEG

L/D	$\Delta P \times 10^{-6}$	$\dot{\gamma}_a$	$\tau_\omega \times 10^{-4}$	$\dot{\gamma}_\omega$	B	B+	t_a
-	PASCAL	1/SEC	PASCAL	1/SEC	-	-	SEC
3.00	.78	21.34	4.13	27.09	1.91	2.01	1.12
	1.02	32.00	5.20	40.47	1.98	2.09	.75
	1.22	42.67	5.96	53.82	2.01	2.13	.56
	1.40	53.34	6.67	67.14	2.07	2.19	.45
	1.50	64.01	6.94	80.51	2.10	2.22	.37
	1.82	85.34	8.12	107.04	2.14	2.25	.28
	2.10	106.68	9.16	133.50	2.17	2.29	.22
	2.38	133.35	10.28	166.52	2.20	2.32	.18
	2.47	138.68	10.70	173.06	2.20	2.32	.17
5.50	1.32	21.34	4.58	27.10	1.70	1.79	2.06
	1.64	32.00	5.51	40.85	1.74	1.84	1.37
	1.94	42.67	6.38	54.67	1.79	1.89	1.03
	2.18	53.34	7.04	68.52	1.82	1.92	.82
	2.43	64.01	7.70	82.42	1.83	1.93	.69
	2.57	71.48	8.03	92.14	1.85	1.95	.62
	2.76	80.01	8.55	103.31	1.86	1.97	.55
	2.88	85.34	8.87	110.30	1.86	1.97	.52
	3.18	106.68	9.66	138.19	1.89	2.00	.41

\+ TEMPERATURE CORRECTED SWELLING RATIOS

LAST SET OF VALUES REFERS TO ONSET OF MELT FRACTURE

LDPE DHDY-6873

TEST TEMPERATURE = 160.0 DEG C

DIAMETER OF CAPILLARY = .066 CM

ENTRANCE ANGLE = 90.0 DEG

L/D	$\Delta P \times 10^{-6}$	$\dot{\gamma}_a$	$\tau_\omega \times 10^{-4}$	$\dot{\gamma}_\omega$	B	B+	t_a
-	PASCAL	1/SEC	PASCAL	1/SEC	-	-	SEC
	1.60	24.00	4.09	28.93	1.67	1.76	2.67
	1.97	32.00	4.96	39.46	1.70	1.79	2.00
	2.29	42.67	5.67	53.44	1.73	1.82	1.50
	2.62	53.34	6.39	67.72	1.74	1.84	1.20
8.00	2.83	64.01	6.80	81.84	1.77	1.87	1.00
	2.91	71.48	6.94	91.59	1.79	1.89	.90
	3.31	85.34	7.79	110.80	1.80	1.90	.75
	3.70	106.68	8.60	140.02	1.82	1.92	.60
	4.15	133.35	9.62	177.20	1.85	1.95	.48
	2.75	24.00	4.81	32.61	1.51	1.60	4.17
	3.10	32.00	5.38	42.97	1.54	1.63	3.12
	3.59	42.67	6.15	56.49	1.57	1.66	2.34
	3.81	48.01	6.48	63.18	1.59	1.68	2.08
12.50	3.96	53.34	6.71	69.94	1.59	1.68	1.87
	4.37	64.01	7.33	83.12	1.62	1.71	1.56
	4.62	71.48	7.71	92.30	1.64	1.73	1.40
	5.08	85.34	8.39	109.17	1.65	1.74	1.17
	5.68	106.68	9.32	134.88	1.67	1.76	.94

+ TEMPERATURE CORRECTED SWELLING RATIOS

LAST SET OF VALUES REFERS TO ONSET OF MELT FRACTURE

LDPE DHDY-6873

TEST TEMPERATURE = 160.0 DEG C

DIAMETER OF DIE ORIFICE = .066 CM

θ DEG	V_p CM/MIN	$\Delta P \times 10^{-5}$ PASCAL	$\dot{\gamma}_a$ 1/SEC	B -	B+ -
90.0	.08	6.06	32.00	2.42	2.56
	.10	7.30	42.67	2.48	2.62
	.13	7.99	53.34	2.53	2.67
	.15	9.18	64.01	2.57	2.72
	.20	11.55	85.34	2.63	2.78
	.25	14.05	106.68	2.68	2.83
	.32	16.11	133.35	2.73	2.88

+ TEMPERATURE CORRECTED SWELLING RATIOS

LDPE DHDY-6873

TEST TEMPERATURE = 200.0 DEG C

DIAMETER OF DIE ORIFICE = .118 CM

θ DEG	V_p CM/MIN	$\Delta P \times 10^{-5}$ PASCAL	$\dot{\gamma}_a$ 1/SEC	B -	B+ -
60.0	1.27	5.31	93.24	2.49	2.65
	1.91	7.30	139.86	2.61	2.78
	2.54	8.43	186.48	2.69	2.87
	3.81	11.55	279.73	2.79	2.97
	5.08	14.67	372.97	2.87	3.06
	6.10	16.17	447.56	2.91	3.10
	7.62	18.10	559.45	3.01	3.20
120.0	1.91	7.43	139.86	2.84	3.03
	2.54	8.43	186.48	2.86	3.05
	3.81	11.36	279.73	3.05	3.25
	5.08	14.17	372.97	3.01	3.21
	5.72	15.61	419.59	3.01	3.21
	6.10	16.23	447.56	3.01	3.21
	7.62	18.42	559.45	3.08	3.28

+ TEMPERATURE CORRECTED SWELLING RATIOS

LDPE DHDY-6873

TEST TEMPERATURE = 200.0 DEG C

DIAMETER OF DIE ORIFICE = .118 CM

θ DEG	V_p CM/MIN	$\Delta P \times 10^{-5}$ PASCAL	$\dot{\gamma}_a$ 1/SEC	B -	B+ -
150.0	1.27	4.68	93.24	2.84	3.02
	1.91	6.87	139.86	2.95	3.04
	2.54	8.12	186.48	2.90	3.10
	3.81	10.61	279.73	2.96	3.16
	5.08	12.61	372.97	3.01	3.20
	6.10	14.48	447.56	3.08	3.28
	7.62	17.17	559.45	3.14	3.35
180.0	1.27	4.99	93.24	2.63	2.81
	1.91	5.93	139.86	2.73	2.91
	2.54	7.80	186.48	2.86	3.05
	3.81	9.99	279.73	2.95	3.14
	5.08	12.80	372.97	3.02	3.22
	6.10	14.67	447.56	3.06	3.26
	7.62	17.67	559.45	3.09	3.29

+ TEMPERATURE CORRECTED SWELLING RATIOS

LDPE DFDD-4400

TEST TEMPERATURE = 220.0 DEG C

DIAMETER OF CAPILLARY = .133 CM

ENTRANCE ANGLE = 90.0 DEG

L/D	$\Delta P \times 10^{-6}$	$\dot{\gamma}_a$	$\tau_\omega \times 10^{-4}$	$\dot{\gamma}_\omega$	B	B+	t_a
-	PASCAL	1/SEC	PASCAL	1/SEC	-	-	SEC
	.97	6.48	.93	8.04	1.42	1.51	30.58
	1.42	12.96	1.34	16.09	1.47	1.57	15.29
	2.62	38.87	2.40	48.28	1.54	1.65	5.10
	3.43	64.79	3.06	80.47	1.57	1.68	3.06
24.76	4.06	97.18	3.55	120.71	1.61	1.72	2.04
	4.84	129.58	4.20	160.96	1.66	1.77	1.53
	6.62	259.15	6.21	321.97	1.72	1.84	.76
	1.03	9.72	1.19	12.52	1.46	1.56	16.46
	1.22	12.96	1.40	16.58	1.52	1.62	12.35
	2.29	38.87	2.53	48.51	1.59	1.69	4.12
	2.73	64.79	2.93	80.35	1.61	1.72	2.47
20.00	3.51	97.18	3.69	119.34	1.65	1.76	1.65
	4.12	129.58	4.28	158.09	1.70	1.81	1.23
	5.71	259.15	6.53	310.36	1.77	1.89	.62

+ TEMPERATURE CORRECTED SWELLING RATIOS

LAST SET OF VALUES REFERS TO ONSET OF MELT FRACTURE

LDPE DFDQ-4400

TEST TEMPERATURE = 220.0 DEG C

DIAMETER OF CAPILLARY = .133 CM

ENTRANCE ANGLE = 90.0 DEG

L/D	$\Delta P \times 10^{-6}$	$\dot{\gamma}_a$	$\tau_\omega \times 10^{-4}$	$\dot{\gamma}_\omega$	B	B+	t_a
-	PASCAL	1/SEC	PASCAL	1/SEC	-	-	SEC
	.79	9.72	1.13	12.10	1.51	1.61	13.16
	.97	12.96	1.36	16.09	1.52	1.62	9.87
	1.84	38.87	2.48	47.94	1.62	1.73	3.29
	2.35	64.79	3.06	79.71	1.68	1.79	1.97
15.98	2.92	97.18	3.68	119.31	1.72	1.84	1.32
	3.34	129.58	4.17	158.84	1.76	1.88	.99
	4.66	259.15	6.53	316.01	1.86	1.98	.49
	.50	9.72	1.08	11.07	1.54	1.65	8.14
	.69	12.96	1.48	15.26	1.59	1.69	6.10
	1.25	38.87	2.50	48.34	1.72	1.83	2.03
	1.65	64.79	3.15	82.42	1.77	1.89	1.22
9.89	2.02	97.18	3.68	125.53	1.80	1.92	.81
	2.50	129.58	4.48	170.55	1.86	1.98	.61
	2.87	194.36	5.33	260.04	1.92	2.05	.41

+ TEMPERATURE CORRECTED SWELLING RATIOS

LAST SET OF VALUES REFERS TO ONSET OF MELT FRACTURE

LDPE DFDQ-4400

TEST TEMPERATURE = 220.0 DEG C

DIAMETER OF CAPILLARY = .133 CM

ENTRANCE ANGLE = 90.0 DEG

L/D	$\Delta P \times 10^{-6}$	$\dot{\gamma}_a$	$\tau_\omega \times 10^{-4}$	$\dot{\gamma}_\omega$	B	B+	t_a
-	PASCAL	1/SEC	PASCAL	1/SEC	-	-	SEC
	.39	9.72	1.01	10.89	1.57	1.68	6.55
	.48	12.96	1.24	14.82	1.61	1.72	4.92
	1.03	38.87	2.44	47.44	1.77	1.89	1.64
	1.34	64.79	2.99	80.56	1.84	1.96	.98
7.96	1.70	97.18	3.61	122.91	1.89	2.01	.66
	2.03	129.58	4.23	166.19	1.95	2.08	.49
	2.42	194.36	5.24	253.99	2.01	2.14	.33
	.27	9.72	.96	10.41	1.65	1.76	4.41
	.37	12.96	1.32	14.68	1.69	1.81	3.30
	.75	38.87	2.35	48.38	1.85	1.97	1.10
	1.01	64.79	2.93	83.41	1.94	2.07	.66
5.35	1.29	97.18	3.53	128.57	2.03	2.17	.44
	1.50	129.58	3.99	174.51	2.09	2.23	.33
	1.75	194.36	4.90	269.49	2.14	2.29	.22

+ TEMPERATURE CORRECTED SWELLING RATIOS

LAST SET OF VALUES REFERS TO ONSET OF MELT FRACTURE

LDPE DFDQ-4400

TEST TEMPERATURE = 220.0 DEG C

DIAMETER OF CAPILLARY = .133 CM

ENTRANCE ANGLE = 90.0 DEG

L/D	$\Delta P \times 10^{-6}$	$\dot{\gamma}_a$	$\tau_\omega \times 10^{-4}$	$\dot{\gamma}_\omega$	B	B+	t_ω
-	PASCAL	1/SEC	PASCAL	1/SEC	-	-	SEC
	.22	12.96	1.19	13.12	1.74	1.85	1.85
	.42	25.92	2.01	30.50	1.89	2.01	.92
	.53	38.87	2.37	47.90	1.97	2.10	.62
	.69	51.83	2.89	67.09	2.04	2.17	.46
2.99	.78	64.79	3.12	85.47	2.09	2.23	.37
	1.00	97.18	3.67	133.24	2.17	2.31	.25
	1.17	129.58	4.15	182.67	2.22	2.37	.18

+ TEMPERATURE COFRECTED SWELLING RATIOS

LAST SET OF VALUES REFERS TO ONSET OF MELT FRACTURE

LDPE DFDQ-4400

TEST TEMPERATURE = 220.0 DEG C

DIAMETER OF DIE ORIFICE = .133 CM

θ DEG	V_p CM/MIN	$\Delta P \times 10^{-5}$ PASCAL	$\dot{\gamma}_a$ 1/SEC	B -	B* -
30.0	.76	1.69	38.87	2.52	2.69
	1.02	2.87	51.83	2.60	2.77
	1.27	3.12	64.79	2.65	2.83
	1.91	4.56	97.18	2.77	2.95
	2.54	6.06	129.58	2.86	3.05

* TEMPERATURE CORRECTED SWELLING RATIOS

LOPE DFDY=6600
TEST TEMPERATURE = 260.0 DEG C
DIAMETER OF CAPILLARY = .133 CM
ENTRANCE ANGLE = 90.0 DEG

L/D	$\Delta P \times 10^{-6}$	$\dot{\gamma}_a$	$\tau_w \times 10^{-4}$	$\dot{\gamma}_w$	B	B+	t_a
-	PASCAL	1/SEC	PASCAL	1/SEC	-	-	SEC
	1.57	6.48	1.47	7.56	1.42	1.53	30.58
	2.00	9.72	1.85	12.09	1.45	1.56	20.38
	2.34	12.96	2.13	16.73	1.47	1.58	15.29
	2.87	19.44	2.54	26.25	1.48	1.60	10.19
24.76	3.28	25.92	2.84	35.98	1.51	1.63	7.64
	3.53	31.10	3.02	43.81	1.53	1.65	6.37
	3.95	38.87	3.34	56.09	1.55	1.67	5.10
	.99	3.89	1.15	4.46	1.43	1.54	41.16
	1.37	6.48	1.57	7.90	1.45	1.57	24.70
	1.70	9.72	1.90	12.29	1.48	1.60	16.46
	1.99	12.96	2.18	16.80	1.51	1.62	12.35
20.00	2.45	19.44	2.61	26.01	1.54	1.65	8.23
	2.83	25.92	2.94	35.40	1.54	1.66	6.17
	3.43	38.87	3.46	54.58	1.57	1.70	4.12

\+ TEMPERATURE CORRECTED SWELLING RATIOS

LAST SET OF VALUES REFERS TO ONSET OF MELT FRACTURE

LDPE DFDY-6600

TEST TEMPERATURE = 260.0 DEG C

DIAMETER OF CAPILLARY = .133 CM

ENTRANCE ANGLE = 90.0 DEG

L/D	$\Delta P \times 10^{-6}$	$\dot{\gamma}_a$	$\tau_w \times 10^{-4}$	$\dot{\gamma}_w$	B	B+	t_a
-	PASCAL	1/SEC	PASCAL	1/SEC	-	-	SEC
	.64	3.89	.92	3.80	1.46	1.57	32.89
	1.00	6.48	1.40	7.25	1.49	1.61	19.73
	1.34	9.72	1.83	11.74	1.54	1.65	13.16
	1.59	12.96	2.13	16.32	1.56	1.68	9.87
15.98	1.97	19.44	2.52	25.60	1.57	1.70	6.58
	2.25	25.92	2.81	35.06	1.59	1.71	4.93
	2.82	38.87	3.39	55.08	1.66	1.78	3.29
	.44	3.89	.97	3.70	1.48	1.60	20.34
	.69	6.48	1.48	7.11	1.54	1.65	12.21
	.94	9.72	1.92	11.55	1.58	1.70	8.14
	1.21	12.96	2.40	16.39	1.61	1.74	6.10
9.89	1.45	19.44	2.72	25.42	1.65	1.78	4.07
	1.71	25.92	3.06	34.96	1.69	1.82	3.05
	2.15	38.87	3.67	54.87	1.73	1.86	2.03

+ TEMPERATURE CORRECTED SWELLING RATIOS

LAST SET OF VALUES REFERS TO ONSET OF MELT FRACTURE

LDPE DFDY-6600

TEST TEMPERATURE = 260.0 DEG C

DIAMETER OF CAPILLARY = .133 CM

ENTRANCE ANGLE = 90.0 DEG

L/D	$\Delta P \times 10^{-6}$	$\dot{\gamma}_a$	$\tau_\omega \times 10^{-4}$	$\dot{\gamma}_\omega$	B	B*	t_a
-	PASCAL	1/SEC	PASCAL	1/SEC	-	-	SEC
	.49	6.48	1.24	6.92	1.58	1.70	9.83
	.71	9.72	1.73	11.28	1.63	1.76	6.55
	.88	12.96	2.06	15.66	1.67	1.80	4.92
	1.09	19.44	2.38	24.29	1.71	1.84	3.28
7.96	1.33	25.92	2.76	33.43	1.75	1.89	2.46
	1.72	38.87	3.36	52.29	1.79	1.93	1.64
	1.97	51.83	3.83	71.61	1.82	1.96	1.23
	.44	6.48	1.52	8.72	1.66	1.79	6.61
	.50	9.72	1.63	12.96	1.72	1.86	4.41
	.62	12.96	1.93	16.89	1.77	1.90	3.30
	.82	19.44	2.33	24.68	1.81	1.95	2.20
5.35	1.08	25.92	2.86	31.96	1.86	2.00	1.65
	1.37	38.87	3.38	46.77	1.94	2.09	1.10
	1.59	51.83	3.99	61.05	1.96	2.11	.83

* TEMPERATURE CORRECTED SWELLING RATIOS

LAST SET OF VALUES REFERS TO ONSET OF MELT FRACTURE

LOPE DFDY-6600

TEST TEMPERATURE = 260.0 DEG C

DIAMETER OF CAPILLARY = .133 CM

ENTRANCE ANGLE = 90.0 DEG

L/D	$\Delta P \times 10^{-6}$	$\dot{\gamma}_a$	$\tau_\omega \times 10^{-4}$	$\dot{\gamma}_\omega$	B	B+	t_a
-	PASCAL	1/SEC	PASCAL	1/SEC	-	-	SEC
	.31	6.48	1.62	6.66	1.75	1.89	3.69
	.47	9.72	2.21	13.26	1.81	1.95	2.46
	.53	12.96	2.31	18.32	1.87	2.02	1.85
	.69	19.44	2.67	30.48	1.94	2.09	1.23
2.99	.84	25.92	2.95	43.46	1.99	2.15	.92
	.88	31.10	2.96	52.19	2.02	2.17	.77
	1.03	38.87	3.30	69.93	2.05	2.21	.62

+ TEMPERATURE CORRECTED SWELLING RATIOS

LAST SET OF VALUES REFERS TO ONSET OF MELT FRACTURE

LDPE DFDY-6600

TEST TEMPERATURE = 260.0 DEG C

DIAMETER OF DIE ORIFICE = .133 CM

θ DEG	V_p CM/MIN	$\Delta P \times 10^{-5}$ PASCAL	$\dot{\gamma}_a$ 1/SEC	B -	B+ -
90.0	.25	2.37	12.96	2.48	2.67
	.38	3.12	19.44	2.59	2.79
	.51	4.06	25.92	2.65	2.85
	.61	4.49	31.10	2.71	2.92
	.76	5.18	38.87	2.74	2.95

+ TEMPERATURE CORRECTED SWELLING RATIOS

PS CV-41113

TEST TEMPERATURE = 180.0 DEG C

DIAMETER OF CAPILLARY = .133 CM

ENTRANCE ANGLE = 90.0 DEG

L/D	$\Delta P \times 10^{-6}$	$\dot{\gamma}_a$	$\tau_\omega \times 10^{-4}$	$\dot{\gamma}_\omega$	B	B+	t_a
-	PASCAL	1/SEC	PASCAL	1/SEC	-	-	SEC
24.76	2.90	3.11	2.70	3.75	1.27	1.30	63.70
	3.38	3.89	3.15	4.86	1.30	1.33	50.96
	5.21	10.37	4.81	14.25	1.39	1.43	19.11
	5.81	12.96	5.35	18.21	1.42	1.46	15.29
	7.49	25.92	6.80	38.24	1.51	1.55	7.64
	7.93	31.10	7.17	46.35	1.54	1.57	6.37
	8.30	38.87	7.45	58.38	1.56	1.59	5.10
	11.36	86.82	9.82	137.37	1.71	1.75	2.28
	12.49	103.66	10.69	166.57	1.74	1.78	1.91
15.98	2.26	3.11	3.12	3.42	1.31	1.34	41.11
	3.67	8.68	5.03	12.06	1.42	1.45	14.73
	4.00	10.37	5.46	14.92	1.45	1.49	12.33
	4.39	12.96	5.97	19.36	1.47	1.50	9.87
	5.46	25.92	7.28	41.85	1.56	1.59	4.93
	6.01	31.10	7.96	51.92	1.60	1.63	4.11
	6.44	38.87	8.43	66.26	1.63	1.67	3.29
	8.05	86.82	10.00	157.01	1.75	1.79	1.47
	8.30	97.18	10.21	177.02	1.77	1.81	1.32

+ TEMPERATURE CORRECTED SWELLING RATIOS

LAST SET OF VALUES REFERS TO ONSET OF MELT FRACTURE

PS CV-41113

TEST TEMPERATURE = 180.0 DEG C

DIAMETER OF CAPILLARY = .133 CM

ENTRANCE ANGLE = 90.0 DEG

L/D	$\Delta P \times 10^{-6}$	γ_a	$\tau_\omega \times 10^{-5}$	γ_ω	B	B*	t_a
-	PASCAL	1/SEC	PASCAL	1/SEC	-	-	SEC
9.89	1.81	5.18	3.76	6.89	1.36	1.39	15.26
	2.18	7.77	4.51	10.70	1.42	1.45	10.17
	2.47	10.37	5.05	14.58	1.46	1.49	7.63
	2.68	12.96	5.47	18.49	1.49	1.52	6.10
	3.12	19.44	6.26	28.42	1.56	1.59	4.07
	3.51	25.92	6.95	38.60	1.60	1.63	3.05
	4.12	38.87	7.93	59.24	1.67	1.71	2.03
	4.62	51.83	8.68	80.21	1.74	1.78	1.53
	5.12	64.79	9.41	101.63	1.79	1.83	1.22
7.96	1.44	5.18	3.55	6.52	1.38	1.41	12.29
	1.78	7.77	4.36	10.40	1.44	1.47	8.19
	2.15	12.96	5.20	18.20	1.49	1.52	4.92
	2.93	25.92	6.84	39.11	1.63	1.67	2.46
	3.34	38.87	7.55	60.11	1.68	1.72	1.64
	3.87	51.83	8.50	82.50	1.75	1.79	1.23
	4.12	64.79	8.82	104.04	1.81	1.85	.98
	4.62	77.75	9.67	127.56	1.87	1.92	.82
	4.85	97.18	9.86	160.16	1.90	1.94	.66

* TEMPERATURE CORRECTED SWELLING RATIOS

LAST SET OF VALUES REFERS TO ONSET OF MELT FRACTURE

PS CV-41113

TEST TEMPERATURE = 160.0 DEG C

DIAMETER OF CAPILLARY = .133 CM

ENTRANCE ANGLE = 90.0 DEG

L/D	$\Delta P \times 10^{-6}$	$\dot{\gamma}_a$	$\tau_\omega \times 10^{-4}$	$\dot{\gamma}_\omega$	B	B+	t_s
-	PASCAL	1/SEC	PASCAL	1/SEC	-	-	SEC
5.35	.81	3.89	2.69	4.47	1.39	1.42	11.02
	.94	5.18	3.14	6.23	1.42	1.45	8.26
	1.14	7.77	3.76	9.85	1.48	1.51	5.51
	1.50	12.96	4.84	17.55	1.55	1.59	3.30
	2.07	25.92	6.39	37.64	1.71	1.75	1.65
	2.50	38.87	7.38	58.44	1.79	1.83	1.10
	2.81	51.83	8.01	79.39	1.85	1.89	.83
	3.06	64.79	8.44	100.43	1.91	1.95	.66
	3.37	77.75	9.03	122.36	1.95	1.99	.55
2.99	.61	3.89	2.96	4.52	1.37	1.40	6.15
	.90	8.68	4.28	10.91	1.53	1.56	2.76
	1.05	12.96	4.90	16.73	1.60	1.64	1.85
	1.46	19.44	6.56	26.53	1.69	1.73	1.23
	1.76	25.92	7.66	36.39	1.77	1.81	.92
	2.00	38.87	8.20	55.27	1.87	1.92	.62
	2.33	51.83	9.11	75.07	1.96	2.00	.46
	2.51	58.31	9.56	85.18	2.00	2.05	.41
	3.06	86.82	10.70	129.30	2.10	2.15	.28

\+ TEMPERATURE CORRECTED SWELLING RATIOS

LAST SET OF VALUES REFERS TO ONSET OF MELT FRACTURE

PS CV-41113

TEST TEMPERATURE = 180.0 DEG C

DIAMETER OF DIE ORIFICE = .133 CM

θ DEG	V_p CM/MIN	$\Delta P \times 10^{-5}$ PASCAL	$\dot{\gamma}_a$ 1/SEC	B -	B+ -
90.0	.20	2.81	10.37	2.01	2.05
	.15	2.31	7.77	1.90	1.94
	.25	3.93	12.96	2.09	2.14
	.51	6.87	25.92	2.38	2.43
	.76	8.43	38.87	2.50	2.56
	1.02	9.99	51.83	2.61	2.67
	1.27	11.55	64.79	2.73	2.79

+ TEMPERATURE CORRECTED SWELLING RATIOS

PS CV-41113

TEST TEMPERATURE = 200.0 DEG C

DIAMETER OF CAPILLARY = .133 CM

ENTRANCE ANGLE = 90.0 DEG

L/D	$\Delta P \times 10^{-6}$	$\dot{\gamma}_a$	$\tau_\omega \times 10^{-4}$	$\dot{\gamma}_\omega$	B	B+	t_a
-	PASCAL	1/SEC	PASCAL	1/SEC	-	-	SEC
	1.07	1.94	1.00	1.88	1.16	1.19	101.92
	2.05	5.18	1.92	6.07	1.24	1.27	38.22
	2.60	7.77	2.43	9.68	1.28	1.31	25.48
	3.43	12.96	3.20	17.24	1.33	1.37	15.29
24.76	4.87	29.15	4.51	41.93	1.39	1.43	6.79
	6.24	58.31	5.73	88.20	1.51	1.55	3.40
	7.43	97.18	6.74	151.92	1.59	1.63	2.04
	8.88	194.36	7.86	313.22	1.67	1.71	1.02
	11.30	388.73	9.72	652.16	1.83	1.88	.51
	1.15	1.94	1.31	2.17	1.20	1.23	82.32
	1.53	5.18	1.74	6.15	1.24	1.28	30.87
	2.01	7.77	2.28	9.75	1.29	1.32	20.58
	3.36	19.44	3.79	26.87	1.38	1.41	8.23
20.00	5.23	58.31	5.82	86.88	1.51	1.55	2.74
	6.41	103.66	7.01	159.34	1.60	1.64	1.54
	7.57	172.34	8.11	271.20	1.69	1.73	.93
	8.32	291.55	8.68	463.74	1.79	1.84	.55
	9.41	388.73	9.69	629.09	1.85	1.90	.41

\+ TEMPERATURE CORRECTED SWELLING RATIOS

LAST SET OF VALUES REFERS TO ONSET OF MELT FRACTURE

PS CV-41113

TEST TEMPERATURE = 200.0 DEG C

DIAMETER OF CAPILLARY = .133 CM

ENTRANCE ANGLE = 90.0 DEG

L/D	$\Delta P \times 10^{-6}$	$\dot{\gamma}_a$	$\tau_w \times 10^{-4}$	$\dot{\gamma}_w$	B	B+	t_a
-	PASCAL	1/SEC	PASCAL	1/SEC	-	-	SEC
	1.13	1.94	1.57	2.45	1.23	1.26	65.78
	1.69	6.48	2.34	8.70	1.28	1.31	19.73
	3.10	25.92	4.27	38.02	1.43	1.47	4.93
	4.43	64.79	5.98	99.59	1.53	1.57	1.97
15.98	5.13	97.18	6.82	152.03	1.60	1.64	1.32
	5.66	129.58	7.43	205.00	1.63	1.68	.99
	6.99	259.15	8.82	419.23	1.79	1.84	.49
	7.82	388.73	9.64	636.00	1.88	1.93	.33
	8.61	485.91	10.55	804.02	1.93	1.98	.26
	.44	1.94	.92	1.71	1.21	1.24	40.69
	.68	5.18	1.43	5.31	1.25	1.28	15.25
	1.29	7.77	2.71	9.60	1.28	1.31	10.17
	1.59	12.96	3.33	16.88	1.33	1.37	6.10
9.89	2.42	38.87	4.95	55.72	1.47	1.51	2.03
	3.26	77.75	6.50	118.40	1.60	1.64	1.02
	4.00	129.58	7.72	204.69	1.68	1.72	.61
	5.04	259.15	9.19	424.26	1.82	1.87	.31
	5.64	388.73	9.95	646.47	1.93	1.97	.20

\+ TEMPERATURE CORRECTED SWELLING RATIOS

LAST SET OF VALUES REFERS TO ONSET OF MELT FRACTURE

PS CV-41113

TEST TEMPERATURE = 200.0 DEG C

DIAMETER OF CAPILLARY = .133 CM

ENTRANCE ANGLE = 90.0 DEG

L/D	$\Delta P \times 10^{-6}$	$\dot{\gamma}_a$	$\tau_\omega \times 10^{-4}$	$\dot{\gamma}_\omega$	B	B+	t_a
-	PASCAL	1/SEC	PASCAL	1/SEC	-	-	SEC
	.42	2.59	1.05	2.44	1.21	1.24	24.58
	.84	6.48	2.11	7.63	1.27	1.31	9.83
	1.47	19.44	3.65	26.48	1.39	1.43	3.28
	2.22	51.83	5.35	77.30	1.54	1.58	1.23
7.96	2.58	77.75	6.09	119.36	1.60	1.64	.82
	3.29	161.97	7.32	258.74	1.75	1.79	.39
	4.11	259.15	8.71	429.17	1.87	1.92	.25
	4.61	388.73	9.40	653.73	1.99	2.04	.16
	5.18	518.30	10.44	890.06	2.06	2.11	.12

+ TEMPERATURE CORRECTED SWELLING RATIOS

LAST SET OF VALUES REFERS TO ONSET OF MELT FRACTURE

PS CV-41113

TEST TEMPERATURE = 200.0 DEG C

DIAMETER OF CAPILLARY = .133 CM

ENTRANCE ANGLE = 90.0 DEG

L/D	$\Delta P \times 10^{-6}$	$\dot{\gamma}_a$	$\tau_\omega \times 10^{-4}$	$\dot{\gamma}_\omega$	B	B+	t_a
-	PASCAL	1/SEC	PASCAL	1/SEC	-	-	SEC
	.42	3.89	1.54	3.94	1.25	1.28	11.02
	.72	8.68	2.63	10.60	1.33	1.36	4.93
	.88	12.96	3.21	16.81	1.37	1.41	3.30
	1.04	19.44	3.74	26.39	1.42	1.45	2.20
5.35	1.44	38.87	5.05	57.30	1.54	1.58	1.10
	2.33	129.58	7.35	209.97	1.78	1.82	.33
	2.76	194.36	8.20	323.16	1.89	1.94	.22
	3.08	259.15	8.71	436.96	1.96	2.01	.17
	3.35	310.98	9.15	530.31	2.02	2.07	.14
	.21	1.94	1.21	2.19	1.21	1.24	12.31
	.44	8.68	2.49	11.16	1.33	1.37	2.76
	.49	12.96	2.70	16.89	1.37	1.41	1.85
	.99	38.87	5.22	56.29	1.55	1.59	.62
2.99	1.19	64.79	5.97	95.72	1.69	1.73	.37
	1.67	129.58	7.53	198.05	1.88	1.93	.18
	1.95	194.36	8.07	300.02	1.98	2.03	.12
	2.34	259.15	9.01	406.33	2.11	2.17	.09
	2.72	388.73	9.44	613.44	2.22	2.27	.06

+ TEMPERATURE CORRECTED SWELLING RATIOS

LAST SET OF VALUES REFERS TO ONSET OF MELT FRACTURE

PS CV-41113

TEST TEMPERATURE = 200.0 DEG C

DIAMETER OF DIE ORIFICE = .133 CM

θ DEG	V_p CM/MIN	$\Delta P \times 10^{-5}$ PASCAL	$\dot{\gamma}_a$ 1/SEC	B -	B+ -
90.0	.17	.69	8.68	1.51	1.55
	.25	1.02	12.96	1.65	1.69
	.38	1.37	19.44	1.74	1.78
	.76	2.98	38.87	2.02	2.07
	1.70	5.93	86.82	2.33	2.39
	3.81	9.80	194.36	2.63	2.70
	5.08	10.99	259.15	2.69	2.76
	6.10	13.59	310.98	2.86	2.93
	7.62	14.36	388.73	2.97	3.04

+ TEMPERATURE CORRECTED SWELLING RATIOS

PS CV-41113

TEST TEMPERATURE = 220.0 DEG C

DIAMETER OF CAPILLARY = .133 CM

ENTRANCE ANGLE = 90.0 DEG

L/D	$\Delta P \times 10^{-6}$	$\dot{\gamma}_a$	$\tau_\omega \times 10^{-4}$	$\dot{\gamma}_\omega$	B	B+	t_a
-	PASCAL	1/SEC	PASCAL	1/SEC	-	-	SEC
	.75	2.59	.70	2.78	1.06	1.09	76.44
	2.56	25.92	2.39	34.03	1.25	1.29	7.64
	4.59	86.82	4.26	123.79	1.42	1.46	2.28
	5.13	129.58	4.75	187.50	1.47	1.51	1.53
24.76	7.58	388.73	6.88	590.55	1.62	1.66	.51
	8.61	583.09	7.73	899.03	1.66	1.71	.34
	10.05	864.27	8.90	1356.18	1.75	1.80	.23
	11.36	1295.76	9.92	2068.80	1.81	1.86	.15
	12.49	1727.24	10.86	2777.31	1.86	1.91	.11
	.67	5.83	.94	5.50	1.17	1.20	21.93
	1.84	25.92	2.56	32.60	1.36	1.39	4.93
	2.57	51.83	3.56	70.56	1.37	1.41	2.47
	3.76	129.58	5.16	191.46	1.51	1.55	.99
15.98	5.52	388.73	7.37	617.66	1.65	1.70	.33
	6.12	583.09	8.02	941.91	1.73	1.78	.22
	7.42	864.27	9.53	1442.79	1.80	1.85	.15
	7.70	1295.76	9.70	2170.32	1.87	1.93	.10
	8.87	1943.63	11.12	3339.08	1.93	1.98	.07

\+ TEMPERATURE CORRECTED SWELLING RATIOS

PS CV-41113

TEST TEMPERATURE = 220.0 DEG C

DIAMETER OF CAPILLARY = .133 CM

ENTRANCE ANGLE = 90.0 DEG

L/D	$\Delta P \times 10^{-6}$	$\dot{\gamma}_a$	$\tau_\omega \times 10^{-4}$	$\dot{\gamma}_\omega$	B	B+	t_a
-	PASCAL	1/SEC	PASCAL	1/SEC	-	-	SEC
	.31	3.89	.66	3.83	1.15	1.18	20.34
	.41	6.48	.86	6.71	1.16	1.19	12.21
	.69	12.96	1.45	14.78	1.21	1.24	6.10
	1.12	29.15	2.36	36.09	1.28	1.32	2.71
9.89	1.87	77.75	3.90	104.00	1.42	1.46	1.02
	2.37	129.58	4.89	179.17	1.49	1.53	.61
	2.75	194.36	5.60	273.99	1.54	1.58	.41
	4.09	518.30	7.94	766.64	1.75	1.80	.15
	5.03	971.82	9.31	1468.37	1.90	1.96	.08
	.71	19.44	1.79	20.75	1.25	1.29	3.26
	1.30	38.87	3.25	48.95	1.37	1.41	1.64
	1.69	97.18	4.16	130.10	1.47	1.51	.66
	1.88	129.58	4.60	177.70	1.52	1.56	.49
7.96	3.75	583.09	8.47	913.79	1.77	1.82	.11
	4.35	864.27	9.50	1386.51	1.85	1.90	.07
	4.87	1295.76	10.29	2111.91	1.99	2.05	.05
	5.31	1619.70	11.11	2679.45	2.10	2.16	.04
	5.51	1943.63	11.56	3240.52	2.11	2.17	.03

\+ TEMPERATURE CORRECTED SWELLING RATIOS

PS CV-41113

TEST TEMPERATURE = 220.0 DEG C

DIAMETER OF CAPILLARY = .133 CM

ENTRANCE ANGLE = 90.0 DEG

L/D	$\Delta P \times 10^{-6}$	$\dot{\gamma}_a$	$\tau_w \times 10^{-4}$	$\dot{\gamma}_w$	B	B+	t_a
-	PASCAL	1/SEC	PASCAL	1/SEC	-	-	SEC
5.35	.34	9.72	1.17	10.27	1.24	1.27	4.41
	.41	12.96	1.38	14.27	1.25	1.29	3.30
	.75	38.87	2.53	49.05	1.36	1.39	1.10
	1.00	64.79	3.35	86.57	1.48	1.52	.66
	1.19	97.18	3.94	134.04	1.50	1.54	.44
	1.59	194.36	5.14	281.86	1.63	1.68	.22
	1.94	291.55	6.10	435.97	1.72	1.76	.15
	2.31	518.30	6.92	792.47	1.84	1.89	.08
	3.06	971.82	8.54	1540.23	2.01	2.07	.04
2.99	.66	48.59	3.27	66.13	1.42	1.46	.49
	.97	129.58	4.65	182.67	1.57	1.62	.18
	1.52	310.98	6.79	454.70	1.82	1.87	.08
	1.68	388.73	7.29	572.24	1.88	1.93	.06
	1.95	583.09	8.02	866.09	1.99	2.04	.04
	2.50	971.82	9.47	1465.78	2.16	2.22	.02
	2.93	1295.76	10.70	1976.34	2.25	2.31	.02
	3.12	1619.70	11.19	2480.50	2.33	2.40	.01
	3.43	1943.63	12.36	3003.33	2.38	2.45	.01

\+ TEMPERATURE COFRECTED SWELLING RATIOS

PS CV-41113

TEST TEMPERATURE = 220.0 DEG C

DIAMETER OF DIE ORIFICE = .133 CM

θ DEG	V_p CM/MIN	$\Delta P \times 10^{-5}$ PASCAL	$\dot{\gamma}_a$ 1/SEC	B -	B+ -
90.0	.76	1.12	38.87	1.63	1.68
	1.27	1.87	64.79	1.74	1.79
	3.81	3.43	194.36	2.09	2.15
	5.08	4.99	259.15	2.32	2.39
	7.62	6.24	388.73	2.44	2.50
	12.70	8.43	647.88	2.61	2.68
	19.05	11.24	971.82	2.83	2.91

+ TEMPERATURE CORRECTED SWELLING RATIOS

PS CV-41113

TEST TEMPERATURE = 200.0 DEG C

DIAMETER OF CAPILLARY = .066 CM

ENTRANCE ANGLE = 90.0 DEG

L/D	$\Delta P \times 10^{-6}$	$\dot{\gamma}_a$	$\tau_\omega \times 10^{-4}$	$\dot{\gamma}_\omega$	B	B+	t_a
-	PASCAL	1/SEC	PASCAL	1/SEC	-	-	SEC
5.50	1.09	16.00	4.73	20.30	1.36	1.40	2.75
	1.37	32.00	5.74	45.71	1.45	1.49	1.37
	1.88	64.01	7.46	105.18	1.57	1.61	.69
	2.15	85.34	8.22	147.10	1.64	1.68	.52
	2.35	106.68	8.71	188.88	1.68	1.72	.41
	2.80	160.02	9.57	295.69	1.79	1.83	.27
	3.18	213.36	10.09	403.61	1.88	1.92	.21
	3.48	256.03	10.43	491.29	1.92	1.97	.17
	3.90	320.04	10.82	623.84	1.98	2.03	.14
3.00	.69	32.00	5.02	39.62	1.53	1.57	.75
	.75	42.67	5.25	54.43	1.57	1.61	.56
	1.00	71.48	6.44	103.33	1.70	1.74	.34
	1.12	85.34	6.97	129.07	1.76	1.80	.28
	1.33	106.68	7.81	171.39	1.83	1.88	.22
	1.72	160.02	8.90	274.45	1.94	1.99	.15
	2.03	213.36	9.41	376.02	2.06	2.11	.11
	2.23	256.03	9.55	454.27	2.15	2.20	.09
	2.50	320.04	9.61	569.44	2.21	2.27	.07

+ TEMPERATURE COFRECTED SWELLING RATIOS

LAST SET OF VALUES REFERS TO ONSET OF MELT FRACTURE

PS CV-41113

TEST TEMPERATURE = 200.0 DEG C

DIAMETER OF CAPILLARY = .066 CM

ENTRANCE ANGLE = 90.0 DEG

L/D	$\Delta P \times 10^{-6}$	γ_a	$\tau_\omega \times 10^{-4}$	γ_ω	B	B+	t_a
-	PASCAL	1/SEC	PASCAL	1/SEC	-	-	SEC
	2.02	16.00	3.96	18.43	1.33	1.37	6.25
	2.46	24.00	4.78	31.02	1.38	1.41	4.17
	3.41	53.34	6.48	80.97	1.48	1.52	1.87
	3.98	80.01	7.39	129.32	1.56	1.60	1.25
12.50	4.44	106.68	8.07	179.34	1.59	1.63	.94
	5.16	160.02	9.00	282.02	1.67	1.71	.62
	5.76	213.36	9.68	387.52	1.73	1.77	.47
	6.06	256.03	9.88	469.04	1.77	1.82	.39
	6.62	320.04	10.35	597.31	1.82	1.86	.31
	1.20	16.00	3.64	17.03	1.33	1.37	4.00
	1.87	40.00	5.48	54.99	1.45	1.49	1.60
	2.19	53.34	6.31	78.97	1.51	1.55	1.20
	2.63	80.01	7.34	127.63	1.59	1.63	.80
8.00	2.98	106.68	8.04	177.53	1.64	1.68	.60
	3.47	160.02	8.83	277.62	1.71	1.75	.40
	3.93	213.36	9.47	381.33	1.82	1.86	.30
	4.23	256.03	9.77	463.66	1.85	1.89	.25
	4.66	320.04	10.14	588.64	1.91	1.96	.20

+ TEMPERATURE CORRECTED SWELLING RATIOS

LAST SET OF VALUES REFERS TO ONSET OF MELT FRACTURE

PS CV-41113

TEST TEMPERATURE = 200.0 DEG C

DIAMETER OF DIE ORIFICE = .066 CM

θ DEG	V_p CM/MIN	$\Delta P \times 10^{-5}$ PASCAL	$\dot{\gamma}_a$ 1/SEC	B -	B+ -
90.0	.10	3.68	42.67	1.85	1.89
	.13	4.31	53.34	1.92	1.97
	.15	5.18	64.01	2.00	2.05
	.19	5.74	80.01	2.09	2.14
	.25	6.87	106.68	2.20	2.25
	.38	9.68	160.02	2.35	2.41
	.51	10.92	213.36	2.48	2.54
	.76	15.92	320.04	2.67	2.73
	1.02	17.92	426.72	2.82	2.89

+ TEMPERATURE CORRECTED SWELLING RATIOS

PS CV-41113

TEST TEMPERATURE = 200.0 DEG C

DIAMETER OF CAPILLARY = .099 CM

ENTRANCE ANGLE = 90.0 DEG

L/D	$\Delta P \times 10^{-6}$	γ_a	$\tau_w \times 10^{-4}$	γ_w	B	B+	t_a
-	PASCAL	1/SEC	PASCAL	1/SEC	-	-	SEC
	1.39	9.48	2.61	11.36	1.38	1.42	10.56
	1.92	21.18	3.58	28.08	1.45	1.49	4.73
	2.42	31.61	4.48	44.75	1.51	1.55	3.17
	3.70	94.83	6.53	148.71	1.67	1.71	1.06
12.51	4.41	158.04	7.52	256.87	1.76	1.80	.63
	5.06	237.07	8.33	395.06	1.86	1.90	.42
	5.47	316.09	8.82	533.98	1.92	1.97	.32
	5.99	395.11	9.53	679.95	1.99	2.04	.25
	6.37	474.13	10.11	827.16	2.05	2.10	.21
	.83	9.48	2.37	12.33	1.35	1.39	6.75
	1.09	15.80	3.09	21.26	1.41	1.45	4.05
	1.51	31.61	4.19	44.18	1.50	1.54	2.02
	2.43	94.83	6.32	139.20	1.71	1.75	.67
8.00	2.86	153.04	7.04	234.92	1.82	1.86	.40
	3.40	237.07	7.98	357.45	1.92	1.97	.27
	3.91	316.09	8.89	482.43	1.99	2.04	.20
	4.48	474.13	9.97	733.02	2.13	2.18	.13
	5.13	632.18	11.85	996.04	2.23	2.29	.10

+ TEMPERATURE CORRECTED SWELLING RATIOS

LAST SET OF VALUES REFERS TO ONSET OF MELT FRACTURE

PS CV-41113

TEST TEMPERATURE = 200.0 DEG C

DIAMETER OF CAPILLARY = .099 CM

ENTRANCE ANGLE = 90.0 DEG

L/D	$\Delta P \times 10^{-6}$	$\dot{\gamma}_a$	$\tau_\omega \times 10^{-4}$	$\dot{\gamma}_\omega$	B	B+	t_a
-	PASCAL	1/SEC	PASCAL	1/SEC	-	-	SEC
	.65	9.48	2.58	12.81	1.36	1.40	4.65
	.92	21.18	3.60	29.63	1.45	1.49	2.08
	1.14	31.61	4.38	45.12	1.49	1.53	1.40
	1.80	94.83	6.31	140.41	1.72	1.76	.47
5.51	2.32	158.04	7.55	238.15	1.85	1.89	.28
	2.62	237.07	8.02	359.29	1.98	2.03	.19
	3.09	316.09	9.06	484.68	2.08	2.13	.14
	3.65	474.13	10.44	736.77	2.21	2.27	.09
	3.96	632.18	11.89	994.36	2.31	2.37	.07
	.33	9.48	2.20	9.94	1.38	1.42	2.53
	.59	21.18	3.81	27.39	1.49	1.53	1.13
	.69	31.61	4.28	42.54	1.57	1.61	.76
	1.25	94.83	6.74	146.80	1.85	1.89	.25
3.00	1.52	158.04	7.36	250.88	2.00	2.05	.15
	1.87	237.07	8.27	388.65	2.13	2.18	.10
	2.15	316.09	8.96	529.45	2.24	2.30	.08
	2.43	395.11	9.81	677.91	2.34	2.40	.06
	2.62	474.13	10.51	828.07	2.41	2.47	.05

\+ TEMPERATURE CORRECTED SWELLING RATIOS

LAST SET OF VALUES REFERS TO ONSET OF MELT FRACTURE

PS CV-41113

TEST TEMPERATURE = 200.0 DEG C

DIAMETER OF DIE ORIFICE = .099 CM

θ DEG	V_p CM/MIN	$\Delta P \times 10^{-5}$ PASCAL	$\dot{\gamma}_a$ 1/SEC	B -	B+ -
90.0	.38	1.94	47.41	2.32	2.38
	.51	2.43	63.22	2.44	2.50
	.76	3.43	94.83	2.62	2.69
	1.27	4.68	158.04	2.88	2.95
	1.91	6.68	237.07	3.11	3.19
	2.54	7.37	316.09	3.28	3.36
	3.81	10.05	474.13	3.51	3.60
	5.08	11.11	632.18	3.66	3.76
	6.10	12.73	758.61	3.77	3.86

+ TEMPERATURE CORRECTED SWELLING RATIOS

PS CV-41113

TEST TEMPERATURE = 220.0 DEG C

DIAMETER OF DIE ORIFICE = .118 CM

θ DEG	V_p CM/MIN	$\Delta P \times 10^{-5}$ PASCAL	$\dot{\gamma}_a$ 1/SEC	B -	B+ -
60.0	.15	1.37	11.19	1.47	1.51
	.19	1.87	13.99	1.57	1.61
	.25	2.00	18.65	1.63	1.68
	.76	4.37	55.95	1.97	2.03
	1.27	5.62	93.24	2.21	2.27
	2.54	8.74	186.48	2.45	2.51
	3.81	11.86	279.73	2.67	2.74
120.0	.15	.94	11.19	1.52	1.56
	.19	1.25	13.99	1.63	1.68
	.25	1.87	18.65	1.70	1.75
	.76	4.37	55.95	2.07	2.13
	1.27	5.12	93.24	2.26	2.32
	2.54	8.74	186.48	2.51	2.58
	3.81	12.17	279.73	2.72	2.79

+ TEMPERATURE CORRECTED SWELLING RATIOS

PS CV-41113

TEST TEMPERATURE = 220.0 DEG C

DIAMETER OF DIE ORIFICE = .118 CM

θ DEG	V_p CM/MIN	$\Delta P \times 10^{-5}$ PASCAL	$\dot{\gamma}_a$ 1/SEC	B -	B+ -
150.0	.25	1.87	18.65	1.74	1.78
	.76	4.00	55.95	2.12	2.18
	1.27	5.49	93.24	2.30	2.37
	1.91	7.37	139.86	2.44	2.51
	2.54	8.30	186.48	2.54	2.61
	5.08	9.99	372.97	2.83	2.91
	7.62	16.36	559.45	3.00	3.08
180.0	.19	1.25	13.99	1.65	1.70
	.25	1.87	18.65	1.71	1.76
	.76	4.00	55.95	2.08	2.14
	1.27	5.49	93.24	2.27	2.33
	2.54	8.61	186.48	2.52	2.59
	5.08	11.74	372.97	2.78	2.85
	7.62	15.29	559.45	2.99	3.07

+ TEMPERATURE CORRECTED SWELLING RATIOS